Defective Dynamics Of Mitochondria In Amyotrophic Lateral Sclerosis And Huntington's Disease

2012

Wenjun Song
University of Central Florida

DEFECTIVE DYNAMICS OF MITOCHONDRIA IN AMYOTROPHIC LATERAL SCLEROSIS AND HUNTINGTON'S DISEASE

by

WENJUN SONG
B.S. Shanghai University, 2007
M.S. University of Central Florida, 2010

A dissertation submitted in partial fulfillment of the requirements
for the degree of Doctor of Philosophy
in the Burnett School of Biomedical Sciences
in the College of Medicine
at the University of Central Florida
Orlando, Florida

Summer Term
2012

Major Professor: Ella Bossy-Wetzel, Ph.D.

ABSTRACT

Mitochondria play important roles in neuronal function and survival, including ATP production, Ca^{2+} buffering, and apoptosis. Mitochondrial dysfunction is a common event in the pathogenesis of neurodegenerative diseases such as amyotrophic lateral sclerosis (ALS) and Huntington's disease (HD); however, what causes the mitochondrial dysfunction remains unclear. Mitochondrial fission is mediated by dynamin-related protein 1 (DRP1) and fusion by mitofusin 1/2 (MFN1/2) and optic atrophy 1 (OPA1), which are essential for mitochondrial function. Mutations in the mitochondrial fission and fusion machinery lead to neurodegeneration. Thus, whether defective mitochondrial dynamics participates in ALS and HD requires further investigation.

ALS is a fatal neurodegenerative disease characterized by upper and lower motor neuron loss. Mutations in Cu/Zn superoxide dismutase (SOD1) cause the most common familiar form of ALS by mechanisms not fully understood. Here, a new motor neuron-astrocyte co-culture system was created and live-cell imaging was used to evaluate mitochondrial dynamics. Excessive mitochondrial fission was observed in mutant $SOD1^{G93A}$ motor neurons, correlating with impaired axonal transport and neuronal cell death. Inhibition of mitochondrial fission restored mitochondrial dynamics and protected neurons against $SOD1^{G93A}$-induced mitochondrial fragmentation and neuronal cell death, implicating defects in mitochondrial dynamics in ALS pathogenesis.

HD is an inherited neurodegenerative disorder caused by glutamine (Q) expansion in the polyQ region of the huntingtin (HTT) protein. In the current work, mutant HTT caused mitochondrial fragmentation in a polyQ-dependent manner in both primary cortical neurons and fibroblasts from human patients. An abnormal interaction between DRP1 and HTT was observed in mutant HTT mice and inhibition of mitochondrial fission or promotion of mitochondrial fusion restored mitochondrial dynamics and protected neurons against mutant HTT-induced cell death. Thus, mutant HTT may increase mitochondrial fission by elevating DRP1 GTPase activity, suggesting that mitochondrial dynamics plays a causal role in HD.

In summary, rebalanced mitochondrial fission and fusion rescues neuronal cell death in ALS and HD, suggesting that mitochondrial dynamics could be the molecular mechanism underlying these diseases. Furthermore, DRP1 might be a therapeutic target to delay or prevent neurodegeneration.

To those who always support me, believe in me, and had confidence in my success.

ACKNOWLEDGMENTS

I thank S. Lubitz, J. Johnson, V. DeAssis, C. Eldon, Y. Song, and B. Kincaid for technical assistance; Dr. B. Bossy for experimental advice; M. Kaliszewski for language suggestion; A. Knott for manuscript editing; and Dr. A. Estevez for advice on purification of motor neurons.

I would like to thank my academic adviser Dr. Ella Bossy-Wetzel for her guidance and my committee members, Dr. Zixi Cheng, Dr. Christina Fernandez-Valle, and Dr. William Self for advice. This work was supported by NIH grants to E.B-W. (R01 EY016164 and R01 NS055193).

TABLE OF CONTENTS

LIST OF FIGURES

LIST OF ABBREVIATIONS

3-NP	3-nitroproprionic acid
Aβ	Amyloid-beta
AD	Alzheimer's disease
ADOA	autosomal dominant optic atrophy
AIF	apoptosis inducing factor
ALS	amyotrophic lateral sclerosis
AMPA	α-amino-3-hydroxy-5-methyl-4-isoxazolepropionic acid
APAF1	Apoptosis protease activating factor 1
BAK	Bcl-2 homologous antagonist killer
BAX	BCL2-associated protein X
BCL2	B-cell lymphoma 2
BCS	bovine calf serum
BDNF	brain-derived neurotrophic factor
BH	BCL2 homology domain
BSA	bovine serum albumin
CCS	copper chaperone for superoxide dismutase
CDK1	cyclin-dependent kinase 1
CHAPS	3-[(3-cholamidopropyl)dimethylammonio]-1-propanesulfonate
CMT	Charcot-Marie-Tooth
CNS	central nervous system
CoIP	co-immunoprecipitation

CR	caloric restriction
CREB	cAMP response element binding protein
CypD	cyclophilin D
DCTN	Dynactin
DIV	days *in vitro*
DMEM	Dulbecco's Modified Eagle Medium
DRP1	dynamin-related protein 1
DTT	Dithiothreitol
EAAT	Excitatory amino-acid transporter
EBSS	Earle's Balanced Salt Solution
EDTA	ethylenediaminetetraacetic acid
ER	endoplasmic reticulum
ETC	electron transport chain
FBS	fetal bovine serum
FIS1	mitochondrial fission 1 protein
FOX	forkhead box
FUS	fused in sarcoma
GED	GTPase effector domain
GLT	glutamate transporter
GSK	glycogen synthase kinase
HAP1	huntingtin-associated protein 1
HD	Huntington’s disease

HEK	human embryonic kidney
HEPES	4-(2-hydroxyethyl)-1-piperazineethanesulfonic acid
HSP60	heat shock protein 60
HTT	Huntingtin
IDH	isocitrate dehydrogenase
IMM	inner mitochondrial membrane
IMS	intermembrane space
JNK	c-Jun N-terminal kinase
KIF	Kinesin superfamily protein
KLC	Kinesin light chain
MARCH5	membrane-associated ring finger 5
MFN	mitofusin
MPTP	mitochondrial permeability transition pore
mtDNA	mitochondrial DNA
NAD^+	nicotinamide adenine dinucleotide
NADH	reduced nicotinamide adenine dinucleotide
NADPH	reduced nicotinamide adenine dinucleotide phosphate
NAM	Nicotinamide
NEM	N-ethylmaleimide
NGF	nerve growth factor
NES	nuclear export signal
NLS	nuclear localization signal

NMDA	*N*-methyl-D-aspartate
NO	nitric oxide
NRF	nuclear respiration factor
NRSE	Neuron-restrictive silencer element
NRSF	Neuron-restrictive silencer factor
OMM	outer mitochondrial membrane
OPA1	optic atrophy 1
OXPHOS	oxidative phosphorylation
PBS	phosphate buffered saline
PD	Parkinson's disease
Pen/Strep	penicillin streptomycin
PGC-1α	peroxisome proliferator-activated receptor gamma coactivator 1-alpha
PINK1	PTEN-induced putative kinase 1
PKA	protein kinase A
PolyP	Polyproline
PolyQ	Polyglutamine
PUMA	p53 upregulated modulator of apoptosis
RILP	Rab-interacting lysosomal protein
ROS	reactive oxygen species
SIR	silent information regulator
SMAC/Diablo	Second mitochondria-derived activator of caspase/direct inhibitor of apoptosis-binding protein with low pI

SMI32	Neurofilament H Non-Phosphorylated
SNOC	S-nitrosocysteine
SNO-DRP1	S-nitrosylation of DRP1
SNPH	Syntaphilin
SOD1	Cu/Zn superoxide dismutase
SOD2	manganese superoxide dismutase
Sp1	specificity protein 1
SUMO	small ubiquitin-like modifier
TDP-43	TAR DNA-binding protein 43
TSA	trichostatin A
VDAC	Voltage-dependent anion channel
WT	wild type

CHAPTER ONE: GENERAL REVIEW

1.1 Overview of Neurodegeneration

Neurodegeneration describes the progressive loss of neuronal structure or function, including neuronal cell death. Millions of people worldwide currently suffer from neurodegenerative diseases including Alzheimer's disease (AD), Parkinson's disease (PD), Huntington's disease (HD), and amyotrophic lateral sclerosis (ALS).

The greatest risk factor of neurodegenerative diseases is thought to be aging because these diseases are late-onset in most cases. Although the causes of neurodegenerative diseases are different, the intracellular mechanisms are strikingly similar. First, protein aggregation, such as amyloid plaques in AD, Lewy bodies in PD, mutant huntingtin (HTT) aggregation in HD, and mutant Cu/Zn superoxide dismutase (SOD1) aggregation in ALS (Selkoe, 2003), is associated with disease progression. The aggregates are believed to block the ubiquitin-proteasome or macroautophagy pathways and may be involved in the pathology of the neurodegenerative diseases. Second, oxidative stress, as a contributor to aging, is a common phenomenon in neurodegenerative disorders (Lin and Beal, 2006). Oxidation of proteins, DNA, and lipids leads to cellular malfunction. Furthermore, increased intracellular levels of reactive oxygen species (ROS) up-regulate pro-apoptotic proteins, including BAX (Bcl2-associated protein X) and PUMA (P53 up-regulated modulator of apoptosis), which leads to apoptosis. Third, mitochondrial dysfunction is an early event during disease progression and is known to play a key role in neurodegeneration (Knott et al., 2008). Mitochondria-mediated ATP production (see 1.2.3.2)

and Ca^{2+} buffering (see 1.2.3.3) are crucial for neuronal function and survival (see detailed discussion later).

Although the impaired intracellular signaling pathways appear similar among different neurodegenerative diseases, it is important to identify how a single gene mutation interferes with signaling pathways and contributes to neuronal dysfunction and cell death. Furthermore, the specificity of the affected cell type during neurodegeneration is also a mystery worthy of investigation.

1.2 Mitochondrial Structure and Function

1.2.1 Mitochondrial structure

Mitochondria are double-membrane-bound organelles with diameters of about 0.5 µm and lengths of 1–10 µm located within the cytoplasm of most eukaryotic cells (Detmer and Chan, 2007). The two membranes are composed of phospholipid bilayers and different proteins, which divide a single mitochondrion into four distinct compartments (Figure 1).

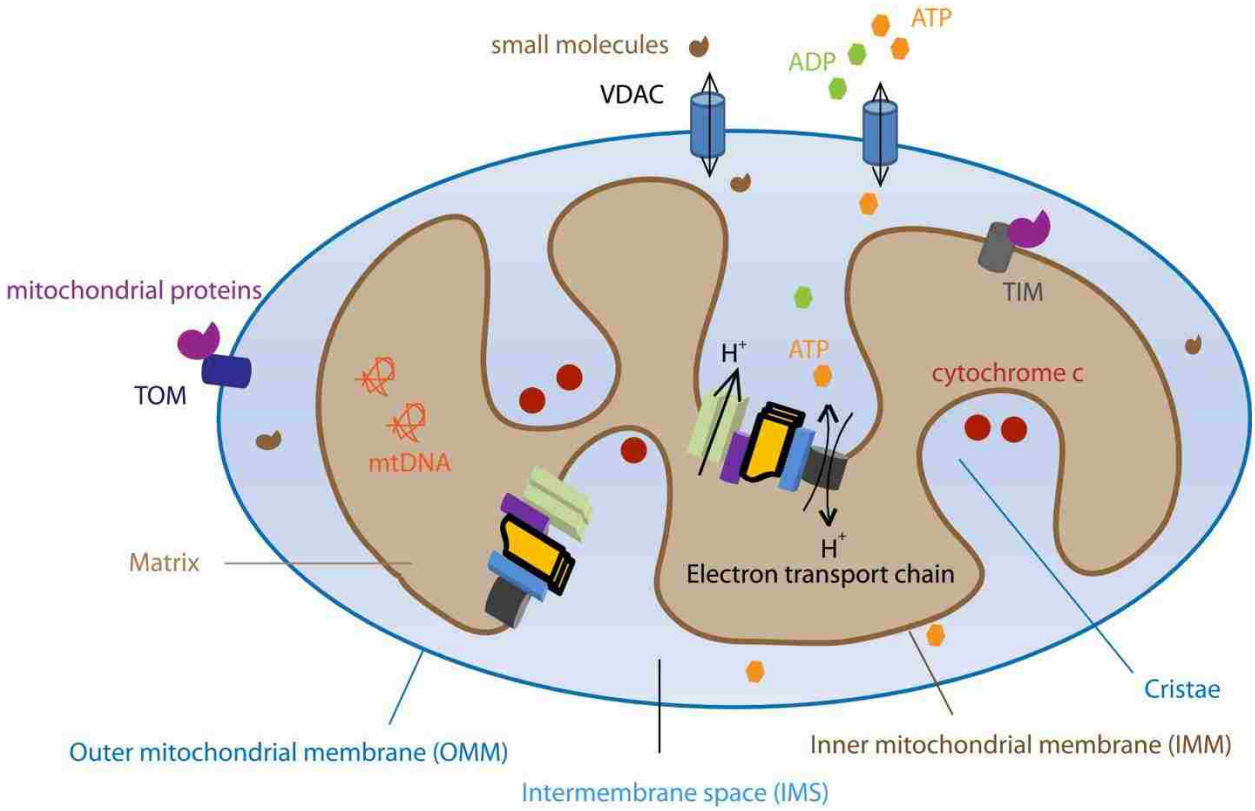

Figure 1 Structure model of a single mitochondrion.

1) Protein import machineries, such as Tom 20, and mitochondrial permeability transition pore components, such as voltage-dependent anion channel (VDAC), are located on the OMM. Proteins involved in important mitochondrial functions are also found on the outer mitochondrial membrane (OMM). For example, the mitochondrial fission and fusion proteins, such as dynamin related protein 1 (DRP1), mitochondrial fission 1 protein (FIS1), mitofusin1/2

(MFN1/2), and proteins involved in apoptosis, including BAX and B-cell lymphoma 2 (BCL2) are all located on the OMM.

2) The intermembrane space (IMS) is the area between the OMM and the inner mitochondrial membrane (IMM). One important function of the IMS is to provide the ions, ADP, and electrochemical proton gradient required for mitochondrial oxidative phosphorylation (OXPHOS) through the electron transport chain (ETC).

3) The IMM is more complex in structure than the OMM. The IMM is only permeable to oxygen, carbon dioxide, and water. The OXPHOS complexes, located within the IMM, pump H^+ ions from the matrix into the IMS to generate a proton gradient, with the resulting flow of ions returning to the matrix and driving ATP production by ATP synthase. In addition, the mitochondrial fusion protein optic atrophy 1 (OPA1) and the protein import machinery Tim complex are also located in the IMM.

Cristae is the term for inner mitochondrial membrane folds, which are thought to expand IMM surface area and enhance mitochondrial OXPHOS. It is also worth noting that cytochrome *c* is usually sequestered here. The release of cytochrome *c* into the cytoplasm is an early signal of apoptosis.

4) The matrix is the space within the IMM that is important for OXPHOS. In addition, the matrix contains mitochondrial ribosomes, tRNA, and mitochondrial DNA (mtDNA). It should be noted that mtDNA encodes 13 peptides, all of which are components of the electron transport chain. Thus, mtDNA is very important for mitochondrial function.

1.2.2 Mitochondrial dynamics

Historically, mitochondria were thought to be immobile inside cells; in fact, mitochondria have been shown to be highly dynamic organelles (Bereiter-Hahn and Voth, 1994; Chan, 2006; Nunnari et al., 1997). Mitochondria can divide by fission, fuse by fusion, move along microtubules, and turn-over by mitophagy. Mitochondrial movement is "saltatory"—stop and go—in response to intracellular energy demands.

1.2.2.1 Mitochondrial fission

Mitochondrial fission is mediated by a large GTPase, DRP1, in mammals (Dnm1 in yeast). DRP1 is primarily located in the cytoplasm, and its recruitment to the OMM is required for mitochondrial fission (Bleazard et al., 1999; Smirnova et al., 2001). DRP1 is composed of four domains: an N-terminal GTPase domain, a middle and a B domain in the central region, and a C-terminal GTP effector domain (GED) (Figure 2). The GTPase domain is highly conserved through yeast to mammals, suggesting its function is important. Purified Dmn1 forms helical rings and spirals *in vitro*, which is consistent with the function of its related protein, dynamin, in endocytosis (Ingerman et al., 2005). Accumulated Dnm1 oligomers form a highly ordered ring structure around mitochondria. Interruption of GTP binding prevents spiral formation and mitochondrial fission, suggesting that GTP binding is required for Dmn1 assemblage. Hydrolysis of GTP to GDP results in disassembly of Dnm1 oligomers and mitochondrial fission (Smirnova et al., 2001).

DRP1 domain model

Mitochondrial fission model

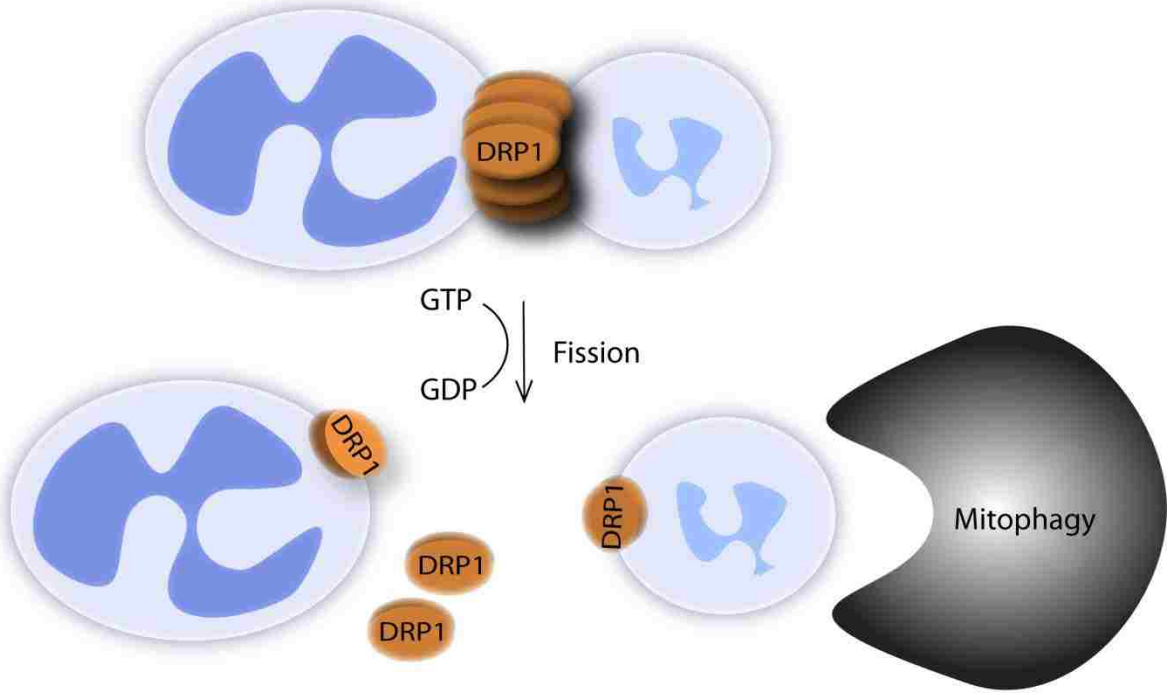

Figure 2 Illustration of DRP1-mediated mitochondrial fission.

A) Domain model of DRP1 (accession number: NP_036192). B) Scheme of mitochondrial fission mediated by DRP1. In the presence of GTP, DRP1 oligomerizes and forms a ring structure around the mitochondrion. Mitochondrial fission occurs when GTP hydrolyzes to GDP, and then the DRP1 oligomer disassembles. Depolarized mitochondria are further degraded by mitophagy.

In yeast, Dnm1 translocates from the cytoplasm to mitochondria through an indirect interaction with an OMM protein, Fis1, via one of two molecular adaptors, Mdv1 or Caf4 (Cerveny and Jensen, 2003; Griffin et al., 2005; Naylor et al., 2006). However, no mammalian homologs of Mdv1 or Caf4 have been identified to date. In addition, FIS1 in mammals seems to play a different role during mitochondrial fission. Knockdown of hFIS1 blocks mitochondrial fission, but does not prevent DRP1 recruitment to the OMM (Lee et al., 2004). Therefore, hFIS1 is not required for DRP1 translocation to mitochondria in mammals. On the other hand, knockdown of hFis1 inhibits mitochondrial fission, suggesting that hFis1 is down-regulated by DRP1. A recent study identified a new OMM protein, Mff, which is involved in mitochondrial fission (Gandre-Babbe and van der Bliek, 2008). However, Mff and hFis1 reside in different complexes, suggesting independent machineries for mitochondrial fission.

Recent studies have revealed that DRP1 GTPase activity can be regulated by post-translational modifications, including phosphorylation, SUMOylation, and ubiquitylation. Protein kinase A (PKA) phosphorylates DRP1 at S637, causing a decrease in GTPase activity and inhibition of mitochondrial fission (Chang and Blackstone, 2007; Cribbs and Strack, 2007). However, cyclin-dependent kinase 1 (CDK1)/cyclin B phosphorylation of DRP1 stimulates DRP1 activity and mitochondrial fission (Kashatus et al., 2011; Taguchi et al., 2007). Thus, it seems that DRP1-mediated mitochondrial fission is involved in different cell signaling pathways. DRP1 has also been shown to be SUMOylated by small ubiquitin-related modifier 1 (SUMO1), promoting mitochondrial fission by protecting DRP1 against degradation (Harder et al., 2004; Wasiak et al., 2007). Furthermore, membrane-associated RING-CHV (MARCH 5) ubiquitinates

DRP1 and promotes mitochondrial fission (Karbowski et al., 2007), although the mechanism of how MARCH5 influences mitochondrial morphology remains unclear.

In sum, DRP1 is required for mitochondrial fission, which can be regulated directly through post-translational modification of DRP1 and probably also through its interaction with other proteins.

1.2.2.2 Mitochondrial fusion

Mitochondrial fusion involves two steps: OMM fusion and IMM fusion.

1) In mammals, OMM fusion is mediated by two large transmembrane GTPases, MFN1 and MFN2 (only one protein, Foz1, in yeast), located at the OMM (Chen et al., 2003). The N-terminal GTPase domains and C-terminal coiled-coil structure are highly conserved in MFNs throughout evolution (Figure 3). Mutations in either of these two domains in Foz1 inhibit mitochondrial fusion in yeast (Griffin and Chan, 2006). MFN1 and 2 are required to form both homo-oligomeric and hetero-oligomeric complexes between opposing mitochondria during OMM fusion (Chen et al., 2003; Koshiba et al., 2004; Meeusen et al., 2004). In addition, both mammalian MFN1 and the bacterial form, BDLP, have been shown to form an anti-parallel coiled coil, promoting membrane tethering and fusion (Koshiba et al., 2004; Low and Lowe, 2006).

2) In yeast, IMM fusion is mediated by Mgm1 (Meeusen et al., 2006). The mammalian homolog, OPA1, is also essential for IMM fusion, with its localization in the IMS and association

with the IMM (Chen et al., 2005b; Cipolat et al., 2004). Compared to DRP1 and MFNs, both Mgm1 and OPA1 contain a N-terminal mitochondrial targeting sequence that mediates mitochondrial import (Figure 3). A transmembrane domain is adjacent to the mitochondrial targeting sequence, which anchors Mgm1 and OPA1 to the IMM. Mgm1 and OPA1 also contain GTPase and GED domains, similar to DRP1. It has been revealed that Mgm1 interacts with itself to tether the IMM and mediate mitochondrial fusion (Meeusen et al., 2006). In addition, both Mgm1 and OPA1 have been shown to have different isoforms (Delettre et al., 2001; Sesaki et al., 2003). Both long-isoform and short-isoform proteins are important for mitochondrial fusion (Hoppins et al., 2007).

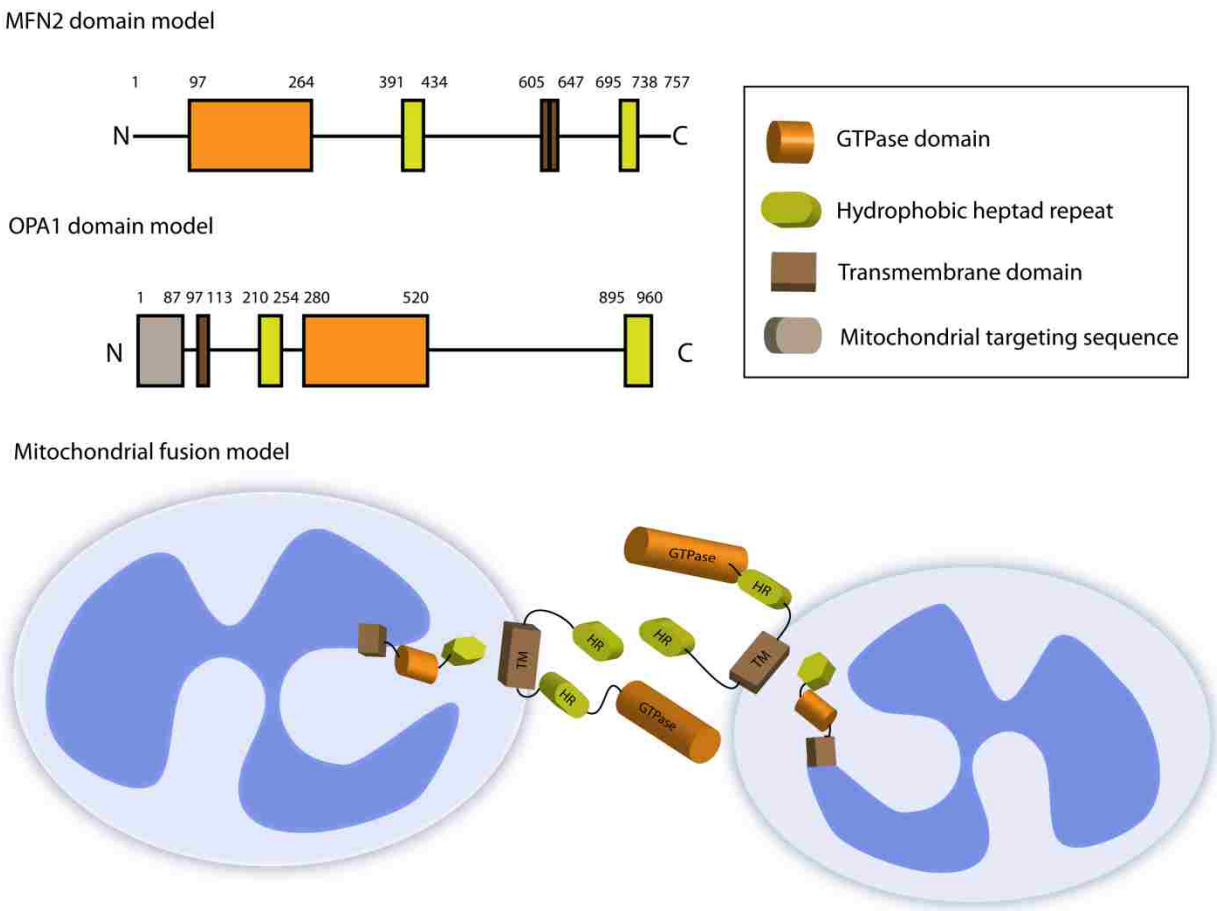

Figure 3 MFNs and OPA1 mediate mitochondrial fusion. Domain models of MFN2 (accession number: NP_001121132) and OPA1 (accession number: NP_056375).

1.2.2.3 Mitochondrial transport

In addition to fission and fusion, mitochondria also move along microtubules and myosins in cells. Microtubule-based mitochondrial transport is responsible for long-distance and fast transport, while actin-based transport is used for short-range and slow movement (Ligon and Steward, 2000).

Myosin-mediated mitochondrial transport along myosins occurs only in areas devoid of microtubules (Ligon and Steward, 2000). In mammalian cells, mitochondrial transport mainly relies on microtubules (Hollenbeck and Saxton, 2005). Microtubules are organized with their plus (+) end towards the periphery of the cell (nerve terminals of the neuron) and minus (-) end towards the nucleus. Anterograde transport is a term that describes movement towards the plus (+) end of the microtubule, while movement in the other direction is known as retrograde transport (Figure 4).

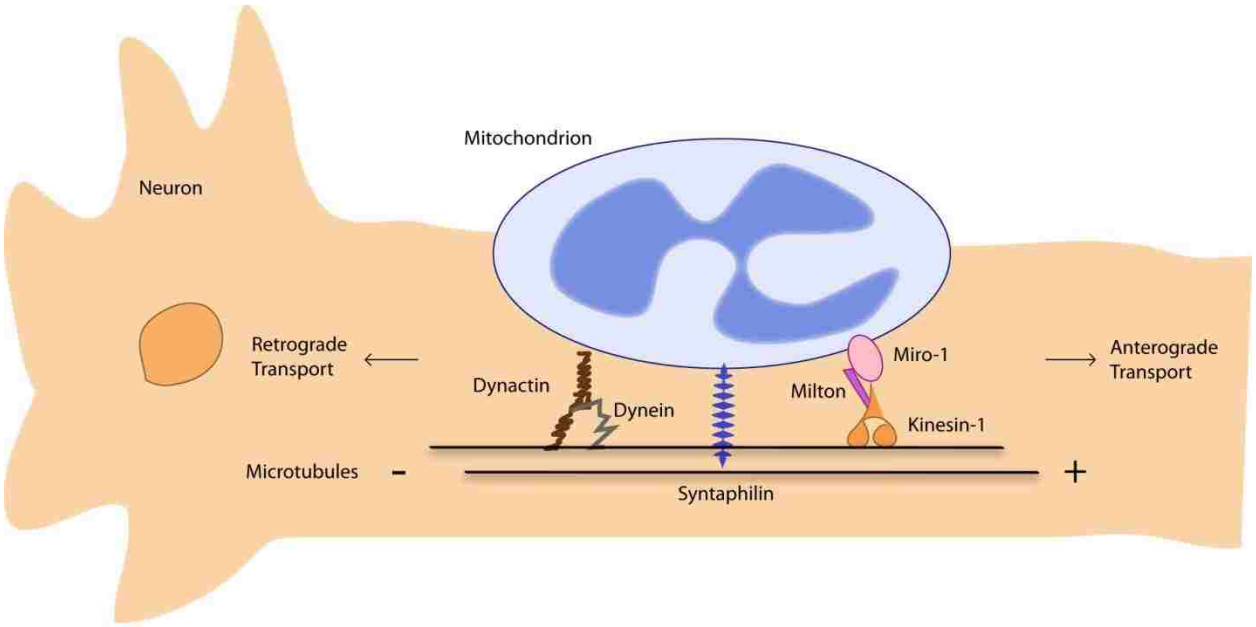

Figure 4 Model of mitochondrial transport machinery.

Recent studies have revealed that Kinesin family and Dynein/Dynactin complexes are involved in mitochondrial anterograde and retrograde transport, respectively (Hollenbeck and Saxton, 2005). Three Kinesin-1 family members have been found to be associated with mitochondria, including Kinesin superfamily protein 1B (KIF1B), KIF5B, and Kinesin light chain 3 (KLC3) (Nangaku et al., 1994; Tanaka et al., 1998; Zhang et al., 2004). Silencing Kinesin heavy chain KIF5B results in inhibition of mitochondrial transport in mouse neurons (Tanaka et al., 1998). Kinesin activity has been found to be regulated by phosphorylation at KLC (De Vos et al., 2000; Lee and Hollenbeck, 1995). The p38-dependent phosphorylation of KLC by glycogen

synthase kinase 3β (GSK3β) releases Kinesin-1 from its cargo and thus inhibits its activity (De Vos et al., 2000). In addition, GSK3β can also be regulated by phosphorylation through the AKT pathway, suggesting that mitochondrial anterograde transport occurs in response to cellular signaling (Jope and Johnson, 2004). Furthermore, mutations in Kinesin-1 inhibit both anterograde and retrograde transport in Drosophila motor neurons, suggesting the existence of an interaction between Kinesin-1 and Dynein (Pilling et al., 2006).

Two cargo adaptor proteins, Miro-1 and Milton, both of which are required for anterograde mitochondrial transport in neurons, have been identified as the link between mitochondria and Kinesin-1, (Guo et al., 2005; Stowers et al., 2002). Mitochondrial rho-like GTPase, Miro-1, is thought to be anchored on the OMM by its C-terminal transmembrane domain (Guo et al., 2005). Miro-1 also contains a GTPase domain and a Ca^{2+} binding EF-hand domain, indicating that Miro-1 might function in regulation of mitochondrial transport and Ca^{2+} sensing (Glater et al., 2006). Mutations in either domain result in abnormal mitochondrial distribution, indicating the importance of both domains in regulating mitochondrial transport (Fransson et al., 2006). Milton acts as an adaptor protein that mediates binding of Miro-1 to Kinesin-1 heavy chain (Glater et al., 2006). However, a recent study indicated that Miro-1 directly interacts with Kinesin-1 in response to intracellular Ca^{2+}, preventing Kinesin from attaching to microtubules (Wang and Schwarz, 2009). Because Ca^{2+} acts as an important signaling molecule, Ca^{2+}-mediated regulation of mitochondrial transport is implicated in multiple biological functions.

Dynein/Dynactin complexes mediate retrograde mitochondrial transport and there is an interesting link between Dynein and DRP1 (Varadi et al., 2004). Varadi *et al* found that Dynein recruits DRP1 to the OMM during mitochondrial retrograde transport. Dynein dysfunction not only causes abnormal subcellular distribution of mitochondria, but also results in elongated mitochondrial morphology. Thus, mitochondrial morphology and transport are tightly regulated by each other.

There is also a "brake" in the regulation mechanism of mitochondrial transport. Syntaphilin (SNPH), an OMM protein, controls docking of mitochondria (Kang et al., 2008). SNPH deletion results in abnormal mitochondrial positioning and cellular dysfunction.

1.2.2.4 Mitophagy

Mitophagy is a type of autophagy that involves selective degradation of mitochondria. Recently, mitophagy has been found to selectively degrade defective mitochondria (Kim et al., 2007b). Mitochondrial fission can yield two uneven daughter mitochondria, with one depolarized and one hyper-polarized (Figure 2). The depolarized daughter mitochondrion fails to fuse and is eventually degraded by autophagocytosis which appears to be a mitochondrial quality control mechanism (Twig et al., 2008). Although mitochondrial fission is required for mitophagy, it is not sufficient for induction of mitophagy.

1.2.3 Biological functions and dynamics of mitochondria

Mitochondria play key roles in multiple cellular events, including ATP production, Ca^{2+} buffering, and apoptosis. Normal mitochondrial dynamics, acting in a housekeeping role, are required to maintain these functions.

1.2.3.1 Role of fission and fusion in mitochondrial maintenance

As mentioned above, mitochondrial fission can result in two uneven daughter mitochondria (Barsoum et al., 2006), and the depolarized one is further recycled by mitophagy (Twig et al., 2008). Such a process is important for mitochondrial quality control and maintenance of a healthy mitochondrial population.

Mitochondrial fusion is also essential for maintenance of mitochondrial functions. Mitochondrial fusion mediates the exchange of mitochondrial contents, including proteins, lipids, and mtDNA. Sometimes, non-functional mitochondria are formed due to the loss of essential components resulting from no fusion. Thus, content exchange through mitochondrial fusion is the most efficient way to restore mitochondrial components and functions.

In the same vein, mitochondrial DNA is a key factor in mitochondrial function. As described before, mtDNA encodes essential subunits of OXPHOS complexes, which are required for maintenance of mitochondrial membrane potential and ATP production (see below). Inhibition of mitochondrial fusion increases the mitochondrial population without mtDNA, which in turn leads to mitochondrial dysfunction (Chen et al., 2007a).

In sum, mitochondrial fission, fusion, and mitophagy are involved in mitochondrial quality control. Mitochondrial transport distributes mitochondria in response to cellular demands. The dynamics of mitochondria support their maximum functioning in cells.

1.2.3.2 ATP production

One of the major roles of mitochondria is ATP production through oxidative phosphorylation driven by oxidation of pyruvate and nicotinamide adenine dinucleotide (NADH). There are four complexes that span the IMM, called Complex I–IV. Electrons flow through this ETC, pump H^+ ions across the IMM from the matrix to the IMS, and generate an electrochemical proton gradient. The energetically unfavorable generation of ATP is driven by protons flowing back from the IMS into the matrix (Wallace and Fan, 2009).

ATP is the main energy source for most cellular functions and helps drive cellular processes, such as 1) synthesis of macromolecules, including DNA, RNA, and proteins; 2) synaptic transmission, such as endocytosis and exocytosis; and 3) maintenance of cell structures by assembly or disassembly of the cytoskeleton. In addition, ATP is also the source of phosphate groups during signaling transduction processes (e.g., phosphorylation) and conversion of ATP to cAMP by adenylate cyclase produces a second messenger molecule in intracellular signaling.

Thus, due to the important roles of ATP, its production is fundamental to maintenance of normal cellular function. In neurons, the importance of ATP production by mitochondrial

oxidative phosphorylation is even more profound, because glycolysis is down-regulated in neurons. In addition, neurons have high energy demands, requiring huge amounts of energy to deliver vesicles from the cell body to the nerve terminal. It has been reported that mitochondria accumulate where neurons need more energy, including synapses, growth cones, and nodes of Ranvier. Moreover, ATP-dependent neurotransmission plays a fundamental role in neurons, requiring mitochondrial transport to synapses and providing ATP.

Recent studies have revealed that defects in mitochondrial dynamics lead to bioenergetic failure. Either inhibition of fission by blockage of DRP1 activity or inhibition of fusion by MFN1/2 knock-out, results in reduced respiratory activity and decreased ATP production (Benard et al., 2007; Chen et al., 2005b). Furthermore, inhibition of mitochondrial transport to synapses results in spine loss, while stimulation of mitochondria in synapses increases spine number (Verstreken et al., 2005). Although the mechanism of this relationship remains unclear, mitochondrial dynamics and the bioenergetic functions of mitochondria, which are essential to neuronal function, are tightly linked.

1.2.3.3 Ca^{2+} homeostasis

Ca^{2+} is the most abundant ion in the human body and plays an essential role in signal transduction, muscle contraction, neuronal transmission, cell growth, and synaptic plasticity. The concentration of Ca^{2+} is usually in the range of 10–100 nM. Mitochondria and endoplasmic reticulum (ER) are the main sites for storage of excess cytoplasmic Ca^{2+} and the main sources of

Ca^{2+} release in response to stimuli. Dysregulation of intracellular Ca^{2+} levels leads to cellular malfunction and even cell death (see further discussion in Section 1.2.3.4).

Mitochondria-mediated Ca^{2+} uptake relies on membrane potential. Failure of mitochondrial fission and fusion disrupts membrane potential and results in more depolarized mitochondria. In addition, Ca^{2+} directs mitochondrial transport in order to buffer the concentrated Ca^{2+} (Glater et al., 2006). Therefore, mitochondrial dynamics is required for maintenance of Ca^{2+} homeostasis.

Ca^{2+} buffering capacity is one of the important functions of mitochondria and is also regulated by mitochondrial dynamics.

1.2.3.4 Apoptosis

Mitochondrial permeability transition pore (MPTP) opening is the first sign of apoptosis, which leads to release of pro-apoptotic proteins from the IMS to the cytoplasm, including cytochrome *c* and second mitochondria-derived activator of caspase (SMAC/Diablo). Cytochrome *c* is sequestered inside the cristae by the IMM protein Cardiolipin. In response to nitration of Cardiolipin or cristae structure remodeling, cytochrome *c* is released from crista junctions into the cytoplasm, where it interacts with apoptotic protease activating factor 1 (APAF1) to facilitate apoptosome formation, and in turn activates Caspase-9, which executes the apoptotic program (Youle and Karbowski, 2005).

Two pro-apoptotic regulators, BAX and Bcl2 homologous killer (BAK), have been shown to form foci with DRP1 and MFN2 during apoptosis (Karbowski et al., 2002; Yuan et al., 2007). Interestingly, inhibition of DRP1 or use of dominant-negative DRP1^{K38A}, decreases mitochondrial fragmentation and blocks or delays cell death in different cell types (Abdelwahid et al., 2007; Cribbs and Strack, 2007; Frank et al., 2001; Goyal et al., 2007; Karbowski et al., 2002). Clearly, mitochondrial dynamics is involved in the apoptotic pathway.

1.3 Defective Mitochondrial Dynamics in Neurodegeneration

As discussed above, mitochondria have several critical functions in cells, particularly neurons. Since mitochondrial dynamics are important to the maintenance of mitochondrial function, defective mitochondrial dynamics may be responsible for neurodegenerative diseases. A number of studies to date have revealed the relationship between mitochondrial dynamics and neurodegeneration.

1.3.1 OPA1 and autosomal dominant optic atrophy

Mutations in OPA1 cause autosomal dominant optic atrophy (ADOA), an optic neuropathy characterized by degeneration of retinal ganglion cells (Alexander et al., 2000; Delettre et al., 2000). Most OPA1 mutations found in patients occur in the GTPase domain, suggesting that defective mitochondrial fusion plays a role in the pathogenesis (Ferre et al.,

2005). In non-neuronal cells from human patients, fragmented mitochondria have been observed. OPA1 mutations are associated with decreased ATP production and reduced mtDNA content, suggesting a relationship between defective mitochondrial fusion and mitochondrial dysfunction in ADOA (Kim et al., 2005; Lodi et al., 2004). In experimental cells with depleted OPA1, fragmented mitochondria, defective respiration, aberrant cristae structure, and increased sensitivity to apoptosis have been observed (Chen et al., 2005b; Griparic et al., 2004; Naylor et al., 2006; Olichon et al., 2003). Moreover, a heterozygous mouse model with OPA1 mutations exhibited a similar phenotype as ADOA patients, marked by degeneration of retinal ganglion cells (Chung et al., 2006). Interestingly, homozygous mice with OPA1 mutations exhibit embryonic lethality, indicating mitochondrial dynamics play a vital role in embryonic development (Davies et al., 2007).

Although the mechanism of how OPA1 mutations lead to ADOA remains unclear, ADOA provides a link between mitochondrial dynamics and neurodegeneration.

1.3.2 MFN2 and Charcot-Marie-Tooth Type 2A

Charcot-Marie-Tooth Type 2A (CMT-2A) is a neurodegenerative disease characterized by peripheral neuropathy. More than 40 mutations in MFN2 that cause CMT-2A have been identified, most of which occur in or near the GTPase domain (Zuchner et al., 2004). Thus, loss of MFN2 fusion activity may result in neuronal loss in CMT-2A. Mitochondrial swelling and aggregation were observed in the sural nerve of CMT-2A patients (Verhoeven et al., 2006). In

addition, mutant MFN2 causes mitochondrial aggregation and defective transport in experimental neurons (Baloh et al., 2007). Interestingly, CMT-2A and ADOA patients have some overlapping symptoms, which probably result from defective mitochondrial fusion (Chung et al., 2006). All of this evidence indicates that defects in mitochondrial dynamics are the primary cause of CMT-2A, although the disease mechanism remains to be elucidated.

1.3.3 Mitochondrial dynamics in Alzheimer's disease

AD is the most common neurodegenerative disease, characterized by cognitive dysfunction and memory loss. Unlike ADOA and CMT-2A, which are caused by mutations in the mitochondrial fusion machinery, most of AD cases are sporadic, marked by neurofibrillary tangles and extracellular amyloid plaques. The mechanism of AD pathology remains unknown, but mitochondrial dysfunction has been implicated.

Amyloid plaques are mainly composed of Aβ. Although amyloid plaques are located in the extracellular matrix, it has been revealed that Aβ is also localized on mitochondria, suggesting mitochondria are involved in Aβ-mediated toxicity in AD (Lustbader et al., 2004). Experimental neuronal cells exposed to Aβ exhibit increased mitochondrial fission, spine loss, and eventually cell death (Cho et al., 2009). The increased mitochondrial fission has been shown to result from increased DRP1 activity, which results from S-nitrosylation of DRP1 (SNO-DRP1) (Cho et al., 2009). Expression of DRP1 (C664A), a mutant resistant to S-nitrosylation, prevents neurons from Aβ-induced mitochondrial fission and neuronal cell death. Importantly,

increased levels of SNO-DRP1 have been observed in both AD mice and patients, confirming the hypothesis that Aβ induces neuronal injury through increased mitochondrial fission. However, a recent paper demonstrated that SNO-DRP1 has no impact on either DRP1 GTPase activity or DRP1 oligomerization (Bossy et al., 2010). Instead, nitrosative stress induces DRP1 phosphorylation at S616, which triggers mitochondrial fragmentation (Bossy et al., 2010). More recently, the abnormal interaction between Aβ and DRP1 was found in AD patients, suggesting that mitochondrial dynamics is implicated (Manczak et al., 2011). Although these results are controversial, there is no doubt that defective mitochondrial dynamics participates in AD.

1.3.4 Mitochondrial dynamics in Parkinson's disease

PD is the second most common neurodegenerative disease, characterized by tremor and rigidity. Sufficient evidence has confirmed the involvement of mitochondria in PD pathogenesis.

The majority of PD cases are sporadic and only about 10% of cases are familial. Mitochondrial involvement in PD was first suggested by a study that showed that inhibition of Complex I in the ETC leads to PD-like symptoms in a mouse model (Betarbet et al., 2000). Many genes have been linked to PD, including PTEN-induced putative kinase 1 (PINK1) and Parkin (Dodson and Guo, 2007). PINK1 is a serine/threonine kinase localized in both the cytoplasm and mitochondria with an N-terminal mitochondrial targeting sequence, while Parkin is an E3-ligase. Although mutations in PINK1 and Parkin failed to produce PD symptoms in mouse models,

there have been observations of mitochondrial defects in respiration and increased sensitivity to oxidative stress (Gautier et al., 2008; Palacino et al., 2004). Genetic ablation of PINK1 results in mitochondrial elongation in COS-7 cells, which can be re-balanced by DRP1 or hFis1 overexpression (Yang et al., 2008). In HeLa cells, PINK1 inhibition leads to mitochondrial fragmentation, which can be rescued by Parkin over-expression (Exner et al., 2007). Moreover, mitochondrial dysfunction was observed in flies with PINK1 or Parkin knock-down. The phenotypes in these mutant flies become even more exaggerated by DRP1 over-expression or inhibition of MFN1, MFN2, and OPA1, suggesting mitochondrial dynamics are involved in the PINK1/Parkin pathway (Deng et al., 2008). More recently, Parkin has been found to be recruited to impaired mitochondria and participate in mitophagy (Narendra et al., 2008). PINK1 is required for maintenance of mitochondrial function (Clark et al., 2006). The functions of PINK1 and PARKIN are so closely related to mitochondrial dynamics and function it is hard to believe that mitochondrial dynamics are not involved in PD pathogenesis.

In sum, mitochondrial dysfunction is a common phenomenon in neurodegeneration. Mitochondrial dynamics is important for maintenance of mitochondrial function, which is essential for neuronal function and survival. In some neurodegenerative diseases, defects in mitochondrial dynamics appear to be the primary cause; however, it remains unknown what triggers these defects in mitochondrial dynamics. Here, the mechanism of mitochondrial fission/fusion in two neurodegenerative diseases, ALS and HD, will be further investigated.

Ultimately, the results may lead to better detection, diagnosis, and even treatment strategies for patients affected by ALS and HD.

CHAPTER TWO: MITOCHONDRIAL DYNAMICS DEFECTS IN ALS

2.1 Overview of ALS

2.1.1 Symptoms and mutations in ALS

ALS is a progressive neurodegenerative disease characterized by the selective degeneration of upper and lower motor neurons in the spinal cord, brainstem, and motor cortex. Dysfunction and death of these motor neurons causes muscle weakness and atrophy leading to paralysis and death within 3–5 years (Shaw, 2005). Respiratory failure is the most common cause of death. The typical age of onset is 45–60, with a life time risk of 1 in 1000 and a male to female ratio of 2:1. Approximately 10% of ALS cases are familial (autosomal dominant in most cases) and the remaining 90% are sporadic.

To date, several proteins have been identified that cause familial ALS, including SOD1, TAR DNA-binding protein (TDP-43), and fused in sarcoma (FUS) (Deng et al., 1993; Kwiatkowski et al., 2009; Neumann et al., 2006; Rosen, 1993; Vance et al., 2009). The cause of sporadic ALS remains unknown; however, we do know that 20% of familial ALS (FALS) cases are linked to mutations in SOD1 (Deng et al., 1993; Rosen, 1993). The hope is that studies of these rare hereditary ALS cases will lead to a better understanding of the mechanisms underlying the more common sporadic disease.

2.1.2 Mutant SOD1-mediated toxicity in ALS

SOD1 is a 154 amino acid homo-dimeric soluble protein found in the cytoplasm that is known to neutralize superoxide radicals. SOD1 converts superoxide, most of which is generated as a by-product of mitochondrial OXPHOS, into hydrogen peroxide. Thus, SOD1 plays an essential role in cytoplasmic antioxidant defense.

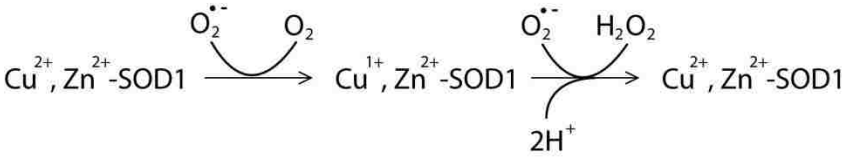

To date, more than 150 SOD1 mutants have been identified in ALS patients (Turner and Talbot, 2008). Due to its important cellular function, it was initially proposed that SOD1-linked FALS results from radical damage caused by decreased SOD1 activity. However, *in vitro* studies showed that different FALS-linked SOD1 mutant proteins have different enzymatic activities, and at least some FALS mutants retain full enzyme activity (Borchelt et al., 1994). Moreover, SOD1 null mice live to adulthood and do not develop motor neuron disease (Reaume et al., 1996). Although these mice are vulnerable to motor neuron loss after axonal injury, this study showed that loss of SOD1 is not required for development of motor neuron disease. In addition, transgenic mice expressing FALS mutants exhibit motor neuron disease with normal SOD1 activity (Bruijn et al., 1997), indicating that mutant SOD1 toxicity is not triggered by a loss of enzymatic activity, but by an unknown gain-of-function.

Previous studies have suggested that mSOD1 causes various cellular events, including glutamate-induced excitotoxicity, ER stress, proteasome inhibition, alteration of gene

expression, abnormal protein interactions, activation of caspases, mitochondrial dysfunction, and cytoskeletal abnormalities (Figure 5) (Ilieva et al., 2009). However, the causal relationship between these events and motor neuron death remains unclear.

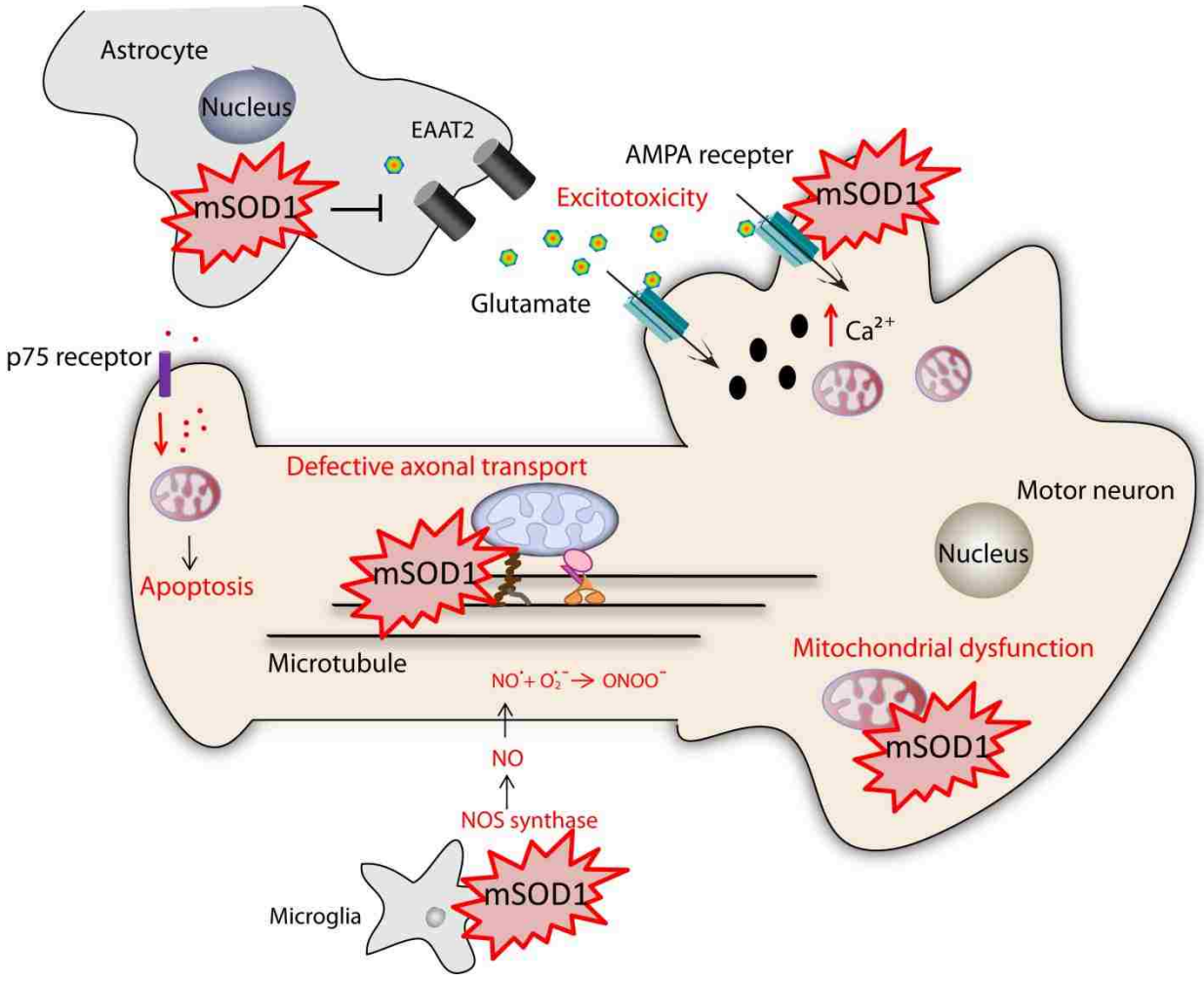

Figure 5 Proposed mechanisms of ALS pathogenesis.

2.1.2.1 Proteasome inhibition

Most SOD1 mutants are misfolded and form aggregates in the cells. Aggregation of mutant SOD1 has been proposed to block and inhibit proteasome-mediated protein degradation. Dorfin, a RING finger type E3 ubiquitin ligase, has been found to specifically bind to mutant SOD1, but not WT SOD1, suggesting that mutant SOD1 is specifically targeted for proteasome (Niwa et al., 2002). In spinal cords of mutant SOD1 mice, decreased proteasome activities were observed (Kabashi et al., 2004). Thus, mutant SOD1 may trigger dysfunction of the proteasome and increases aggregation of misfolded proteins, leading to damage in the cells.

2.1.2.2 Glutamate-induced excitotoxicity

Glutamate-induced excitotoxicity has been observed in ALS patients (Shaw and Ince, 1997). Failure to remove glutamate from synaptic clefts results in repetitive activation of glutamate receptors in motor neurons, which in turn causes Ca^{2+} influx and intracellular Ca^{2+} dyshomeostasis. GluR2 receptors are known to be impermeable to Ca^{2+} and thus regulate Ca^{2+} influx during glutamate stimulation. Unfortunately, motor neurons have a lower expression of GluR2 than other type of cells and have mostly 2-amino-3-(5-methyl-3-oxo-1,2- oxazol-4-yl) propanoic acid (AMPA) receptors. Moreover, mutant SOD1 interacts with AMPA receptors and increases their expression and function, leading to increased sensitivity to glutamate-induced toxicity (Spalloni et al., 2004). On the other hand, accumulation of excessive glutamate is also a

result of reduced expression of the glutamate transporter excitatory amino acid transporter 2 (EAAT2) in astrocytes (Bruijn et al., 1997; Howland et al., 2002; Rothstein et al., 1995). Mutant SOD1 has been shown to be responsible for disrupting the translation of EAAT2 (Bendotti et al., 2001). In addition, caspase 3 activation is responsible for reduced EAAT2 expression and activity (Boston-Howes et al., 2006).

2.1.2.3 Non-cell autonomous mechanism in ALS

In addition to research on motor neurons, more recent studies began to implicate non-neuronal cells and non-cell-autonomous pathways in ALS pathogenesis. For example, transplantation of mSOD1 microglia into mice is not sufficient to cause motor neuron disease. On the other hand, WT microglia in mSOD1 mice had a protective effect, slowing down ALS-like disease progression (Beers et al., 2006). The same study also shows that activated mSOD1 microglia release more neurotoxins, such as nitric oxide (NO), than do WT microglia. Moreover, reduced nicotinamide adenine dinucleotide phosphate (NADPH) oxidase from glial cells is the main source of reactive oxygen species during inflammation. Therefore, mSOD1-induced microglia malfunction leads to reduced neuron survival, because microglia serve as macrophages in the central nervous system (CNS).

Astrocytes are also potentially poisonous neighbors of motor neurons. A study by the Przedborski lab indicated that mSOD1 present only in motor neurons was not sufficient for development of motor neuron degeneration, while mSOD1 expression in astrocytes selectively

killed spinal cord primary motor neurons, but not interneurons, GABAergic neurons, or dorsal root ganglion neurons, by a soluble toxic factor acting through a Bax-dependent mechanism (Nagai et al., 2007). Unfortunately, they failed to identify the soluble toxic factor in the medium conditioned by mSOD1-expressing astrocytes, but researchers are suspect three potential substances: glutamate, NO, and nerve growth factor (NGF).

Astrocytes play an essential role in the rapid recovery of synaptic glutamate, the primary excitatory neurotransmitter (Lobsiger and Cleveland, 2007). Therefore, with mSOD1 expression, glutamate uptake is reduced in astrocytes and leads to glutamate-driven excitotoxicity in motor neurons (Lobsiger and Cleveland, 2007). On the other hand, some studies have shown that reactive astrocytes up-regulate NO production and NGF expression, which induces motor neuron death through p75 receptor signaling (Cassina et al., 2005; Cassina et al., 2002; Pehar et al., 2004). Furthermore, elevated NO levels induce mitochondrial defects and mitochondrial-targeted antioxidants are able to prevent its dysfunction in $SOD1^{G93A}$ astrocytes and restore motor neuron survival (Cassina et al., 2008). These studies not only indicate the importance of mutant astrocytes in the disease progression, but also suggest that mitochondria might be an important target in ALS.

2.1.2.4 Mitochondrial dysfunction in ALS

Experimental evidence indicates that mitochondrial dysfunction is involved in ALS and begins prior to the clinical and pathological onset of the disease. SOD1 has been considered to

be cytosolic protein, while mSOD1 is concentrated inside vacuolated mitochondria (Liu et al., 2004). The aggregates affect protein import, which results in mitochondrial dysfunction (Liu et al., 2004). It has been proposed that mitochondrial dysfunction triggers motor neuron death by at least four pathways.

1) Apoptosis. Mutant SOD1 has been shown to bind mitochondrial Bcl-2 specifically (Pasinelli et al., 2004). Mutant SOD1 binds to Bcl-2 and promotes Bcl-2 conformational change, which leads to toxic BCL2 homology (BH) 3 domain exposure, and finally, apoptosis. Moreover, BAX-induced motor neuron death mediated by astrocytes is strong evidence that mSOD1-mediated toxicity triggers activation of the mitochondrial apoptotic pathway (Nagai et al., 2007).

2) Excitotoxicity. Previous studies indicated that mitochondrial dysfunction reduces Ca^{2+} loading capacity and impairs rapid calcium transient buffering, leading to increased sensitivity to glutamate toxicity from the astrocytes, which results in synaptic malfunction (Damiano et al., 2006).

3) Impaired protein import. Mutant SOD1 has been found to be misfolded and to form aggregates on the cytoplasmic face of the OMM (Liu et al., 2004; Vande Velde et al., 2008). Recently, VDAC1 has been found to be directly bound by mutant SOD1 (Israelson et al., 2010). VDAC1 is an integral membrane protein located in the OMM, which modulates ATP/ADP flux across the OMM. This abnormal interaction results in reduced VDAC1 activity, and thus, reduced ATP generation.

4) Oxidative stress. Mutant SOD1 binds to the IMM and disrupts the redox state of mitochondria (Ferri et al., 2006). This more oxidizing environment impairs ETC, which increases ROS generation (Ferri et al., 2006). Both decreased respiratory activities of Complexes I, II, III, and IV and increased ROS levels have been found in the spinal cords of ALS patients (Murata et al., 2008; Wiedemann et al., 2002). Increased concentration of 3-nitrotyrosine, which is formed by protein nitration through peroxynitrite, was observed in the CSF of human patients, (Tohgi et al., 1999). Peroxidation of Cardiolipin, an anionic IMM component, disrupts its interaction with cytochome *c* and leads to its release into the IMS, which ultimately results in apoptosis (Kirkinezos et al., 2005; Paradies et al., 2009).

In addition, impaired axonal transport has been proposed to participate in ALS pathogenesis (Magrane and Manfredi, 2009). Due to the long processes of motor neurons, fast axonal transport is crucial for maintenance of ATP supply to maintain synaptic function, neurotransmitter release, vesicle recycling, and mitochondrial Ca^{2+} buffering. Slowing of mitochondrial axonal transport has been proposed to be a very early event in the toxicity of ALS-linked SOD1 mutants in motor neurons (Williamson and Cleveland, 1999). Given these findings, mitochondria appear to be central players in ALS pathogenesis.

2.1.3 Mitochondrial dynamics and ALS

As previously discussed, mitochondrial dynamics are essential for maintenance of mitochondrial function, which is required for cellular function and cell survival. Abnormal mitochondrial dynamics have been observed in different models of ALS.

2.1.3.1 Mitochondrial dysmorphology in ALS

Vacuolated mitochondria and their fragmented network have been observed in both ALS patients and mutant $SOD1^{G93A}$ mice (Gurney et al., 1994; Sasaki and Iwata, 2007). A number of studies have indicated that mitochondrial vacuolation occurs at the pre-symptomatic stage and increases with disease progression (Jaarsma et al., 2001; Kong and Xu, 1998). It has been speculated that mutant SOD1 accumulation in the mitochondrial IMS initiates expansion of the IMS and eventually triggers mitochondrial degeneration (Jaarsma et al., 2000; Jaarsma et al., 2001).

Mitochondrial fragmentation is indicative of an imbalance in mitochondrial fission and fusion. Fragmented mitochondria have been reported in transgenic mice and neuronal cell lines. Components of the mitochondrial fission and fusion machinery might be involved in ALS pathogenesis. DRP1, MFN2, and OPA1 are all involved in not only mitochondrial fission and fusion, but as described above, also play important roles in maintenance of mitochondrial function. Most importantly, mutations in MFN2 result in motor defects (Baloh et al., 2007).

Thus, defective mitochondrial fission and fusion balance might be the primary cause of ALS, and mitochondrial dysfunction may be a secondary effect of defective mitochondrial dynamics.

2.1.3.2 Defective mitochondrial axonal transport in ALS

Motor neurons contain long axons, which may be up to 1 meter in length. Such a unique feature requires effective axonal transport to deliver different components synthesized in the soma to the synapses and nerve terminals.

In ALS patients and mice, motor neuron loss begins with distal axonal degeneration (Fischer et al., 2004). Defects in axonal transport of mitochondria and vesicles have been well studied in ALS mice (Warita et al., 1999; Williamson and Cleveland, 1999). Because defective axonal transport is an early sign of the disease, it could be the mechanism of the axonal degeneration characteristic of ALS.

Mutations in the trafficking machinery have been found to be associated with motor neuron degeneration. A point mutation in KIF1B, a member of the Kinesin-3 family, has been identified in CMT-2A patients who suffer from muscle weakness and atrophy (Zhao et al., 2001). This point mutation is conserved in its ATP-binding domain and causes impaired axonal transport of synaptic vesicles. KIF5A mutants have been identified in another motor neuron disease, hereditary spastic paraplegia (Reid et al., 2002). These mutants inhibit anterograde axonal transport, and thus, cause axonal degeneration. In addition, mutations in Dynein affect sensory neurons rather than motor neurons (Chen et al., 2007b). One of the most promising

pieces of evidence is that a mutation in the p150 subunit of Dynactin is involved in FALS cases (Puls et al., 2003). This Dynactin mutant has lower affinity to microtubules and in turn disrupts Dynein/Dynactin function. Although the reason why defective axonal transport affects different types of neurons is unclear, these findings support the notion that defects in axonal transport could be the mechanism underlying ALS.

How might mutant SOD1 interfere with mitochondrial axonal transport in motor neurons? First, mutant SOD1 may interact with motor proteins and impair axonal transport. A number of mutations in motor complexes have been found to cause motor atrophy, including KIF5B and Dynactin mutations (Puls et al., 2003; Zhao et al., 2001). Because mutant SOD1 specifically accumulates on mitochondria, it is not surprising that the abnormal interactions between mutant SOD1 and motor proteins impair axonal transport of mitochondria. To date, the only report about the interaction between mutant SOD1 and motor proteins is of the Dynein complex, which is responsible for retrograde transport (Zhang et al., 2007). Although there was no other interaction detected, it is possible that the abnormal interaction between mutant SOD1 and motor proteins interferes with mitochondrial transport.

Second, mutant SOD1 may reside on or inside mitochondria and cause mitochondrial dysfunction. It has been reported that 1–2% of WT SOD1 is localized to mitochondria, while mutant SOD1 preferentially accumulates in mitochondria of the spinal cord (Liu et al., 2004). A number of proteins in mitochondria have been found to interact with mutant SOD1 specifically, including heat shock proteins (HSPs), Lysyl-tRNA synthetase, and Bcl2 (Kunst et al., 1997; Okado-Matsumoto and Fridovich, 2001; Pasinelli et al., 2004). Recently, Magrane *et al.* found

that mitochondrial-targeted SOD1 is sufficient to cause cell death in NSC-34 cells (Magrane et al., 2009). Moreover, enrichment of SOD1 in mitochondria by copper chaperone for SOD1 (CCS) leads to abnormal mitochondrial dynamics and accelerates disease progression (Son et al., 2007). Thus, it is possible that the abnormal interaction between mutant SOD1 and mitochondrial proteins interferes with normal mitochondrial function and thus impairs transport.

Finally, mutant SOD1 may interfere with regulation of the cytoskeleton and molecular motors through cell signaling pathways. Abnormal activation of p38, c-Jun N-terminal kinases (JNKs), and cyclin-dependent kinase 5 (CDK5) has been observed in the transgenic mouse model of ALS, which could directly result in phosphorylation of neurofilaments and disruption of mitochondrial transport (Ackerley et al., 2004). Moreover, p38 can also phosphorylate the Kinesin-1 light chain, preventing Kinesin-1-mediated mitochondrial transport (De Vos et al., 2000). In addition, activation of JNK results in Kinesin-1 heavy chain phosphorylation and inhibits Kinesin-1 microtubule-binding activity (Morfini et al., 2006).

Collectively, mutant SOD1-mediated defective mitochondrial dynamics could be the primary cause of ALS, although the manner by which mutant SOD1 mediates this impairment is unknown. Here, our lab proposes that imbalance of mitochondrial fission and fusion is implicated in ALS, and restoration of this balance might rescue mitochondrial transport and mutant SOD1-induced neuronal cell death.

2.1.4 Motor neuron and astrocyte co-culture system

Several previous studies suggested defects in mitochondrial dynamics in a model of ALS (De Vos et al., 2007; Magrane et al., 2009; Magrane et al., 2012). The first report identified a decrease in anterograde mitochondrial transport in pure motor neuron cultures isolated from mutant SOD1 rats (De Vos et al., 2007). To visualize mitochondria, the authors used MitoTracker Red, a fluorescent membrane potential sensitive dye. This probe is not incorporated in depolarized mitochondria. Therefore, it predominantly stains mitochondria with high membrane potential. In addition, this fluorescent probe tends to lack specificity, as it does not label only mitochondria, and can be neurotoxic. A second report demonstrated a decrease in both anterograde and retrograde transport, increased mitochondrial fragmentation, and a tendency toward increased cell death in NSC34 cells expressing mutant SOD1 targeted to the mitochondrial IMS (Magrane et al., 2009). However, this study was carried out only in a cell line and not primary motor neurons. The most recent study on defective mitochondrial transport used pure motor neuron cultures as the experimental model (Magrane et al., 2012). Defective mitochondrial axonal transport was well described, but little retrograde transport was observed. While these reports suggest a role for defective mitochondrial dynamics in SOD1-mediated motor neuron dysfunction, further studies are needed to resolve discrepancies in the findings.

To reconcile this apparent controversy and to improve the experimental model, we set out to investigate whether mitochondrial dynamics is impaired in primary motor neurons

expressing mutant SOD1^{G93A}. We chose this SOD1 mutation because it is among the most frequently observed SOD1 mutations in humans and is commonly used in experimental models. To visualize mitochondria, we co-expressed DsRed2-Mito, a red fluorescent protein, which exhibits no toxicity in primary neurons. In addition, we co-cultured motor neurons on top of a spinal cord astrocyte monolayer. Astrocytes play a pivotal role in motor neuron physiology, and both cell-autonomous and non-autonomous pathways have been proposed to account for ALS pathogenesis. Therefore, an astrocyte and motor neuron co-culture system is a good model for ALS study. These key modifications make this experimental system of greater physiological relevance compared to cell lines and pure neuronal cultures, and because we use fluorescent fusion proteins that have no toxicity, our study provides an important step forward in the exploration of mitochondrial dynamics defects in ALS.

2.2 Materials and Methods

In the experiments in this section, three systems have been used:

1. Primary motor neuron cultures: astrocytes co-cultured with isolated motor neurons from E15 rat spinal cords.

2. Spinal cord tissue isolated from pre-symptomatic (2 month) and symptomatic (5 month) mSOD1^{G93A} transgenic mice. The transgenic mice exhibit the first signs of motor neuron disease, hyperflexia, after day 91, and reduced locomotor activity and weight loss after day 115.

3. Human embryonic kidney (HEK) 293 cell line.

2.2.1 Reagents

The pDsRed2-Mito vector was obtained from Clontech. The pcDNA3.1-SOD1^{WT} and -SOD1^{G93A} were obtained from Dr. Alvaro G. Estevez (University of Central Florida, Orlando, FL, USA). The pcDNA3-DRP1^{K38A} was obtained from Dr. Alexander M. van der Bliek (David Geffen School of Medicine at UCLA, Los Angeles, CA, USA). The pβ-actin-Map2c/EGFP was obtained from Dr. Doll (Novartis Institute for Biomedical Research, Basel, Switzerland). All plasmids were purified using the Endotoxin-free Marligen Maxiprep Kit (Diagnostic technology, Belrose, Australia). 4-(2-hydroxyethyl)-1-piperazineethanesulfonic acid (HEPES) was purchased from Omega Scientific (Tarzana, CA, USA). Poly-L-lysine, bovine serum albumin (BSA), DNase I, Opti-prep, phenol-red, Penicillin-streptomycin (Pen/Strep), formaldehyde, glutamine, pyruvate, F-12 HAM, sucrose and rabbit antibodies to MFN2 (M6444) were all obtained from Sigma-Aldrich (St.

Louis, MO, USA). Custom-made phenol-free Dulbecco's Modified Eagle Medium (DMEM)/high glucose, phosphate buffered saline (PBS), and bovine calf serum (BCS) were obtained from Thermo Scientific (Rockford, IL, USA). Trypsin (2.5%, 10×), L-15, glutamax, and Earle's Balanced Salt Solution (EBSS) were purchased from Gibco (Carlsbad, CA, USA). Lipofectamine 2000, Hoechst 33342, and neurobasal medium were purchased from Invitrogen (Carlsbad, CA, USA). Protease inhibitor cocktails were purchased from Roche (Indianapolis, IN, USA). D-mannitol was obtained from J.T. Baker (Austin, TX, USA). Ethylenediaminetetraacetic acid (EDTA) and mouse antibodies to actin were purchased from Calbiochem (Darmstadt, Germany). Alexa 488-conjugated goat anti-mouse secondary antibodies were obtained from Molecular Probes (Grand Island, NY, USA). The Amaxa Nucleofector kit for rat neurons was purchased from Lonza (Basel, Switzerland). Mouse anti-rat p75 antibody MC-192 and mouse monoclonal anti neurofilament H non-phosphorylated (SMI-32) were obtained from Abcam (Cambridge, MA, USA). Rat anti-mouse IgG1 microbeads and MACS separation columns were obtained from Miltenyi Biotec (Auburn, CA, USA). Mouse antibodies to DRP1 (clone8/DLP1) and OPA1 were obtained from BD Biosciences (San Jose, CA, USA), MFN2 (XX-1) and MFN2 (50331) from Santa Cruz Biotechnology (Santa Cruz, CA, USA), and heat shock protein 60 (HSP60) was obtained from Stressgen (Farmingdale, NY, USA). Rabbit antibodies to pDRP1 (S616) were obtained from Cell Signaling (Danvers, MA, USA).

2.2.2 Mice and rats

SOD1^{G93A} transgenic mice (B6.Cg-Tg (SOD1-G93A) 1Gur/J) were purchased from Jackson Laboratory. Here, mSOD1^{G93A} mice at pre-symptomatic (2 month) and symptomatic stages (5 month) were used. Heterozygous mSOD1^{G93A} mice develop hind limb paralysis at 4 months with rapid progression, and thereafter, resemble human ALS neuropathology.

Timed-pregnant Sprague Dawley rats were purchased from Charles River. All experiments were approved by the Institutional Animal Care and Use Committee of University of Central Florida College of Medicine.

2.2.3 Isolation of astrocytes

Astrocytes were prepared from E18 rat embryos. Spinal cords were isolated and then incubated for 40 min at 37°C in 0.025% Trypsin in EBSS with frequent agitation. Tissues were transferred into a new tube with 1 ml L15 supplemented with 0.4% BSA and 0.1mg/ml DNase I and triturated about 10 times using a P1000 pipette. The fragments were allowed to settle for 2 min and trituration was repeated until cells were well dissociated. Cells were then spun down through 2 ml 4% BSA cushion at 470 rpm and room temperature for 5 min using a centrifuge with swing-out rotor (Eppendorf 5810R). The cell pellet was resuspended in medium supplemented with 10% FBS, Pen/Strep, and 15 mM HEPES and cultured at 37°C, 5% CO_2 for one week. After reaching confluence, the astrocyte cultures were placed on a shaking platform and 300 rpm shaking was applied to eliminate microglia for 24 h at 37°C. Supernatant with

floating cells was removed and shaking was repeated for another 24 h. After removing the supernatant, the last shaking was applied with 10 μM cytosine arabinoside in the medium for 48 h. The remaining cells comprised of astrocytes were trypsinized and plated onto Lab-Tek II (#1.5 German coverglass) 8-chamber slides (Thermo Fisher Scientific, Pittsburgh, PA, USA) at a density of 2×10^6 cells/cm^2 in phenol-free DMEM medium supplemented with 10% BCS, 2 mM glutamine, 25 mM HEPES, 10% F-12 HAM, and 0.25% Pen/Strep. Motor neurons were seeded on top after 5 days and grown in culture.

2.2.4 Motor neuron isolation and transfection

The following motor neuron isolation protocol was established by Dr. Henderson and Dr. Estevez with some modifications.

Briefly, Motor neurons were prepared from one litter of E15 rat embryos. Spinal cords were isolated, separated into two 15 ml polystyrene tubes, and then incubated for 10 min at 37°C in 1 ml 0.025% Trypsin (2.5%, 10×) in EBSS under frequent agitation. The fragments of the spinal cords were transferred into a new 15 ml tube with 1 ml L-15 supplemented with 0.4% BSA and 0.1mg/ml DNase I. The tissues were then dissociated using a p1000 Gilson blue tip by triturating 8 times and allowed to settle for 2 min at room temperature. The supernatant was then centrifuged at 470 g at room temperature for 5 min on top of a 2 ml 4% BSA cushion in L-15. After removing the supernatant, cell pellet was resuspended in Amaxa Nucleofector buffer (for rat neurons) and 4 μg DNA was added, followed by electroporation using the

electroporator device (Amaxa) and G13 program (Basel, Switzerland). The transfected cells were then diluted in 4 ml L-15 and layered on top of 2 ml solution containing 12% OptiPrep, 88% L-15, and 0.4% Phenol red followed by gradient centrifugation for 15 min at 830 g, room temperature. Motor neurons, located at the interface between the clear and red phases, were collected into 1 ml using a P1000 pipette, and pelleted by centrifugation at 470 g at room temperature for 5 min through a 2 ml 4% BSA cushion. After removing the supernatant, cell pellets were resuspended in 98 μl PBS with 0.5% BSA. Two microliter mouse monoclonal anti-rat p75 MC-192 antibodies were added to the motor neurons and incubated for 10 min at 4 ^{o}C. Cells were washed with 10 ml 0.5% BSA in PBS followed by centrifugation for 15 min at 470 g, room temperature through a 2 ml 4% BSA cushion. Pellets were resuspended in 80 μl 0.5% BSA in PBS and 20 μl rat anti-mouse IgG1 microbeads were added to the motor neuron-p75 antibody mix. After 15 min incubation at 4 ^{o}C, cells were washed with 10 ml 0.5% BSA in PBS followed by centrifugation for 15 min at 470 g, room temperature through a 2 ml 4% BSA cushion. Cell pellets were resuspended in 500 ml 0.5% BSA in PBS and applied onto MACS separation columns, which were already placed in the mini MACS magnet and pre-washed with 500 μl 0.5% BSA in PBS. The columns were rinsed 3 times with 500 μl 0.5% BSA in PBS and then removed from the magnet. One ml 0.5% BSA in PBS was applied onto the column and the positive fraction was collected as the purified motor neuron fraction. The purified motor neurons were seeded on top of an astrocyte monolayer in 50% conditioned medium from astrocyte culture and 50% fresh neuronal medium composed of DMEM medium supplemented

with 10% BCS, 2 mM glutamine, 25 mM HEPES, 10% F-12 HAM, and 0.25% Pen/Strep. Analysis was performed at 2 DIV.

2.2.5 Cortical neuron isolation and transfection

Pure cortical neuronal cultures were prepared from embryonic day E-18 rat embryos (Barsoum et al., 2006). Cells were placed on poly-L-lysine (1mg/ml) coated coverslips at 40,000 cells per well in 24-well plates. Transfection was performed on 5 DIV using Lipofectamine 2000.

2.2.6 Live-cell time-lapse imaging and quantification

Time-lapse imaging was performed using an Axiovert Zeiss 100M inverted fluorescence microscope equipped with a Plan-Apochromat 63×1.4 NA oil objective, a DG-4/Lambda 10-2 combo Xe-arc illumination unit (Sutter), and a Sensicam QE cooled CCD camera (PCO AG, Germany) and controlled by MetaMorph 7.5 software (Molecular Devices). Motor neurons were grown on Lab-Tek II 8-chamber slides (#1.5 German coverglass) in DMEM medium supplemented with 10% BCS, 2 mM glutamine, 25 mM HEPES, 10% F-12 HAM, and 0.25% Pen/Strep without phenol red. Time-lapse images were acquired in a controlled environment using Axiovert Incubator XL 100/135 (37°C, humidified 5% CO_2). To visualize DsRed2-Mito, the excitation filter was S555/28× (Chroma) and the emission filter was S617/73m (Chroma). To visualize EGFP, the excitation filter was S490/20× (Chroma) and the emission filter was S528/38m (Chroma). 3D images were acquired with the Multi-Dimensional Acquisition module

in MetaMorph 7.5. For the mitochondrial movement experiments, one neurite (~ 100 μm in length) was selected for 10 neurons per group at 2 DIV (Song et al., 2011). The mitochondrial movement was recorded for 5 min at 5 second intervals (5 planes, 1 μm step size). The kymographs generated were of 25 μm in width by average projections of all planes without background subtraction using MetaMorph 7.5. The measurements of mitochondrial velocity and moving distance were exported to Microsoft Excel for further analysis.

2.2.7 Imaging of fixed samples

Two days after transfection, the cortical neurons were fixed with 3.7% formaldehyde and 5% sucrose in PBS for 15 min at 37 °C. Three-dimensional images were acquired (2×2 binning, 0.2 μm step size, 20-25 z-planes) with the Multi-Dimensional Acquisition module in Metamorph 7.5. Images were surface rendered using Metamorph 4D-viewer and exported as TIFF files. Mitochondrial numbers and length were measured as previously described (Song et al., 2008).

2.2.8 Immunocytochemistry of motor neurons and cell death

Two days after transfection, neuronal cultures were fixed with 3.7% formaldehyde and 5% sucrose in PBS for 15 min at 37 °C. After fixation, the cultures were permeabilized with 0.1% Triton X-100 in PBS, pH 7.4, for 10 min at room temperature. Unspecific binding was blocked with 3% BSA, 3% FBS in PBS, pH 7.4, for 1 h at room temperature. Mouse monoclonal anti- SMI-

32 antibodies (Abcam) were used for motor neuron staining at 1:5000 dilution in blocking solution and incubated overnight at 4°C. After washing three times with PBS, the cultures were incubated with Alexa 488-conjugated goat anti-mouse secondary antibodies (Molecular Probes) at 1:200 dilution in blocking solution (1 h, room temperature). After washing three times with PBS, nuclei were stained using Hoechst 33342 (1:10,000 in PBS) at room temperature for 10 min.

2.2.9 Cell death and mitochondrial fragmentation counts

Two days after transfection, the cortical neurons were fixed and nuclei were stained using Hoechst 33342 (1:10,000 in PBS) at room temperature for 10 min. Neuronal cell death was scored by microscopy. Neurons with reduced soma size, retracted processes, fragmented mitochondria, and condensed nuclei were scored as dead.

Cell death scoring was performed on triplicate coverslips from three independent experiments (Barsoum et al., 2006; Song et al., 2011).

2.2.10 Cell lysate and western blot

HEK293T cells were grown in DMEM supplemented with 10% FBS, Pen/Strep, and 1 mM pyruvate. Two days after seeding, cells were transfected with different plasmids using Turbofect according to manufacturer's instructions. 36 or 48 hours later, cells were harvested using lysis buffer (50 mM Tris, 150 mM NaCl, 1 mM $MgCl_2$, 5 mM EDTA, 1% NP40, 1 mM NaF, 1

mM Na_3VO_4, 10 mM NAM with protease inhibitor), and centrifuged at 22,000 g, 4°C, for 15 min, followed by BCA test (Piece) to determine protein concentration. Twenty micrograms of protein were used for western blot using 4–12% Bis-Tris SDS PAGE (Invitrogen). After transferring to ECL nitrocellular membrane (GE healthcare), overnight blocking was applied using Odyssey blocking buffer (Li-Cor Biosciences), followed by incubation with DRP1 (BD Biosciences), Actin (Calbiochem), GFP (Abcam), MFN2 (Sigma), OPA1 (BD Biosciences), and phospho-DRP1 Ser616 (Cell Signaling) antibodies. Protein signals were detected using the Li-Cor infrared imaging system. Data were further quantified by Image J.

2.2.11 Protein extractions in mice

Spinal cords were isolated and homogenized in the medium containing 225 mM mannitol, 75 mM sucrose, 1 mM EGTA, and 10 mM HEPES, pH 7.4 in a dounce-type homogenizer. Homogenates were centrifuged at 12,000 g for 10 min and supernatants were kept as cellular fractions. Pellet were re-suspended in T-PER buffer (Thermo Scientific) with protease inhibitors (Roche) and centrifuged at 22,000 g, 4°C, for 15 min. Supernatants were kept as mitochondrial fractions and BCA tests (Piece) were performed to determine protein concentration. Twenty micrograms of protein were used for western blot in each sample.

2.2.12 Statistics

Data from populations or velocity of mitochondria are represented as means ± S.E.M. Student's *t*-test was used to compare groups. Statistical analyses were performed using Microsoft Excel.

2.3 Results

2.3.1 Motor neurons in the co-culture system

To investigate the effects of mutant SOD1^{G93A} on mitochondrial morphology, we first isolated rat spinal cord motor neurons using the new motor neuron and astrocyte co-culture system (described in Methods). In addition, motor neurons were transfected with DsRed2-Mito by electroporation to visualize mitochondrial morphology. Mitochondria exhibited elongated morphology and neurites of 7 DIV motor neurons could grow up to a length of several hundred microns, indicating that the motor neuron was in good condition and well differentiated (Figure 6).

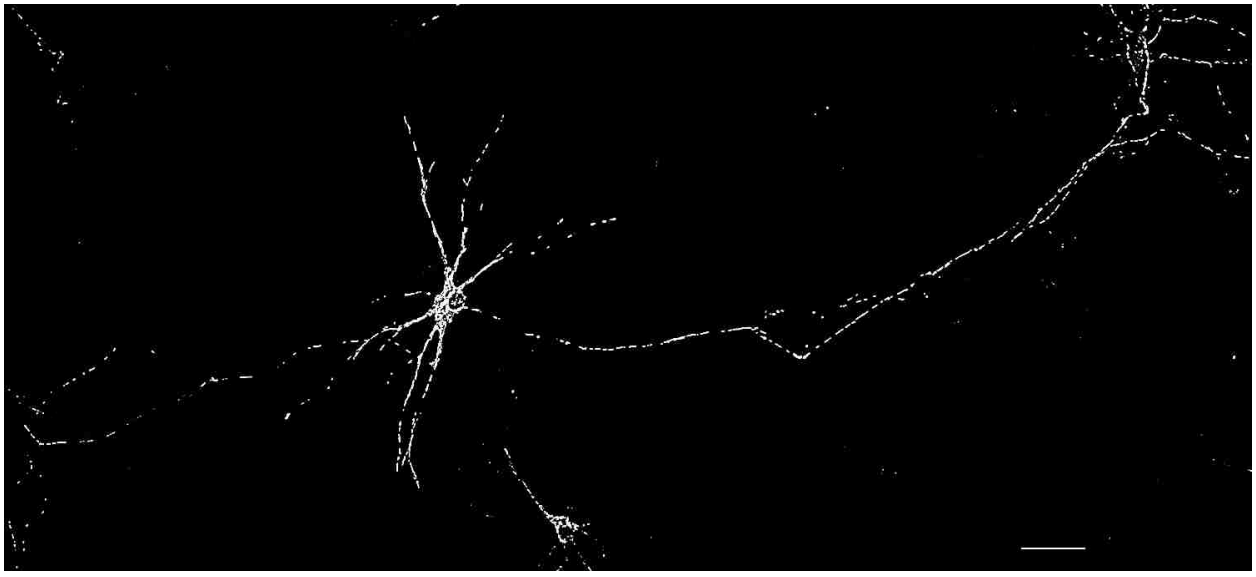

Figure 6 Motor neuron and astrocyte co-culture.

A representative fluorescence wide-field microscopic image of 7 DIV rat motor neurons co-cultured with astrocytes. The motor neurons were transfected with DsRed2-Mito. Scale bar: 100 μm.

2.3.2 Mitochondrial fragmentation in SOD1^{G93A} motor neurons

Abnormal mitochondrial dynamics have been previously reported in “pure” motor neurons, “pure” cortical neurons, and motor neuron-like NSC-34 cells (De Vos et al., 2007; Magrane et al., 2009; Magrane et al., 2012). However, the results are partially controversial, which may be due to different experimental models.

To investigate if mitochondrial morphology is altered by SOD1^{G93A} in our new motor neuron-astrocyte co-culture system, DsRed2-Mito and SOD1^{WT} or SOD1^{G93A} were transfected by electroporation in motor neurons. Mitochondria of SOD1^{WT} motor neurons exhibited normal elongated and tubular morphology, while mutant SOD1^{G93A} motor neurons contained smaller and more rounded mitochondria. The reduced size may result from either increased mitochondrial fission or an inhibition of mitochondrial fusion (Figure 7A). Further quantitative analysis revealed that the mean length of mitochondria was decreased in SOD1^{G93A} motor neurons (Figure 7B). Excessive fission led to increased mitochondrial number in the neurites of SOD1^{G93A} motor neurons compared to SOD1^{WT} neurons (Figure 7C). To further quantify the reduced mitochondrial length, we scored individual motor neurons. The percentage of neurons exhibiting short, round mitochondria was significantly greater in SOD1^{G93A} motor neurons compared to SOD1^{WT} neurons (Figure 7D). In addition, the change in mitochondrial morphology was associated with elevated motor neuron cell death (Figure 7E). In summary, these results indicate that mutant SOD1^{G93A} triggers an increase in round mitochondria in spinal cord motor neurons, suggesting that mitochondrial fragmentation may occur.

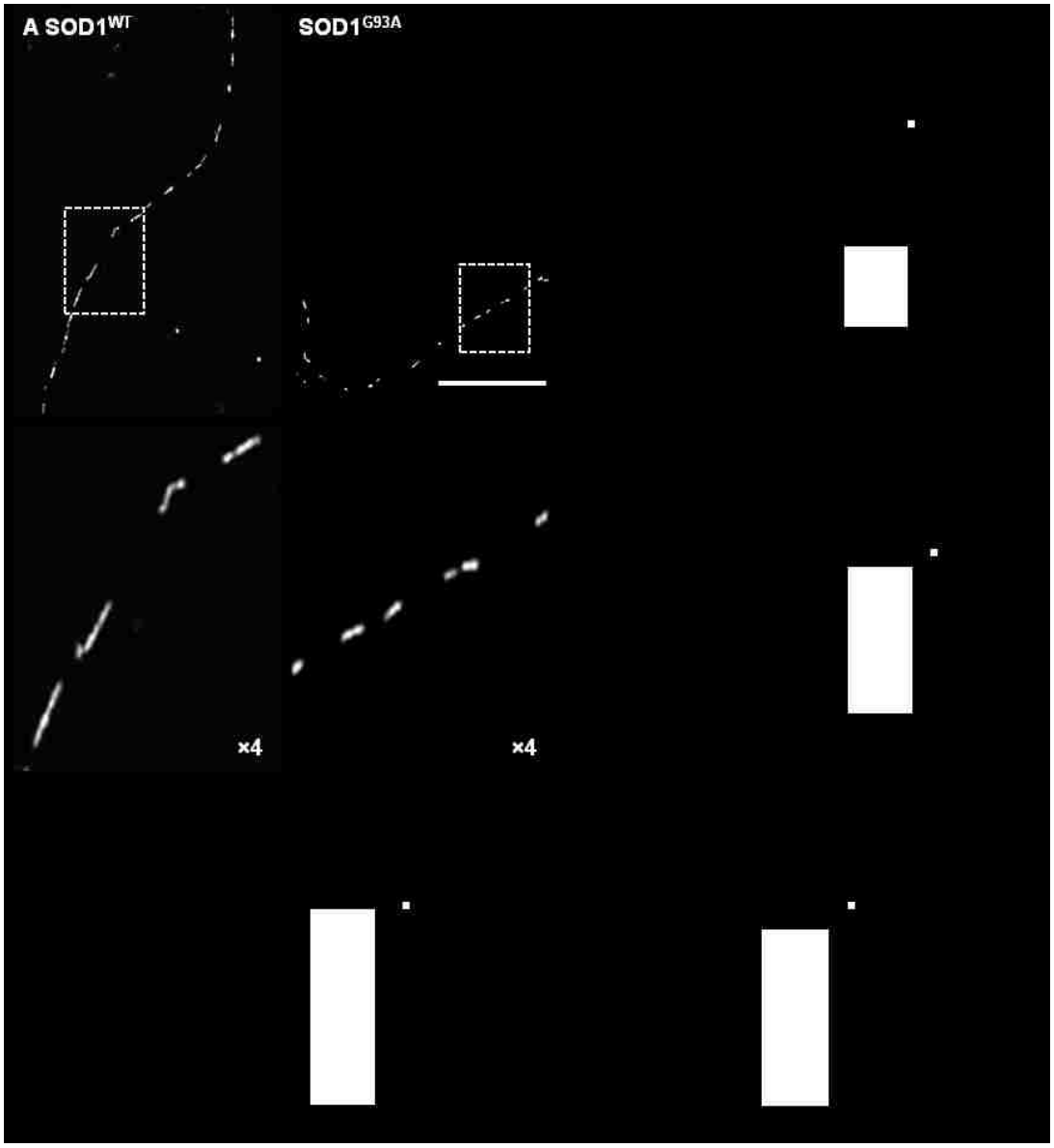

Figure 7 Mitochondrial fragmentation occurs in mutant $SOD1^{G93A}$ motor neurons.

A) Fluorescence micrographs (top panels) and close up views (bottom panels) of mitochondria in 2 DIV motor neurons expressing DsRed2-Mito and either $SOD1^{WT}$ or $SOD1^{G93A}$ co-cultured with astrocytes. Scale bar: 50 μm. B) Mean length of mitochondria in motor neurons expressing DsRed2-Mito and either $SOD1^{WT}$ or $SOD1^{G93A}$ (n = 10). C) Number of mitochondria in 100 μm neurites of motor neurons expressing DsRed2-Mito and either $SOD1^{WT}$ or $SOD1^{G93A}$ (n = 10). D) Mitochondrial fragmentation of motor neurons expressing DsRed2-Mito and either $SOD1^{WT}$ or $SOD1^{G93A}$ in mixed cultures. E) Cell death of 2 DIV motor neurons expressing DsRed2-Mito and either $SOD1^{WT}$ or $SOD1^{G93A}$. P value: two-tail paired Student's t-test.

2.3.3 Abnormal mitochondrial axonal transport in SOD1^{G93A} motor neurons

Mitochondrial morphology and transport are tightly linked. To investigate how changes in SOD1^{G93A}-induced mitochondrial morphology affect mitochondrial axonal transport in our motor neurons and astrocyte co-culture system, fast acquisition fluorescence time-lapse imaging was used to measure mitochondrial directional (anterograde and retrograde) movement and mean velocity over a period of 5 minutes. To better present the results, kymographs were generated from the original time-lapse images to illustrate mitochondrial mobility and directional movement (Figure 8A). Kymographs are 2D representations of 3D movies, and the horizontal lines indicate either anterograde or retrograde movement of mitochondria, while the vertical lines represent stationary mitochondria. A representative kymograph of SOD1^{WT} motor neurons contains both vertical and horizontal lines, indicating that mitochondria are mobile and exhibit substantial movement in both anterograde and retrograde directions (Figure 8A, top panel). By contrast, a representative kymograph of mutant SOD1^{G93A} motor neurons contains mostly vertical lines, indicating very little mitochondrial movement and axonal transport (Figure 8A, bottom panel). Quantitative analysis demonstrated that both anterograde and retrograde movement of mitochondria were decreased in SOD1^{G93A} neurons (Figure 8B). In addition, the velocity of mitochondrial transport and mitochondrial mobility were also decreased in SOD1^{G93A} motor neurons (Figure 8C and D). These results demonstrate that SOD1^{G93A} triggers defects in bi-directional axonal transport of mitochondria in motor

neurons co-cultured with astrocytes. In addition, it suggests that changes in mitochondrial morphology may cause the observed decrease in axonal transport.

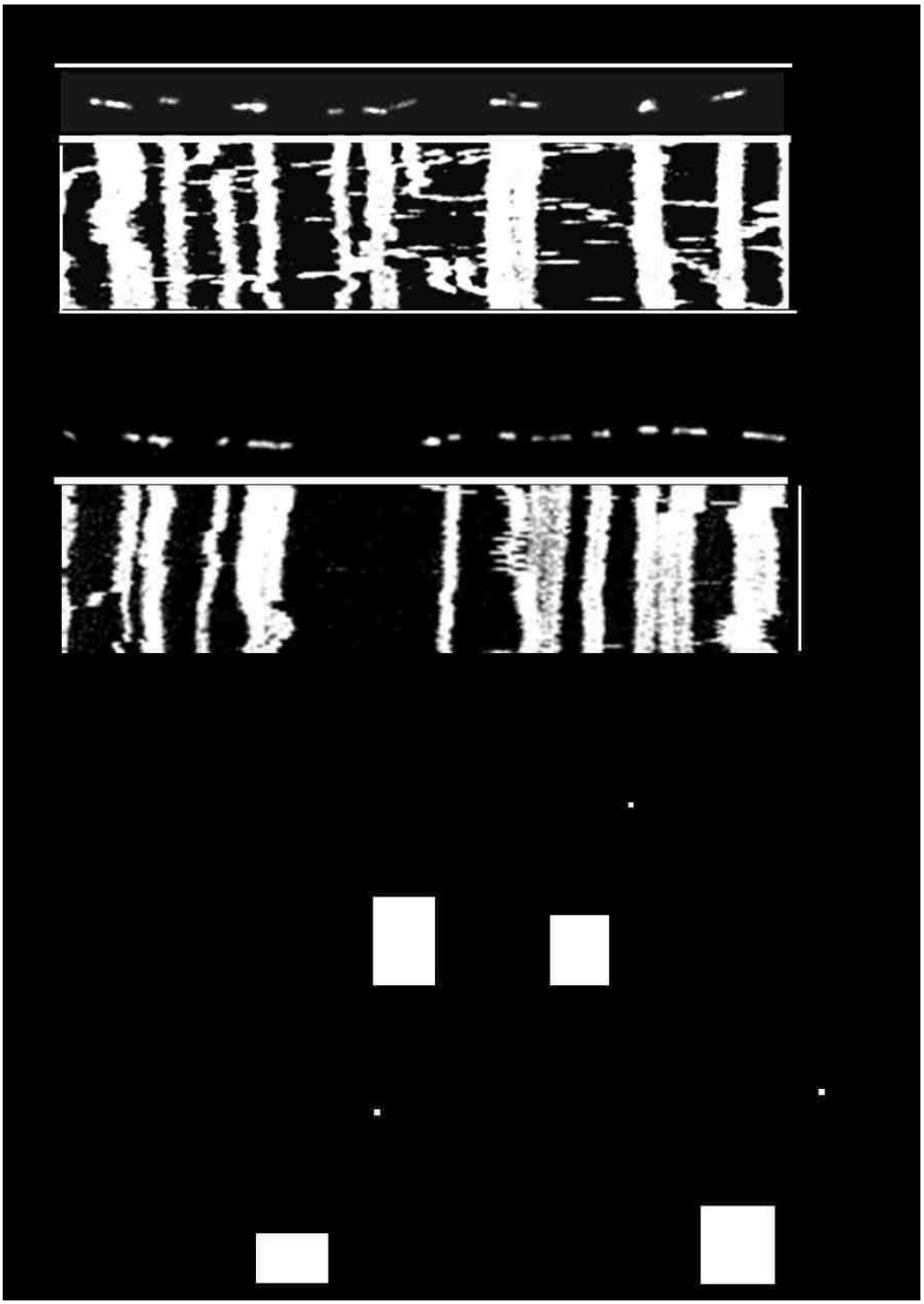

Figure 8 Mutant SOD1^{G93A} triggers a decrease in axonal anterograde and retrograde transport of mitochondria in 2 DIV motor neurons.

A) Kymographs of motor neurons expressing DsRed2-Mito and either SOD1^{WT} or SOD1^{G93A}. B) Mitochondrial directional movement in motor neurons expressing DsRed2-Mito and either SOD1^{WT} or SOD1^{G93A}. C) Mean velocity of mitochondria in the axons of motor neurons expressing DsRed2-Mito and either SOD1^{WT} or SOD1^{G93A}. D) Mitochondrial mobility in motor neurons expressing DsRed2-Mito and either SOD1^{WT} or SOD1^{G93A}. P value: two-tail paired Student's t-test, n = 10.

2.3.4 Defective neuronal development in SOD1^{G93A} motor neurons

To investigate whether the defects in mitochondrial transport impact neuronal differentiation, we transfected spinal cord motor neurons with SOD1^{WT} or SOD1^{G93A} plus DsRed2-Mito and MAP2-GFP to allow visualization of both mitochondria and neurites. In SOD1^{WT} motor neurons, mitochondria were elongated and evenly distributed along neurites (Figure 9A, left). By contrast, more fragmented mitochondria in mutant SOD1^{G93A} motor neurons accumulated in growth cones (Figure 9A, right). Furthermore, the average neurite length of 1655 μm in SOD1^{WT} motor neurons (n = 10) was significantly decreased to 1057 μm in mutant SOD1^{G93A} motor neurons (n = 10) (Figure 9B). To further characterize the apparent developmental defect caused by SOD1^{G93A}, we quantified the number of neurite branches. The neuronal extensions were grouped into primary, secondary, and tertiary arbors as illustrated (Figure 9C). Quantification revealed that the number of secondary and tertiary arbors was significantly decreased in SOD1^{G93A} motor neurons, suggesting a reduced complexity in neurite

branching (Figure 9D). Thus, SOD1^{G93A}-induced mitochondrial fragmentation and defects in axonal trafficking were accompanied by altered neuronal morphology and differentiation.

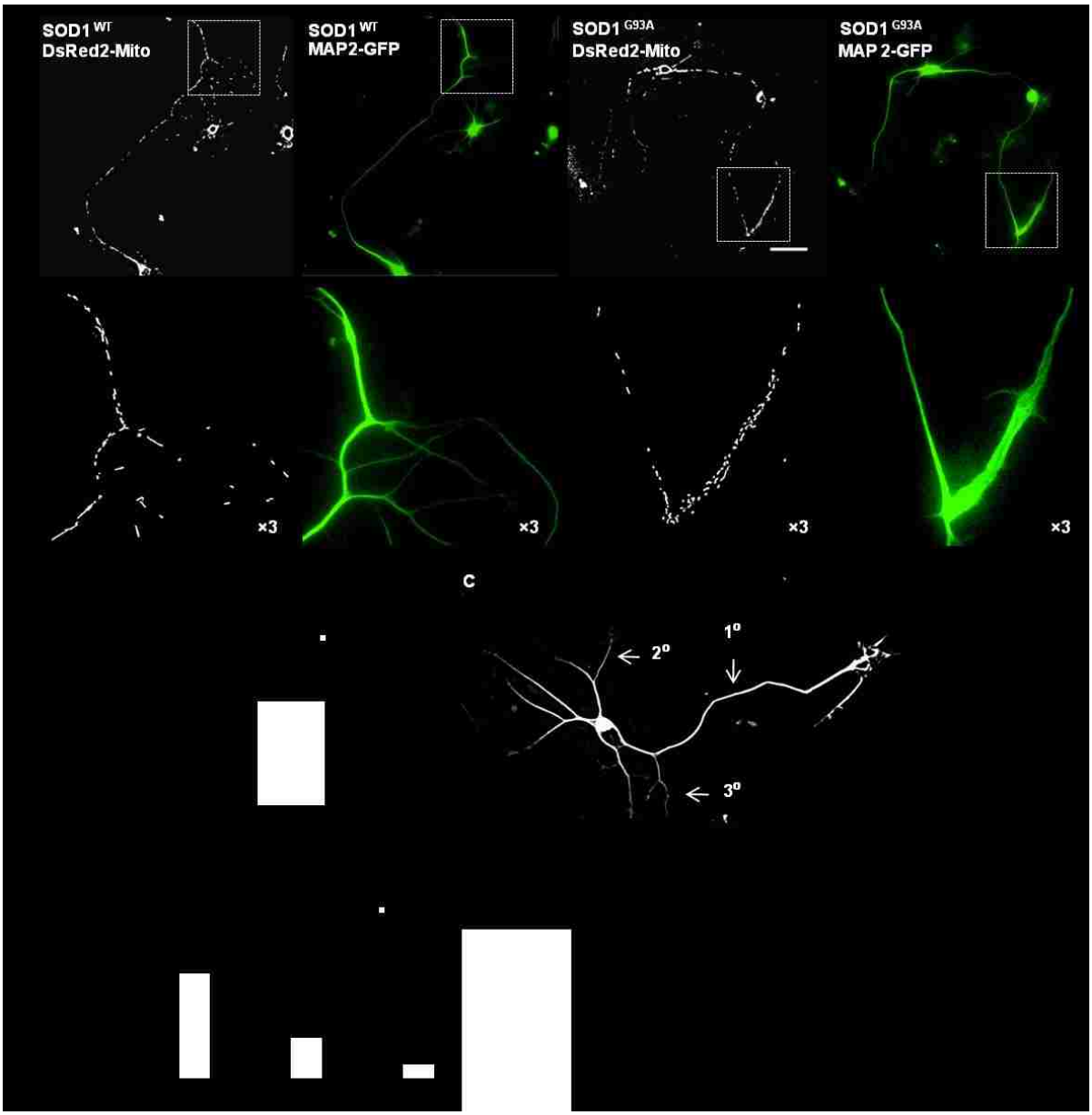

Figure 9 Mutant SOD1^{G93A} triggers defective neurite branching and abnormal mitochondrial accumulation in growth cones.

A) Representative 3D fluorescence wide-field microscopic images, and close up views below, of motor neurons expressing DsRed2-Mito, MAP2-EGFP, and either SOD1^{WT} or SOD1^{G93A}. Scale bar: 50 μm. B) Total neurite length of motor neurons expressing DsRed2-Mito, MAP2-GFP, and either SOD1^{WT} or SOD1^{G93A}. C) Scheme for neurite branching quantification. D) Number of branches of motor neurons expressing DsRed2-Mito, MAP2-GFP, and either SOD1^{WT} or SOD1^{G93A}. P value: two-tailed paired Student's t-test, n = 10.

2.3.5 DRP1^{K38A} restores mitochondrial morphology in SOD1^{G93A} neurons

Altered mitochondrial morphology has been demonstrated in both ALS patients and cell culture models (Kong and Xu, 1998; Magrane and Manfredi, 2009; Sasaki and Iwata, 2007). Therefore, impaired mitochondrial dynamics may play a causal role in ALS pathogenesis. Dominant-negative DRP1^{K38A} harbors an inactive GTPase domain and thus inhibits mitochondrial fission activity (Smirnova et al., 2001; Smirnova et al., 1998; van der Bliek et al., 1993). It has been reported that DRP1^{K38A} restores mitochondrial fission and fusion balance and provides protection against cell death in neurodegenerative models (Song et al., 2011). However, the effect of DRP1^{K38A} on mitochondrial dynamics in ALS has yet to be examined. To test whether blocking excessive mitochondrial fission by Drp1^{K38A} could rescue SOD1^{G93A}-induced mitochondrial fragmentation and neuronal cell death, we co-transfected primary cortical neurons with SOD1^{WT} or SOD1^{G93A}, DsRed2-Mito, and DRP1^{K38A}. Co-expression of SOD1^{G93A} and DRP1^{K38A} produced elongated mitochondria similar to those in neurons

expressing $SOD1^{WT}$ (Figure 10A). To validate these observations, we scored the neurons and found that $SOD1^{G93A}$ neurons had 61% mitochondrial fragmentation, which was decreased to 48% by $DRP1^{K38A}$ co-expression (Figure 10B). The mitochondrial fragmentation scheme was also correlated with neuronal cell death (Figure 10C). In summary, these results indicate that $DRP1^{K38A}$ is able to rescue mitochondrial fragmentation and neuronal cell death caused by $SOD1^{G93A}$. Moreover, they suggest that imbalanced mitochondrial fission and fusion might be the mechanism implicated in ALS, providing the basis for future studies investigating whether decreasing DRP1 activity protects against motor neuron death *in vivo* in animal models of ALS.

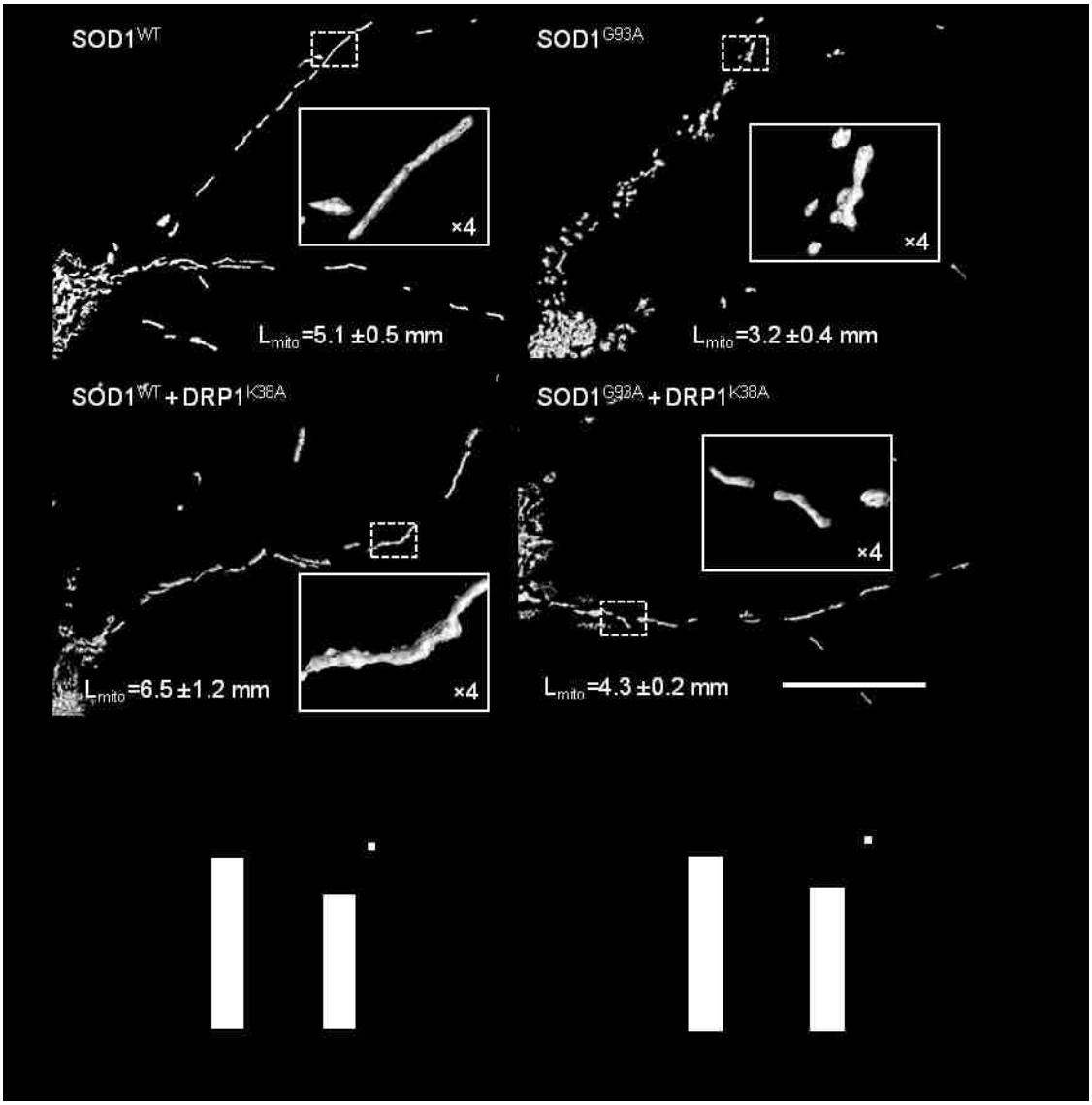

Figure 10 Inhibiting mitochondrial fission with the GTPase-defective DRP1^{K38A} mutant rescues mitochondrial fragmentation and neuronal cell death caused by mutant SOD1^{G93A}.

A) Fluorescence micrographs and close up views of cortical neurons expressing DsRed2-Mito and either SOD1^{WT} or SOD1^{G93A} alone or in combination with DRP1^{K38A} introduced at day 2 post transfection. Scale bar, 50 μm. Mitochondrial length (L_{mito}) is indicated as mean ± S.E.M. (n = 10). B) Mitochondrial fragmentation of cortical neurons expressing DsRed2-Mito and either SOD1^{WT} or SOD1^{G93A} alone or in combination with DRP1^{K38A}. C) Cell death of cortical neurons expressing DsRed2-Mito and either SOD1^{WT} or SOD1^{G93A} alone or in combination with DRP1^{K38A}. *P* value: two-tailed paired Student's *t*-test.

2.3.6 DRP1^{K38A} rescues mitochondrial trafficking defects in SOD1^{G93A} neurons

To determine whether restoration of mitochondrial fission and fusion balance can also rescue mitochondrial axonal transport, we co-expressed SOD1^{WT} or SOD1^{G93A} and DsRed2-Mito either alone or in combination with dominant-negative DRP1^{K38A} in cortical neurons. As the kymographs show (Figure 11A), there were more horizontal lines in neurons expressing both SOD1^{G93A} and DRP1^{K38A} than SOD1^{G93A} alone, which indicates that DRP1^{K38A} expression increased mitochondrial bi-directional movement. Quantitative analysis indicates that both mitochondrial anterograde and retrograde movement were rescued by Drp1^{K38A} co-expression (Figure 11B). Moreover, both mitochondrial velocity (Figure 11C) and motility (Figure 11D) were significantly increased by about three-fold in neurons co-expressing SOD1^{G93A} and DRP1^{K38A}. Collectively, our data show that mitochondrial transport is rescued by dominant-negative DRP1^{K38A}.

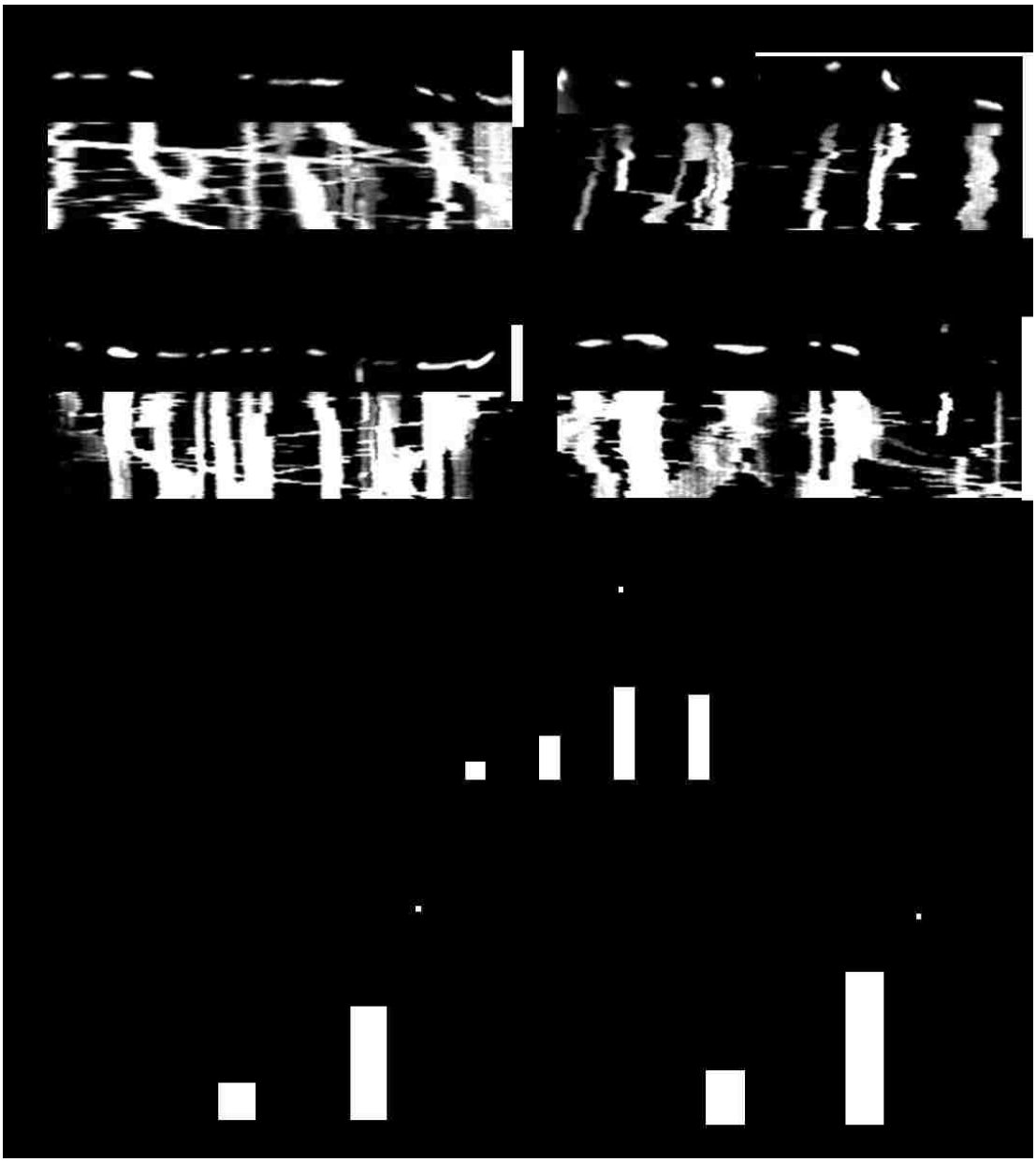

Figure 11 DRP1^{K38A} rescues neurons from mitochondrial trafficking defects.

A) Kymographs of mitochondrial transport in cortical neurons expressing DsRed2-Mito and either SOD1^{WT} or SOD1^{G93A} alone or in combination with DRP1^{K38A}. B) Mitochondrial directional movement in cortical neurons expressing DsRed2-Mito and either SOD1^{WT} or SOD1^{G93A} alone or in combination with DRP1^{K38A}. C) Mitochondrial velocity in cortical neurons expressing DsRed2-Mito and either SOD1^{WT} or SOD1^{G93A} alone or in combination with DRP1^{K38A}. D) Mitochondrial mobility in cortical neurons expressing DsRed2-Mito and either SOD1^{WT} or SOD1^{G93A} alone or in combination with DRP1^{K38A}. *P* value: two-tailed paired Student's *t*-test, n = 10.

2.3.7 MFN2 cleavage in SOD1^{G93A} transgenic mice

Previous results indicate that impairment of the mitochondrial fission and fusion machinery might interfere with axonal transport and jeopardize cell survival. Mitochondrial fragmentation results from either excessive fission or inadequate fusion. By chance, abnormal MFN2 cleavage has been observed in SOD1^{G93A} transgenic mice.

As an OMM protein, full-length MFN2 is slightly decreased in the mitochondrial fraction of SOD1^{G93A} transgenic mice (Figure 12). Interestingly, there is a significant increase in the signal in the cytoplasmic fraction of transgenic mice. Using different MFN2 antibodies (Santa Cruz 50331 and Sigma M6664), which recognize different domains in MFN2, two different fragments (60 KD and 45 KD) were observed. Coincidently, both of the fragments were located in the cytoplasm with a stronger signal in SOD1^{G93A} transgenic mice, suggesting the cleaved fragments were released from the mitochondria.

Although it has not been proven that these fragments were part of MFN2, these findings suggest that MFN2 was cleaved by abnormal protease activation in SOD1^{G93A} transgenic mice. Such cleavage may directly impair mitochondrial fission and fusion balance, and thus, mitochondrial dysfunction in ALS mice.

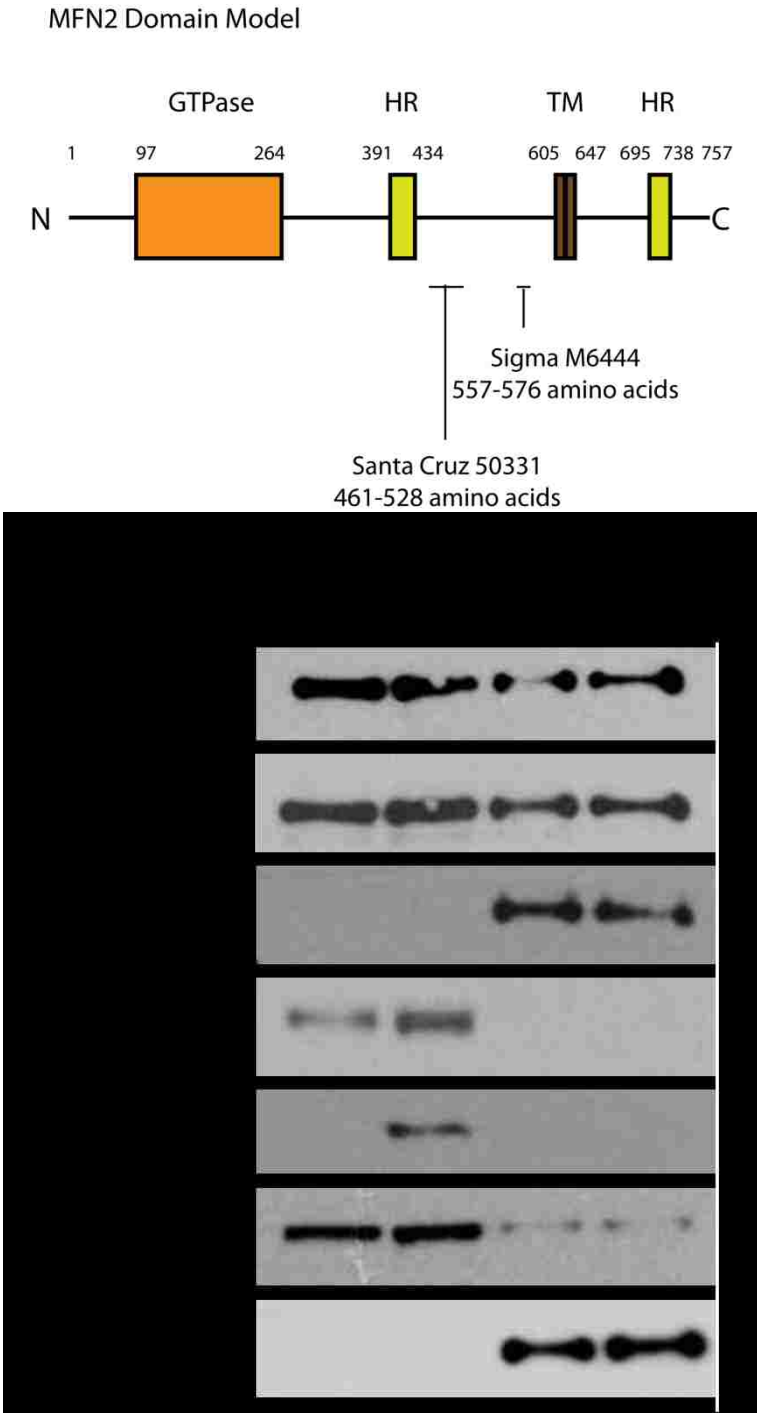

Figure 12 MFN2 cleavage in ALS mice.

Western Blot of MFN2, ACTIN, and HSP60 in 5-month-old control or SOD1^{G93A} mice spinal cords with MFN2 antibody recognition domains.

2.3.8 Disruption of mitochondrial dynamics in response to SNOC treatment

Elevated NO levels have been implicated in ALS pathogenesis. NO reacts with superoxide and forms peroxynitrite, which causes oxidative stress (Bossy-Wetzel et al., 2004). Nitrosative stress is known to trigger mitochondrial fragmentation and neuronal cell death (Barsoum et al., 2006). To investigate whether NO causes mitochondrial fragmentation by negatively regulating the mitochondrial fission and fusion machinery, time course experiments were performed using S-nitrosocysteine (SNOC) treatment in HEK cells.

As expected, NO directly interferes with expression of mitochondrial fission and fusion machinery proteins. Two hours after 100 μM SNOC treatment, DRP1 expression level starts to increase (Figure 13), suggesting more mitochondrial fission might occur. In addition to DRP1 protein levels, it is known that posttranslational modifications also regulate DRP1 GTPase activities, such as phosphorylation, SUMOylation, and ubiquitination. Therefore, it will be worthwhile in the future to investigate whether NO induces mitochondrial fragmentation through direct enhancement of DRP1 activity by posttranslational modification.

In addition to increasing DRP1 expression levels, SNOC triggers cleavage of the OPA1 long-isoform into the short-isoform, resulting in a loss of mitochondrial fusion (Figure 13). OPA1 has different isoforms resulting from both alternative mRNA splicing and proteolytic cleavage (Akepati et al., 2008; Song et al., 2007). Further studies revealed that only the long-isoform of OPA1 is required for mitochondrial fusion, because only long-isoform OPA1 was able to protect

against mitochondrial fragmentation (Ishihara et al., 2006). Thus, cleavage of the long-isoform results in loss of fusion activity, and in turn, mitochondrial fragmentation.

Moreover, full-length MFN2 (86 KD) protein levels decreased while fragment (64 KD and 46 KD) levels increased (Figure 13). Fragments were of the same molecular weight as those observed in ALS transgenic mice (Figure 12). Although it remains to be confirmed that these fragments belong to MFN2, full-length MFN2 was definitely degraded in response to SNOC treatment.

Collectively, these data suggest that NO impairs protein expression and proteolytic cleavage of the mitochondrial fission and fusion machinery, including DRP1, OPA1, and MFN2, which in turn shifts the balance of mitochondrial dynamics toward fission.

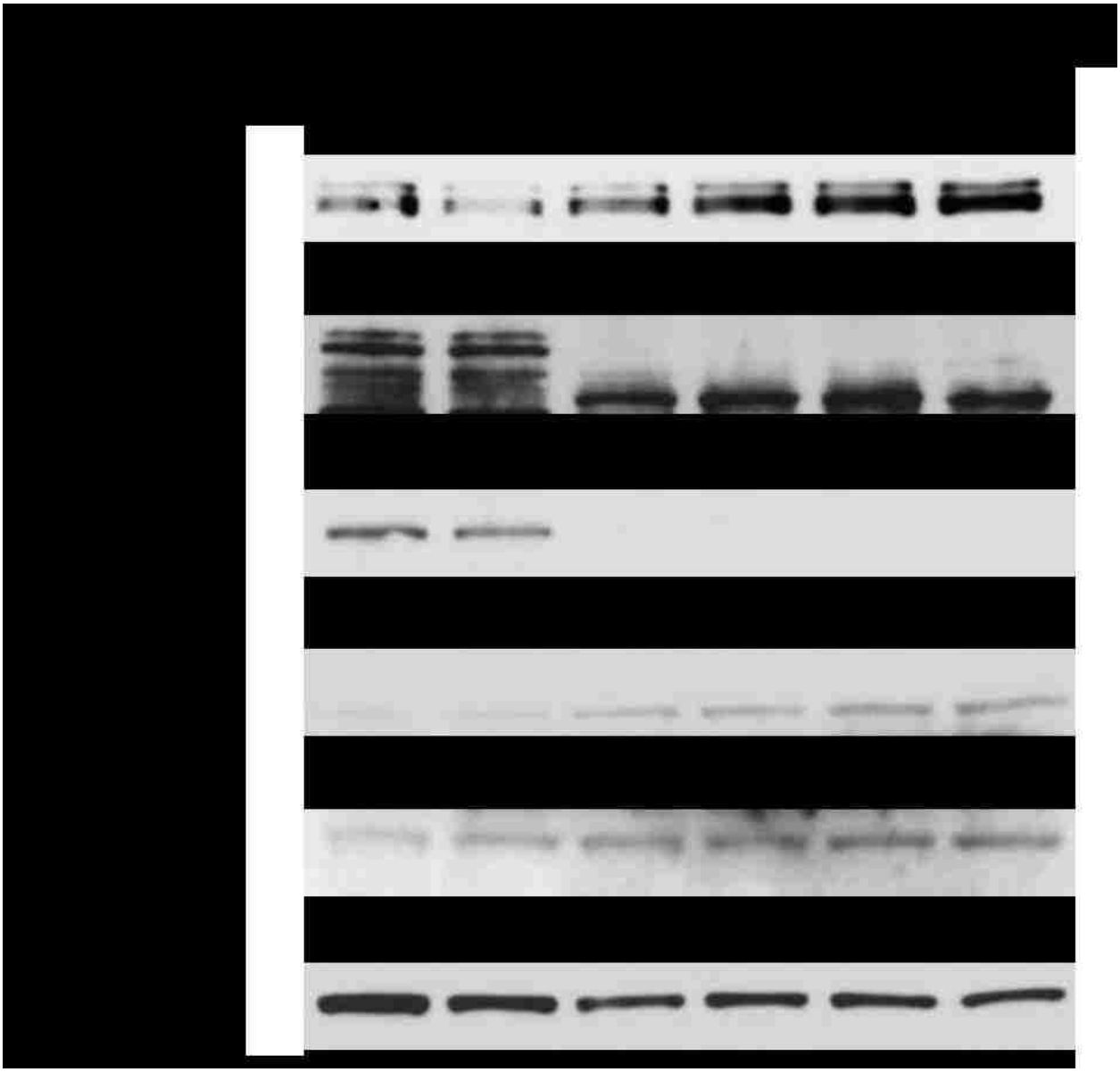

Figure 13 Alteration of protein levels in mitochondrial fission and fusion machinery.

Western blots of DRP1, OPA1, MFN2, and Actin in HEK cells after 300 μM SNOC time-course treatment.

2.4 Discussion

Mitochondrial dysfunction occurs in both ALS patients and animal models of ALS (Damiano et al., 2006; Mattiazzi et al., 2002; Wiedemann et al., 2002). Altered mitochondrial morphology has been reported in ALS patients, mice, and cell culture models (Kong and Xu, 1998; Magrane et al., 2009; Sasaki and Iwata, 2007). Thus, abnormal mitochondrial dynamics may participate in ALS pathogenesis.

DRP1 mediates mitochondrial fission and its overexpression increases vulnerability to mitochondrial fragmentation and neuronal cell death (Barsoum et al., 2006). In addition, we recently reported that DRP1 is activated in HD and decreasing DRP1 activity by expression of dominant-negative $DRP1^{K38A}$ mutant restores mitochondrial dynamics, and in turn, rescues neuronal cell death (Song et al., 2011). However, the role of DRP1 in ALS has not been studied. In the current work, we report the presence of defective axonal mitochondrial dynamics in motor neurons expressing mutant $SOD1^{G93A}$ (Figures 7-9). We also demonstrate that $DRP1^{K38A}$ expression restores mitochondrial dynamics (Figure 10). Similarly, neuronal cell death is inhibited by decreasing DRP1 activity (Figure 11). Therefore, aberrant mitochondrial dynamics might play a causal role in ALS-linked motor neuron degeneration. Recently, Magrane *et al.* reported impaired mitochondrial fusion using photo-switchable fluorescent MitoDendra in "pure" motor neuron cultures, which correlated with fewer mitochondria at synapses and synaptic loss (Magrane et al., 2012). Fission and fusion are not independent events and impact each other. Defects in mitochondrial fusion may result from increased fission rates, which is

consistent with our observations. This provides the basis for future studies using animal models of ALS to investigate if decreasing DRP1 activity might mediate neuroprotection *in vivo*.

One important consideration in the types of experiments described here is that motor neurons are among the most difficult neuronal types to culture *in vitro*. Recently published work has shown abnormal mitochondrial dynamics in ALS models *in vitro* using either “pure” motor neurons, “pure” cortical neurons, or motor neuron-like NSC34 cells (De Vos et al., 2007; Magrane et al., 2009; Magrane et al., 2012). However, the reported defects in mitochondrial movement are in part inconsistent, which may be due to different experimental models. It is our experience that "pure" motor neuron cultures, without astroglial support, are stressed and therefore require ample amounts of neurotrophic factors in the culture medium for cell survival. An artificial excess of neurotrophins may obfuscate the physiological response of motor neurons, and result in conflicting experimental findings. The characteristics of motor neurons make analysis a laborious and technically challenging task. Here, we report an improved motor neuron-astrocyte co-culture system. Astrocytes, as supportive cells, are important for motor neuron development and functioning (Sidoryk-Wegrzynowicz et al., 2011; Walz, 2002). In our system, medium supplementation with neurotrophins is not required for motor neuron survival *in vitro*, providing an advantage. Thus, our motor neuron-astrocyte co-culture system might represent an improved experimental model for motor neuron studies, one which may mimic more closely *in vivo* conditions. We grew an astrocyte mono-layer and seeded the DsRed2-Mito electroporated purified motor neurons on top of the established mono-layer (Figure 6). The neurites of these motor neurons not only grew up to several

hundred microns in length, but also connected to their astrocyte or motor neuron targets. Previous studies have shown that disease progression in ALS might not be cell-autonomous (Beers et al., 2006; Harraz et al., 2008; Nagai et al., 2007). There are also several studies indicating that mutant SOD1 astrocytes have significant effects on motor neuron degeneration in ALS models (Nagai et al., 2007; Yamanaka et al., 2008). Therefore, we believe it is better not to omit astrocytes in any study of motor neurons. Future investigations will test the effects of mutant $SOD1^{G93A}$ astrocytes on the mitochondrial dynamics of wild-type motor neurons.

Mitochondrial fragmentation may result from either excessive fission or inhibition of fusion. Although defective mitochondrial dynamics have been shown to be causal events in ALS pathogenesis, what causes these defects and how they are caused remain to be illustrated. A reduction in MFN protein level was observed in ALS mice with several small fragments (Figure 12), suggestive of a novel cleavage of MFN2. Further studies are required to prove novel protein processing of MFN2. To date, no direct interaction between SOD1 and MFN2 has been identified, but it is possible that $SOD1^{G93A}$-induced reduction of MFN2 may be mediated by ROS signaling. Previous reports have already indicated that nitrosative/oxidative stress triggers mitochondrial fragmentation by a mechanism that is not fully understood (Barsoum et al., 2006). Of note, nitrosative/oxidative damage has also been implicated in ALS pathogenesis (Mattiazzi et al., 2002). Recently, Bosco *et al.* reported that purified oxidized $SOD1^{WT}$ from sporadic ALS patient tissues can induce defects in fast axonal transport (Bosco et al., 2010). These findings not only suggest an SOD1-dependent mechanism in sporadic ALS, but also highlight the critical role of nitrosative/oxidative stress. Here, levels of proteins involved in

mitochondrial fission and fusion changed in response to SNOC treatment (Figure 13). DRP1 levels increased after 4 h SNOC treatment, while both OPA1 and MFN2 were cleaved (Figure 13). Therefore, ROS may mediate an increase in mitochondrial fragmentation in ALS by enhancing DRP1 protein stability and inducing cleavage of MFN2 and OPA1.

In summary, we generated a novel astrocyte-motor neuron co-culture system, which provides an improved model for studies of mutant $SOD1^{G93A}$-induced toxicity *in vitro*. Moreover, we found that defects in the mitochondrial fission and fusion equilibrium play a functional role in mutant $SOD1^{G93A}$-induced defects in mitochondrial trafficking and neuronal cell death. Although the precise underlying mechanisms require further investigation, our study suggests that ROS signaling may be involved in the regulation of proteins mediating mitochondrial fission and fusion. Agents that modulate DRP1 activity may hold potential to slow motor neuron neurodegeneration linked to ALS.

CHAPTER THREE: MITOCHONDRIAL DYNAMICS DEFECTS IN HD

3.1 Overview of HD

3.1.1 Mutant HTT and HD

HD is a fatal dominant inherited neurodegenerative disorder characterized by involuntary movements and cognitive defects (Burns et al., 1990; Lin and Beal, 2006; Vonsattel et al., 1985). The ratio of HD occurrence is 1 in 10,000 and patients usually die within 10–15 years of disease onset. Usually HD onset occurs between the ages of 35 and 50 and 10% of patients develop symptoms before age 20. Common symptoms of HD include weight loss and disturbances in emotion, memory, and movement. Most HD patients die from aspiration pneumonia. Medium spiny neuronal loss has been reported in the striatum of basal ganglia, and further MRI studies revealed a significant reduction in the cortex and hippocampus of HD patients (Byers et al., 1973; Vonsattel et al., 1985).

Nearly 20 years ago, the IT-15 gene with abnormal CAG trinucleotide repeats in its exon-1 was identified as the cause of this inherited disease (Group, 1993). IT-15 is also called the HTT gene, which encodes the HTT protein. Because CAG codes for glutamine (Q), the CAG repeat region is named the polyglutamine (PolyQ) domain. In normal persons, PolyQ repeats range from 6 to 35, while expansion to 40–120 repeats leads to HD. Persons carrying 36 to 40 repeats may or may not develop HD. However, due to the instability of CAG repeats, an increase in the length of the PolyQ expansion can occur from generation to generation.

Therefore, descendants may be at risk of getting the disease even if the parents were healthy (Ranen et al., 1995). Disease onset correlates with the number of polyQ repeats with more repeats generally resulting in earlier onset (Reddy et al., 1999a; Reddy et al., 1999b). In particular, an expansion of more than 60 polyQ is usually associated with juvenile HD.

3.1.2 Huntingtin

3.1.2.1 Huntingtin structure

HTT is a 348 KD scaffold protein with 3144 amino acids, which is mostly located in the cytoplasm (Figure 14). The PolyQ domain is found in the N-terminal portion of HTT and has been proposed to form a polar zipper structure, binding other PolyQ regions in transcription factors to regulate transcription (Perutz et al., 1994). In addition, the PolyQ region has been found to bind directly with a number of partners (Harjes and Wanker, 2003). Depending on the binding partner, the PolyQ stretch undergoes a conformational change, forming an α-helix, random coil, and extended loop (Kim et al., 2009). Furthermore, the structure of the PolyQ is stabilized by a polyproline region (PolyP) directly adjacent to the PolyQ towards the C-terminus.

The HEAT domain, which favors protein-protein interactions, repeats several times in HTT (Andrade and Bork, 1995). Such a feature further supports protein interactions between PolyQ and its binding partners, which might be the physiological function of HTT.

HTT also contains sequences for a nuclear export signal (NES) and nuclear localization signal (NLS), indicating that HTT shuttles between the nucleus and cytoplasm (Cornett et al.,

2005; Xia et al., 2003). In addition, sequences involved in the association with other organelles have been identified, including mitochondria, Golgi, and ER (Kegel et al., 2002; Rockabrand et al., 2007; Strehlow et al., 2007).

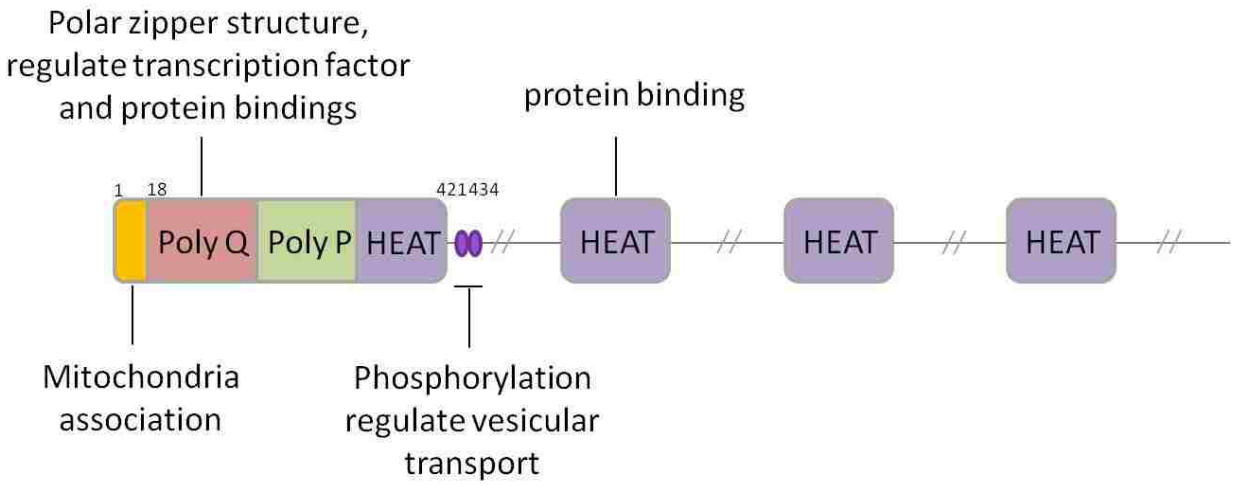

Figure 14 Domain model of HTT.

3.1.2.2 Huntingtin function

HTT is a ubiquitous protein expressed in all types of tissues. Neurons have the highest expression levels of HTT, particularly in cortical pyramidal neurons that project to striatal neurons (Fusco et al., 1999). Because both cortical and striatal neurons are the major targets of

mutant HTT in HD, it is possible to speculate that HTT plays an extremely important role and mutant HTT may lose its normal function in these two neuronal types. Thus, the question remains, what function does HTT play in neurons?

The evolution of the HTT gene provides some hints about its function in neurons. HTT is highly conserved in vertebrates; however, little HTT is found in invertebrates, which contain fewer conserved regions (Li et al., 1999). The evolution of the HTT sequence is aligned with the development of the nervous system, suggestive of a specific role in neuronal functions (Candiani et al., 2007; Gissi et al., 2006; Tartari et al., 2008). In particular, the N-terminus of HTT, which contains a PolyQ tract, is a region newly acquired during evolution, indicating its importance (Tartari et al., 2008).

Recently, more detailed functions of HTT have been identified. HTT is essential for embryonic development, as embryonic death occurs in double HTT knock-out mice (Nasir et al., 1995). Further studies revealed that HTT is important in development and neuronal survival of the forebrain (Reiner et al., 2003). Degeneration is specific to Hdh-/- cells (HTT homolog in mouse) in the cortex and striatum, the regions most affected in HD (Reiner et al., 2003). Thus it is clear that HTT normally functions in neuronal development and survival in the cortex and striatum, suggesting that mutant HTT disrupts the normal function of WT HTT, which leads to HD.

Studies of the role of HTT in neuronal survival have revealed an anti-apoptotic function of HTT. Both *in vitro* and *in vivo* studies have proved that WT HTT protects neurons from apoptosis in response to different toxins, while HTT depletion increases caspase-3 activity (Ho

et al., 2001; Rigamonti et al., 2000; Zhang et al., 2006). The mechanism of WT HTT protection may be involved in the blockage of apoptosome formation (Rigamonti et al., 2000). In addition, HTT directly interacts with caspase-3, inhibits its proteolytic activity, and protects cells from further apoptosis (Zhang et al., 2006). Therefore, loss of HTT directly increases caspase activity and cell death.

Another important activity of HTT is its association with brain-derived neurotrophic factor (BDNF) transcription, transport, and synaptic secretion. BDNF is highly expressed in the cerebral cortex, where it is secreted and induces synaptic growth of medium spiny neurons (Zuccato and Cattaneo, 2007). WT HTT up-regulates transcription of BDNF, while loss of HTT leads to 50% reduction in BDNF transcription (Zuccato et al., 2001). The mechanism of how HTT regulates BDNF transcription has been well defined. Neuron-restrictive silencer element (NRSE) is located in the promoters of a number of neuron-specific genes including BDNF and regulates gene expression during neuronal development through recognition by neuron-restrictive silencer factor (NRSF) (Ooi and Wood, 2007). WT HTT has been shown to interact with NRSF through Huntingtin-associated protein 1 (HAP1) and Rab-interacting lysosomal protein (RILP) in the cytoplasm, preventing NRSF recruitment to the NRSE in the nucleus, which in turn activates gene transcription (Shimojo, 2008). Thus, it is clear that HTT participates in the regulation of BDNF gene transcription during neuronal development.

After transcription, BDNF gets translated in the ER and moves to the synapses via vesicular transport along microtubules. HTT has been shown to regulate vesicular transport through interaction with the p150 subunit of Dynactin via HAP1 (Gauthier et al., 2004). The

Dynactin/Dynein motor complex is responsible for both vesicular and mitochondrial transport, suggesting that mitochondrial transport is also regulated by HTT. There is evidence indicating that loss of HTT causes defective axonal transport of both vesicles and mitochondria (Trushina et al., 2004). In addition, phosphorylation of HTT at S421 mediates anterograde transport, further suggesting a role of HTT in regulation of axonal transport (Colin et al., 2008). Thus, HTT appears to be involved in the vesicular transport of BDNF, as well as mitochondria.

Synaptic activity is one of the most important functions of neurons. HTT has been shown to regulate synaptic activity via interactions with both vesicles and cytoskeletons (Smith et al., 2005). Therefore, in addition to BDNF transcription and transport, HTT is also involved in its transmission, which in turn regulates the survival and development of other neurons. Of course, HTT could also participate in synaptic functions other than BDNF release.

Collectively, HTT seems to be involved in multiple functions, including transcription regulation, axonal transport, and synaptic activity. Multiple studies suggest that HTT plays an essential role in neuronal survival and development. Thus, it is not surprising that loss of HTT function results in neurodegeneration.

3.1.3 Mutant HTT-mediated toxicity in HD

Although the exact function of HTT is not fully understood, abnormal polyQ expansion has been thought to interfere with normal HTT function and produce a toxic gain of function.

Several underlying mechanisms have been proposed to explain HD pathogenesis, including transcriptional dysregulation, excitotoxicity, and mitochondrial dysfunction (Figure 15).

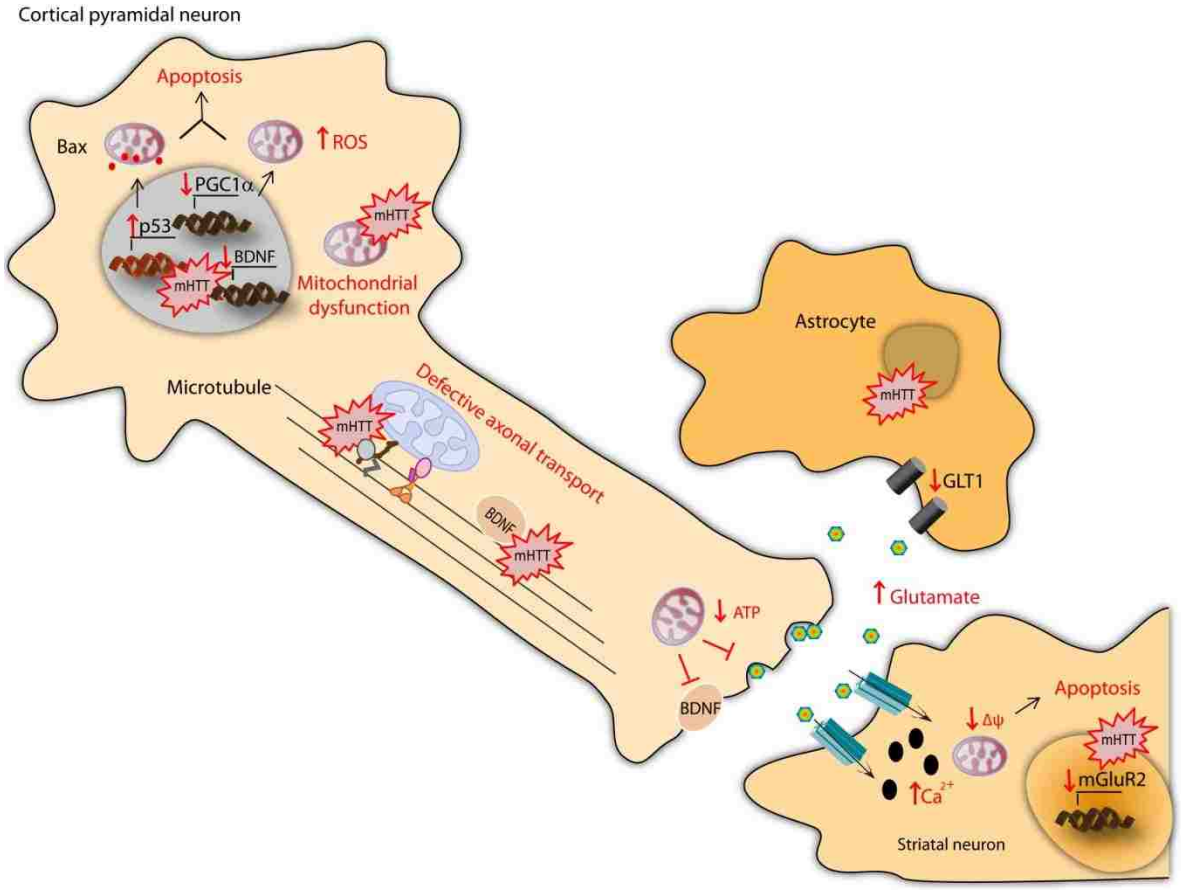

Figure 15 Proposed mechanisms for HD.

3.1.3.1 Transcriptional dysregulation

HTT is a large scaffold protein that interacts with more than 200 proteins (Li and Li, 2004; Sugars and Rubinsztein, 2003). The PolyQ region is an important domain involved in protein interactions. Thus, abnormal PolyQ expansion can either interfere with normal protein-protein bindings or promote abnormal interactions to mediate mutant HTT toxicity.

Abnormal PolyQs interact with the nuclear pore protein TPR, resulting in mutant HTT accumulation in the nucleus (Cornett et al., 2005). Several transcriptional factors have been identified that bind to mutant HTT, including the cAMP response element binding protein (CREB), specificity protein 1 (Sp1), TAFII130, p53, and the nuclear scaffold protein NAKAP (Bae et al., 2005; Huang et al., 1998; Sayer et al., 2005; Shimohata et al., 2000; Sugars and Rubinsztein, 2003). Such abnormal interactions may disrupt gene transcription, expression, and in turn, activity. For example, mutant HTT interacts with Sp1, interfering with its binding to DNA and reducing transcriptional activity (Dunah et al., 2002; Li et al., 2002). Moreover, less binding affinity between mutant HTT and NRSF enhances NRSE recognition by NRSF, which decreases gene transcription (Zuccato and Cattaneo, 2007). Thus, by transcriptional regulation, mutant HTT can directly interfere with multiple signaling pathways in neurons. Several important signaling pathways have been identified.

1) Apoptosis. Mutant HTT binds to p53, up-regulates p53, and increases p53 activity, which in turn up-regulates transcription of BAX and PUMA and mediates mitochondrial damage (Bae et al., 2005). BAX and PUMA, members of Bcl-2 family, are both known to be pro-

apoptotic proteins. Up-regulation of BAX and PUMA triggers apoptosis by releasing mitochondrial apoptogenic proteins, such as cytochrome *c*, SMAC, and apoptosis inducing factor (AIF). Silencing of p53 by RNAi protects against mitochondrial depolarization and neuronal cell death (Bae et al., 2005).

2) Neuronal survival. BDNF is a crucial neurotrophin for neuronal survival, whose transcription is also regulated by mutant HTT through enhanced recruitment of REST/NRSF to its promoter (Zuccato et al., 2003). Mutant HTT impairs BDNF expression, and thus, neurons are more vulnerable in response to toxic stressors (Zuccato et al., 2001; Zuccato et al., 2003). BDNF -/- mice are phenotypically similar to HD mice, suggesting that BDNF loss could be a critical contributor to HD pathogenesis (Baquet et al., 2004).

3) Mitochondrial biogenesis and ROS suppression. Peroxisome proliferator-activated receptor-γ co-activator 1α (PGC-1α) is a transcriptional co-activator involved in mitochondrial biogenesis, oxidative defense, and thermogenesis (Puigserver and Spiegelman, 2003). PGC-1α binds to transcription factor nuclear respiration factor-1 and -2 (NRF-1, 2), which regulate transcription of mitochondrial proteins, including cytochrome *c* and components of the ETC complexes. In addition, PGC-1α participates in ROS suppression by up-regulating antioxidant enzymes, such as SOD1, manganese superoxide dismutase (SOD2), catalase, and glutathione peroxidase (St-Pierre et al., 2006). It is well known that the PGC-1α pathway is impaired in HD (Cui et al., 2006; St-Pierre et al., 2006; Weydt et al., 2006). Mutant HTT interferes with the formation of CREB/TAF4 complexes at the PGC-1α promoter, causing a decrease in PGC-1α transcription (Cui et al., 2006). Reduced PGC-1α expression has been observed in both HD

transgenic mice and HD postmortem brains. Therefore, this reduction by mutant HTT directly mediates mitochondrial dysfunction and cellular oxidative stress.

3.1.3.2 Impaired axonal transport

As discussed above, WT HTT interacts with the p150 subunit of Dynactin via HAP1 and mediates its association with microtubules. However, mutant HTT has an abnormally increased binding affinity with HAP1, which leads to a reduced association between the p150 subunit of Dynactin and the microtubules. Such reduction directly causes defective axonal trafficking (Zala et al., 2008). In addition, phosphorylation of HTT S421 has been shown to regulate directional axonal transport. A reduction in phosphorylated HTT S421 has been observed in both HD animal models and human post mortem tissues (Colin et al., 2008; Warby et al., 2005). The aberrant post-translational modification further impairs vesicular and mitochondrial distribution in neurons. For example, mutant HTT not only interferes with BDNF transcription, but also impairs its vesicular trafficking (del Toro et al., 2006). The impaired axonal anterograde transport further reduces BDNF release and abolishes BDNF-mediated neuronal protection in the brain. It has been shown that hyperphosphorylation of HTT at S421 restores vesicular transport and BDNF release (Zala et al., 2008). Other organelles, such as mitochondria, might also be affected by mutant HTT-induced defective transport (discussion later).

3.1.3.3 Excitotoxicity

Synapses are the functional sites in neurons. Excitotoxicity has been proposed to be a pathogenic mechanism that results in synaptic dysfunction and cell death, which is a common phenomenon in neurodegeneration characterized by the "dying back" pattern. As the major excitatory neurotransmitter, glutamate over-stimulation is associated with excessive ion influx, resulting in excitotoxicity and neuronal cell death. There are three contributors to glutamate receptor overstimulation: increased glutamate release from cortical neurons, reduced glutamate up-take by astrocytes, and altered sensitivity of NMDA receptors (Fan and Raymond, 2007).

As one of the first mechanisms proposed for HD, decreased NMDA receptor levels were first observed in human HD patients more than 20 years ago (Albin et al., 1990; Young et al., 1988). Striatal neurons usually have high expression levels of NMDA and NMDA receptors, and loss of NMDA receptors makes them vulnerable to glutamate stimulation.

Along the cortico-striatal track, pre-synaptic activities of cortical neurons directly interfere with survival and growth of their downstream targets, striatal neurons. Increased glutamate release has also been observed in HD patients, resulting in excitotoxicity in striatal neurons (Reilmann et al., 1994). Excessive calcium influx is accompanied by glutamate over stimulation. The elevated intracellular Ca^{2+} levels may cause mitochondrial Ca^{2+} overload and trigger apoptosis.

Decreased glutamate up-take by astrocytes further induces excitotoxicity. Mutant HTT impairs not only transcription of the glutamate transporter (GLT1), but also glutamate up-take activity in astrocytes, resulting in glutamate accumulation in the synaptic clefts (Arzberger et al., 1997; Hassel et al., 2008). Up-regulating GLT1 expression attenuated neuropathy in a HD mouse model, suggesting the glutamatergic pathway plays a role in HD pathogenesis (Miller et al., 2008).

In sum, excitotoxicity by glutamate over stimulation causes high levels of intracellular Ca^{2+}, which in turn leads to apoptosis through impaired mitochondrial buffering.

3.1.3.4 Mitochondrial dysfunction

As previously discussed, transcriptional dysregulation and excitotoxicity can indirectly impair mitochondrial function and mediate apoptosis caused by mutant HTT through transcriptional regulation of PGC1-α and p53. There is also strong evidence indicating that mutant HTT can directly bind to mitochondria and cause mitochondrial dysfunction.

1) Decreased glucose metabolism. Increased lactate has been reported in the striatum of HD patients, suggestive of decreased glucose utilization (Jenkins et al., 2005) and reflective of altered mitochondrial metabolism that occurs in HD patients. Such defects have been demonstrated to correlate with impaired recall memory and verbal learning in HD patients (Hayden et al., 1986; Kuhl et al., 1982; Kuwert et al., 1990; Young et al., 1986).

2) Decreased ETC complex activity. The decreased mitochondrial metabolism may be associated with decreased mitochondrial respiration. Severe impairments in Complexes II and III and minor defects in Complex IV have been observed in postmortem brain samples of HD patients (Brennan et al., 1985; Browne et al., 1997; Butterworth et al., 1985; Gu et al., 1996). Moreover, in transgenic HD mouse models, impairment of Complexes I, II, III, and IV was observed (Pandey et al., 2008). The decrease in respiratory complex activity might result from both impaired transcription in the nucleus and mitochondrial DNA deletion (Horton et al., 1995). In addition, reduced OXPHOS activity can lead to decreased ATP production, which directly impairs all ATP-dependent cell signaling pathways (Lodi et al., 2000).

One good example of the relationship between mitochondrial respiration and HD is the OXPHOS complex II inhibitor 3-NP that mimics HD pathogenesis. Inhibition of Complex II results in ROS induction and oxidative damage, which is crucial for mutant HTT-mediated neuronal cell death (Browne and Beal, 2006).

3) Reduced Ca^{2+} buffering and depolarized mitochondrial membrane potential. Mutant HTT might directly interact with the OMM, forming aggregates and impairing mitochondrial functions, including Ca^{2+} buffering capacity and mitochondrial membrane potential (Choo et al., 2004). Reduced Ca^{2+} buffering capacity has been observed in HD transgenic mice and in lymphocytes from HD patients (Panov et al., 2002). One piece of convincing evidence is that incubation of mutant HTT and mitochondria *in vitro* results in impaired Ca^{2+} up-take capacity (Choo et al., 2004; Panov et al., 2002). Moreover, this effect is tissue specific and mitochondria in the striatum appear to be more sensitive (Brustovetsky et al., 2005).

4) Impaired mitochondrial trafficking. HTT has been shown to interact with several molecular motors and regulate microtubule-based transport, including Kinesin and Dynein (Gauthier et al., 2004; McGuire et al., 2006). Phosphorylation of HTT determines the direction of vesicular transport (Colin et al., 2008). Because mitochondria and vesicles share similar molecular motors for transport, HTT might play an important role in regulation of mitochondrial trafficking. Loss of WT HTT or expression of mutant HTT results in defective transport of mitochondria in Drosophila (Gunawardena et al., 2003). On the other hand, aggregates of mutant HTT are believed to physically block mitochondrial transport (Chang et al., 2006; Trushina et al., 2004). Due to the importance of mitochondria, mutant HTT-mediated defective mitochondrial trafficking may directly result in neurodegeneration and eventual cell death.

3.1.4 Mitochondrial dynamics and HD

Mitochondrial dynamics, including fission, fusion, and transport, are essential for maintenance of normal mitochondrial function. As described previously, mitochondrial dysfunction is implicated in HD; however, the molecular mechanism by which mutant HTT causes mitochondrial dysfunction requires further investigation. Here, we propose that mutant HTT-mediated imbalance in mitochondrial fission and fusion is the mechanism involved in HD.

Much evidence indicates that altered mitochondrial fission and fusion balance directly leads to neurodegeneration. Mutations in MFN2, a GTPase that mediates OMM fusion, cause CMT-2A (Kijima et al., 2005; Zuchner et al., 2004). In addition, mutations in OPA1, the IMM

fusion protein, lead to ADOA (Alexander et al., 2000; Delettre et al., 2000). Mutations in these two proteins not only cause mitochondrial fragmentation, but also affect mitochondrial trafficking and respiration (Chan, 2006; Kang et al., 2008). DRP1, the mitochondrial fission GTPase, is recruited to mitochondria by Dynein (Varadi et al., 2004). Disruption of the Dynactin/Dynein complex results in lack of DRP1 recruitment to mitochondria, and in turn, abnormal mitochondrial morphology and distribution. In sum, mitochondrial fission and fusion are tightly coupled to mitochondrial transport. Moreover, disruption of this balance clearly leads to neuronal dysfunction.

As described above, mutant HTT causes mitochondrial dysfunction, including impaired Ca^{2+} buffering, mitochondrial DNA deletion, and decreased respiration. All these defects may result from an imbalance in mitochondrial fission and fusion. Thus, we hypothesize here that an imbalance in mitochondrial dynamics causes mitochondrial dysfunction, which in turn may be the primary mechanism implicated in HD.

Interestingly, mutant HTT has been observed to form aggregates, which localize to the mitochondrial membrane in a DRP1-like pattern around the mitochondria, suggesting that mutant HTT may be involved in the mitochondrial fission complex and regulation of mitochondrial fission (Panov et al., 2002). In addition, HTT has been shown to bind to Dynamin, which is involved in synaptic transmission (Kaltenbach et al., 2007; Qin et al., 2004). As the homolog of Dynamin, it is reasonable to speculate that DRP1 interacts with mutant HTT and enhances mitochondrial fission. Moreover, it has been shown that DRP1, MFN2, and BAX are co-localized in the foci during apoptosis (Karbowski et al., 2002). Mutant HTT may interfere

with this complex formation, mediating mitochondrial fission and inducing apoptosis. In addition, it has been found that HTT interacts with Dynactin through HAP1, thus regulating mitochondrial trafficking (McGuire et al., 2006). DRP1 is most likely also involved in this complex, because the Dynein/Dynactin complex recruits DRP1 during mitochondrial transport.

In sum, mutant HTT may interact with DRP1, induce mitochondrial fission and defective transport, mediate mitochondrial dysfunction, and eventually lead to neuronal cell death.

3.2 Materials and Methods

3.2.1 Reagents

The pDsRed2-Mito was purchased from Clontech. The plasmids pGW1-htt exon1-Q17-EGFP, pGW1-htt exon1-Q46-EGFP, and pGW1-htt exon1-Q97-EGFP were obtained from Dr. S. Finkbeiner (University of California-San Francisco). The pcDNA3.1-Q25-GFP and pcDNA3.1-Q97-GFP were provided by Dr. L. Thompson (University of California-Irvine). The YFP-DRP1 plasmid was obtained from Dr. R. Youle (US National Institutes of Health (NIH)). The pcDNA3-DRP1^{K38A} plasmid was obtained from Dr. A. van der Bliek (University of California-Los Angeles). The MFN2 (p82-FzoRV12pECFP-C1) was obtained from Dr. R. Slack (University of Ottawa). The pcDNA3.1β-shRNA-DRP1 and pcDNA3.1β-scramble were obtained from Dr. S. Strack (University of Iowa). All plasmids were purified using the Endotoxin-free Marligen Maxiprep Kit (Diagnostic technology, Belrose, Australia).

HEPES was purchased from Omega Scientific (Tarzana, CA, USA). Poly-L-lysine, BSA, Penicillin-streptomycin (Pen/Strep), formaldehyde, pyruvate, and F-12 HAM were all obtained from Sigma-Aldrich (St. Louis, MO, USA). Custom-made phenol-free DMEM/high glucose and bovine calf serum (BCS) were obtained from Thermo Scientific (Rockford, IL, USA). Glutamax was purchased from Gibco (Carlsbad, CA, USA). Lipofectamine 2000, Hoechst 33342, and neurobasal medium were purchased from Invitrogen (Carlsbad, CA, USA). Protease inhibitor cocktails were purchased from Roche (Indianapolis, IN, USA). EDTA was purchased from Calbiochem (Darmstadt, Germany). Mouse antibodies to HTT (MAB2166) were obtained from

Millipore (Billerica, MA, USA). Rabbit antibodies to DRP1 (H300) were obtained from Santa Cruz (Santa Cruz, CA, USA). Sheep anti-mouse IgG-HRP was purchased from GE Healthcare (Pittsburgh, PA, USA).

3.2.2 Mice and rats

YAC18 (line 212) and YAC 128 (line 53) mice in FVB/N background were used for co-immunoprecipitation experiments. These mice were generated to express full-length human huntingtin with 18 and 128 glutamines, respectively.

Pregnant rats of the Sprague-Dawley background (Charles River) were used for primary cortical cultures.

All experiments were approved by the Institutional Animal Care and Use Committee of University of Central Florida College of Medicine.

3.2.3 Human fibroblasts

Untransformed fibroblasts from HD patients GM05539 (onset at 2 year-old), GM04693 (onset at 41 year-old), and normal subject I91L17, were purchased from the Coriell Institute for Medical Research and cultured following their instructions.

3.2.4 Primary cortical neurons and transfection

Cortical neurons (400,000 cells/ml) were prepared from E18 rat embryos (Barsoum et al., 2006; Song et al., 2011) and transfected at 5 DIV with Lipofectamine 2000 (Invitrogen). Cells were cultured in neurobasal medium (Gibco) supplemented with 2% Neuronal Supplement 21, 1× Pen/Strep, 2 mM GlutaMAX. Neuronal Supplement 21 was prepared according to Chen *et al.* (Chen et al., 2008). Experiments were carried out two days after transfection.

3.2.5 Fluorescence microscopy

Both fixed and live-cell imaging of neurons was performed using an Axiovert Zeiss 100M inverted fluorescence microscope equipped with a Plan Apochromat 63×1.4 NA oil objective, a DG-4/Lambda 10-2 combo Xe-arc illumination unit (Sutter), and a Sensicam QE cooled CCD camera (PCO AG, Germany) controlled by MetaMorph 7.1 software (Molecular Devices) as previously described (Song et al., 2008). The excitation filter for DsRed2-Mito was S555/28× (Chroma) and the emission filter was S617/73m (Chroma). The excitation filter for EGFP was S490/20× (Chroma) and the emission filter was S528/38m (Chroma). Images were acquired using the Multi Dimensional Acquisition module in MetaMorph 7.1 (2×2 binning, 0.2 μm step size, and 15-20 z-planes). The z-series were processed by de-hazing followed by Fast Fourier Transform. Images were saved and exported as TIFF files after surface rendering using MetaMorph 4D-viewer.

For live-cell imaging, cortical neurons were plated on Lab-Tek II (#1.5 German Coverglass) 8-chamber slides (Thermo Fisher) at a density of 150,000 to 200,000 cells per chamber in neurobasal medium without phenol red (see detail in 3.2.4). A region containing 100 μm neurites in 10 neurons were selected and recorded for 5 min with 5 sec intervals at 37 °C under a humidified 5% CO_2 atmosphere. To limit photobleaching and phototoxicity, a 5 μm z-stack was acquired with 1 μm step size (2×2 binning) for each time point. Each z-stack was de-hazed and maximum projected in MetaMorph 7.1. To quantify mitochondrial movement, kymographs were generated with all planes, 25 μm line width, and average projected without background subtraction. The parameters of mitochondrial velocity and moving distance were exported from MetaMorph 7.1 into Excel for further analysis. Mitochondrial velocity ≥ 20 μm/min was classified as motile, while velocity < 20 μm/min was classified as stationary.

3.2.6 Confocal microscopy

Images of fibroblasts were acquired using a Leica TCS SP5 confocal microscope with a 40× oil HCXPLAPO objective controlled by LAS AF software. Z-stacks with 0.3 μm step size (1024 × 1024 dpi) were obtained using a 543 HeNe laser. The stacks of the representative images were processed by surface rendering using MetaMorph 4D-viewer.

Images of the co-localization were acquired using a NikonA1R VAAS Laser Point- and Resonant-Scanning confocal microscope equipped with a 32-channel spectral detection, deconvolution, ultra-sensitive VAAS detector, Perfect Focus (PFS), and a CFI Plan Apochromat

VC 60× WI NA 1.20, W.D. 0.27 mm objective. Single photon Ar-ion laser was emitted at 488 nm and 514 nm; diode laser, emitting at 561 nm. Both image acquisition and processing were performed using Nikon Elements.

3.2.7 Scoring of mitochondrial fragmentation and neuronal cell death

Two days after transfection, the primary cortical neurons were fixed with 3.7% formaldehyde and 5% sucrose in PBS for 15 min at 37 °C. Nuclei were stained by Hoechst 33342 (1:10,000 in PBS) at room temperature for 10 min.

Fibroblasts were seeded at a density of 10,000 cell/ml and analyzed at 6 DIV. Mitochondria were stained with MitoTracker Red CMXRos (100 nM).

Scoring was performed by two individuals independently. Statistics: ANOVA post-hoc test.

3.2.8 Immune precipitation and western blotting

Brain tissues from 2 month old YAC18 and YAC128 mice were lysed in T-PER buffer (1:10) (Thermo Scientific) with protease inhibitors (Roche). Protein concentrations were determined by BCA test (Pierce). Lysates (500 μg) were used to perform immune precipitation by incubating with 30 μl monoclonal mouse-anti-DRP1 antibodies (Santa Cruz) at 4 °C, overnight, and then incubating with 50 μl protein G sepharose (GE Healthcare) at 4 °C for 2 h. Unbound proteins were removed by washing 3 times with ice-cold lysis buffer and the

remaining proteins were then loaded onto NuPAGE 3-8% Tris-Acetate gels (Invitrogen) under reduced conditions and transferred to nitrocellulose membranes (Hybond-ECL Nitrocellulose, 0.22 μm, GE Healthcare). The membranes were blotted with monoclonal mouse-anti-HTT antibodies at 1:1,000 (Millipore) followed by sheep-anti-mouse IgG-HRP at 1:10,000 (GE Healthcare).

3.2.9 Statistics

Results are expressed as means ± S.E.M. Data from two populations were compared using a Student's *t*-test, paired, two-sided. Data from multiple populations were analyzed with ANOVA post-hoc test.

3.3 Results

3.3.1 Mutant HTT triggers mitochondrial fragmentation and neuronal cell death

Mitochondrial dynamics are important for neuronal function and survival, and defects in mitochondrial dynamics have been implicated in neurodegeneration. To investigate whether mutant HTT triggers defective mitochondrial dynamics, primary cortical neurons were transfected with vectors encoding HTT exon1-EGFP with variable length polyQ repeats and DsRed2-Mito to visualize mitochondrial morphology.

Neurons expressing HTT exon1-Q17 exhibited tubular and elongated mitochondrial morphology (Figure 16A, top), while in neurons expressing HTT exon1-Q46 some mitochondria had elongated morphology, but others had rounded morphology, suggesting that excessive mitochondrial fission might have occurred (Figure 16A, middle). By contrast, neurons expressing HTT exon1-Q97 exhibited only round mitochondria, suggestive of profound mitochondrial fragmentation (Figure 16A, bottom). Further quantification indicated that the percentage of mitochondrial fragmentation increased in neurons expressing HTT exon1-Q46 and -Q97, in a polyQ dependent manner (Figure 16B). To evaluate whether mitochondrial fragmentation results from excessive fission or inhibition of fusion, each single mitochondrion was tracked for 5 minutes using time-lapse imaging. Quantitative analysis revealed an increase in the number of mitochondrial fission events relative to total fission and fusion events (Figure 16C). Moreover, mitochondrial fragmentation was correlated with neuronal cell death and was

dependent on polyQ length (Figure 16D). Thus, mutant HTT exon1 triggers mitochondrial fragmentation and cell death in primary cortical neurons.

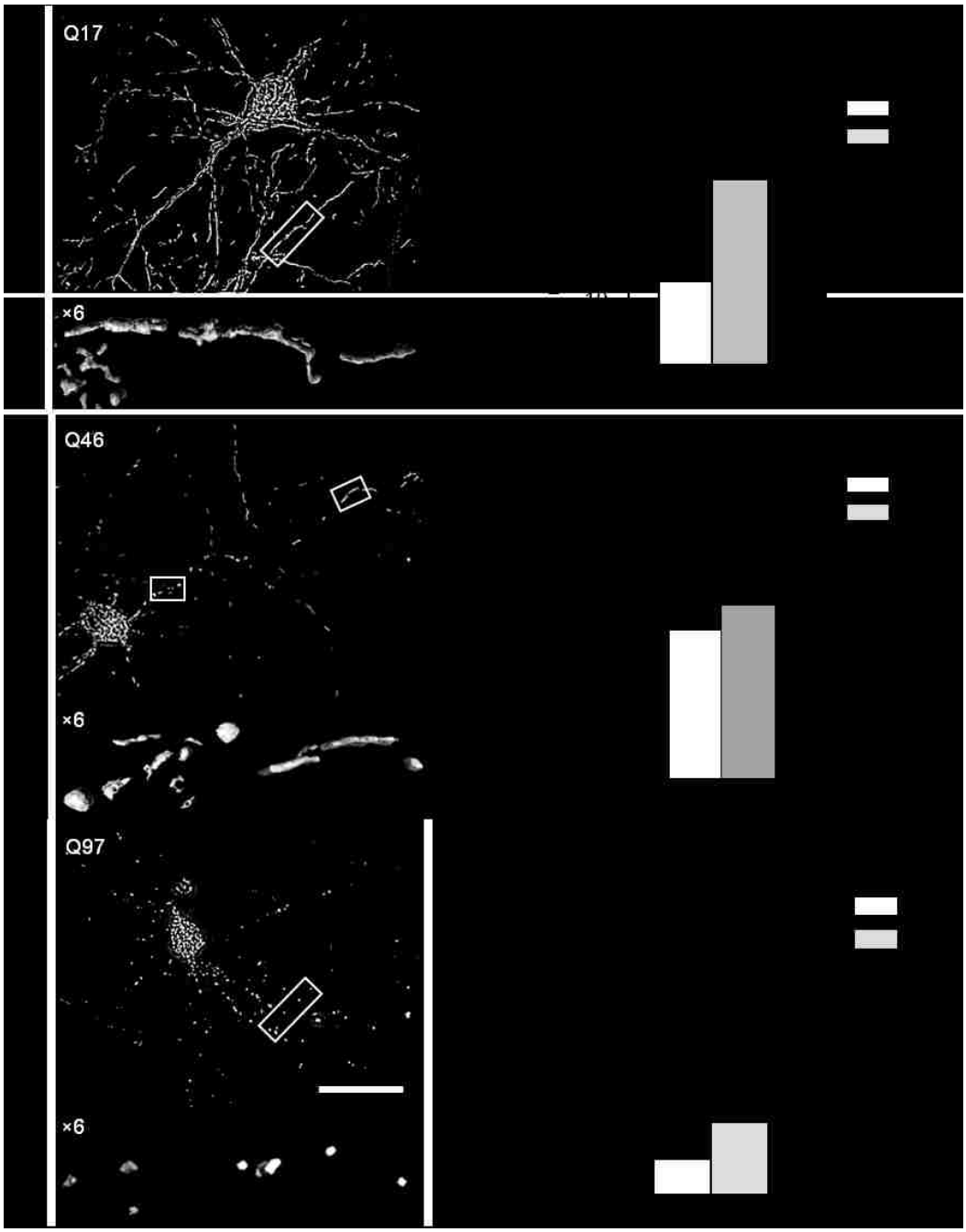

Figure 16 Mutant HTT triggers mitochondrial fragmentation and neuronal cell death, dependent on polyQ length.

A) Three-dimensional fluorescent micrographs and 6x zooms of boxed regions of neurons expressing HTT exon1-Q17, -Q46, or -Q97 and DsRed2-Mito. Scale bar, 50 μm. B) Mitochondrial fragmentation of neurons expressing HTT exon1-Q17, -Q46, or -Q97 and DsRed2-Mito. C) Trend of excessive mitochondrial fission in Q97-HTT cortical neurons. Percentage of mitochondrial fission events over total fission and fusion events in cortical neurons expressing DsRed2-mito, and HTT exon1-Q17, -Q46, or -Q97 in 5 min. n=10, 10, 5, for HTT exon1-Q17, -Q46, and -Q97, respectively. D) Cell death of neurons expressing HTT exon1-Q17, -Q46, or -Q97 scored by chromatin condensation. ANOVA one-way test.

3.3.2 Mutant HTT triggers mitochondrial fragmentation in human fibroblasts

To investigate whether full-length mutant HTT also triggers mitochondrial fragmentation, human fibroblasts from HD patients were used. As expected, mitochondria exhibited a tubular network in fibroblasts expressing WT full-length HTT (Figure 17A, top). In contrast, mitochondria appeared fragmented in fibroblasts expressing mutant full-length HTT (Figure 17A, bottom). Further quantitative analysis revealed that the percentage of fragmented mitochondria increased in fibroblasts from HD patients, with fibroblasts from juvenile onset fibroblasts exhibiting the most profound fragmentation. Therefore, mutant full-length HTT triggers mitochondrial fragmentation in human HD patients, which results from polyQ toxicity. Moreover, both mutant HTT exon1 (Figure 16B) and full length HTT cause mitochondrial fragmentation, suggesting that HTT exon1 can be used instead of full-length HTT for studies *in*

vitro. Moreover, the result confirms our previous data that mitochondrial fragmentation occurs in neurons expressing mutant HTT, which is not due to overexpression.

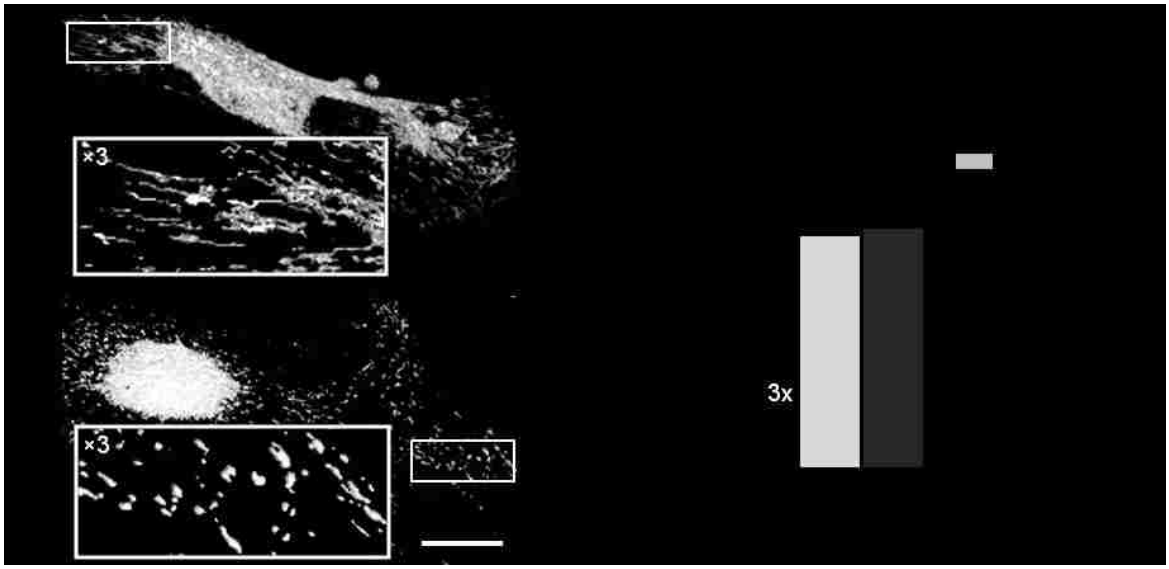

Figure 17 Mutant HTT triggers mitochondrial fragmentation in human fibroblasts.

A) Three-dimensional fluorescent micrographs and 3x zoom of boxed regions of human fibroblasts from a normal individual (top panel) and an HD patient with adult onset (bottom panel) visualized by MitoTracker Red CMXRos staining. Scale bar, 25 µm. B) Mitochondrial fragmentation in human fibroblasts from a normal individual, an HD patient with adult onset, and an HD patient with juvenile onset.

3.3.3 Mutant HTT impairs mitochondrial transport in neurons

Mitochondrial transport is closely linked with mitochondrial morphology. To investigate whether mitochondrial fragmentation is associated with defects in mitochondrial transport, live-cell imaging was used to track single mitochondria. Primary cortical neurons were transfected with HTT exon1-Q17, -Q46, -Q97, and DsRed2-Mito.

To analyze mitochondrial movement, kymographs were generated to illustrate velocity, mobility, and directional trafficking. Kymographs are 3D representations of movies acquired from time-lapse imaging. The horizontal lines represent mitochondrial movement in either the anterograde or retrograde direction, while vertical lines represent stationary mitochondria. In neurons expressing HTT exon1-Q17, a substantial number of horizontal lines are evident in the kymograph, demonstrating that mitochondria were very dynamic (Figure 18A, top). In contrast, fewer horizontal lines are evident in neurons expressing HTT exon1-Q46, suggestive of decreased mitochondrial movement (Figure 18A, middle). More strikingly, kymographs of neurons expressing HTT exon1-Q97 exhibited mostly vertical lines, suggestive of stalled mitochondrial movement (Figure 18A, bottom). To better illustrate mitochondrial movement, scatter plots of mitochondrial velocity and distances traveled were performed for anterograde and retrograde movement. Mitochondria in neurons expressing HTT exon1-Q17 had the highest speed and traveled the longest distance (Figure 18B, top). However, both anterograde and retrograde mitochondrial velocity and distance traveled was reduced in neurons expressing HTT exon1-Q46 (Figure 18B, middle), with the lowest values observed in neurons expressing HTT

exon1-Q97 (Figure 18B, bottom). Thus, it is evident that mutant HTT impairs mitochondrial movement in a polyQ-dependent manner. Furthermore, quantitative analysis revealed that directional movement, mobility, and velocity of mitochondria were impaired dependent in a polyQ-dependent manner (Figure 18C-E). In sum, mutant HTT causes defective mitochondria dynamics, including fission/fusion balance and transport, in primary cortical neurons.

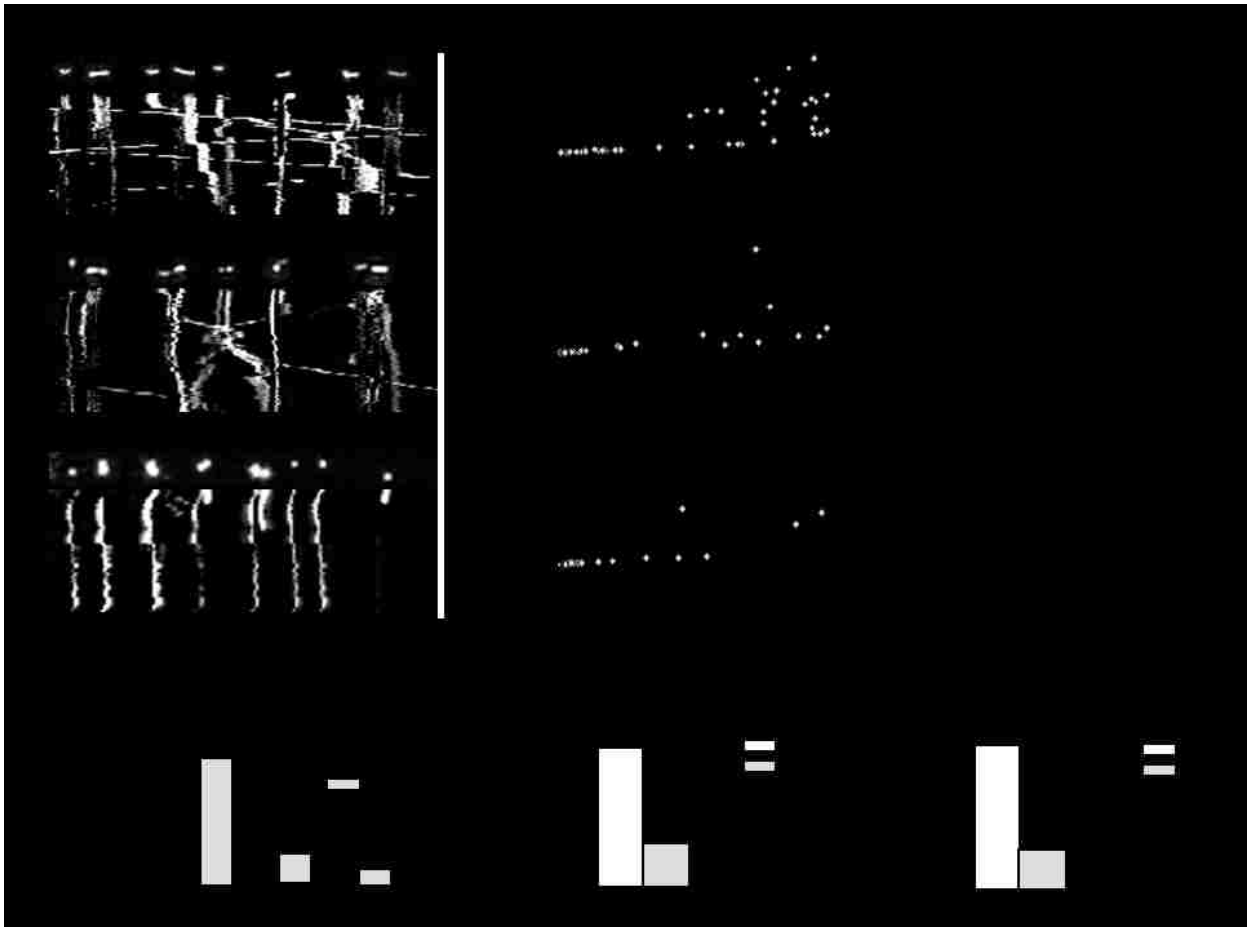

Figure 18 Mutant HTT triggers a decrease in mitochondrial anterograde and retrograde transport in a polyQ-dependent manner.

A) Kymographs of mitochondrial transport in neurons expressing HTT exon1-Q17, -Q46, or -Q97 and DsRed2-Mito. See also Movies S1, S2, S3. B) Scatter plots of mitochondrial velocity in the retrograde or anterograde directions as a function of distance traveled in 5 minutes in neurons (n = 10) expressing HTT exon1-Q17, -Q46, or -Q97 and DsRed2-Mito. C-E) Anterograde and retrograde movement, motility, and mean velocity of mitochondria in the same neurons analyzed in B). Data are means ± S.E.M. of triplicate samples of representative experiments. Results are representative of three or more independent experiments. Statistics: one-way ANOVA test.

3.3.4 Mutant HTT aggregates on mitochondria

A previous immune-EM study reported that mutant HTT forms aggregates and localizes on mitochondria (Panov et al., 2002), which implied that mutant HTT might directly impair mitochondrial function. To confirm whether mutant HTT co-localizes with mitochondria in cortical neurons, bright field fluorescence microscopy was used. HTT exon1-Q25 or -Q97-GFP and DsRed2-Mito were co-transfected to visualize HTT and mitochondria.

In neurons expressing HTT exon1-Q25, HTT was evenly distributed and diffused along the neurites (Figure 19A, left). Higher magnification images demonstrated that there is no specific co-localization of HTT and mitochondria; however, HTT exon1-Q97 formed large and bright spots in cortical neurons, suggestive of aggregation (Figure 19A, right). Moreover, mutant HTT aggregates were localized either on the fissioning mitochondrion or nearby right after fission, suggesting that mutant HTT participates in mitochondrial fragmentation. Further

quantification confirmed that mutant HTT was co-localized to mitochondria in cortical neurons (Figure 19B).

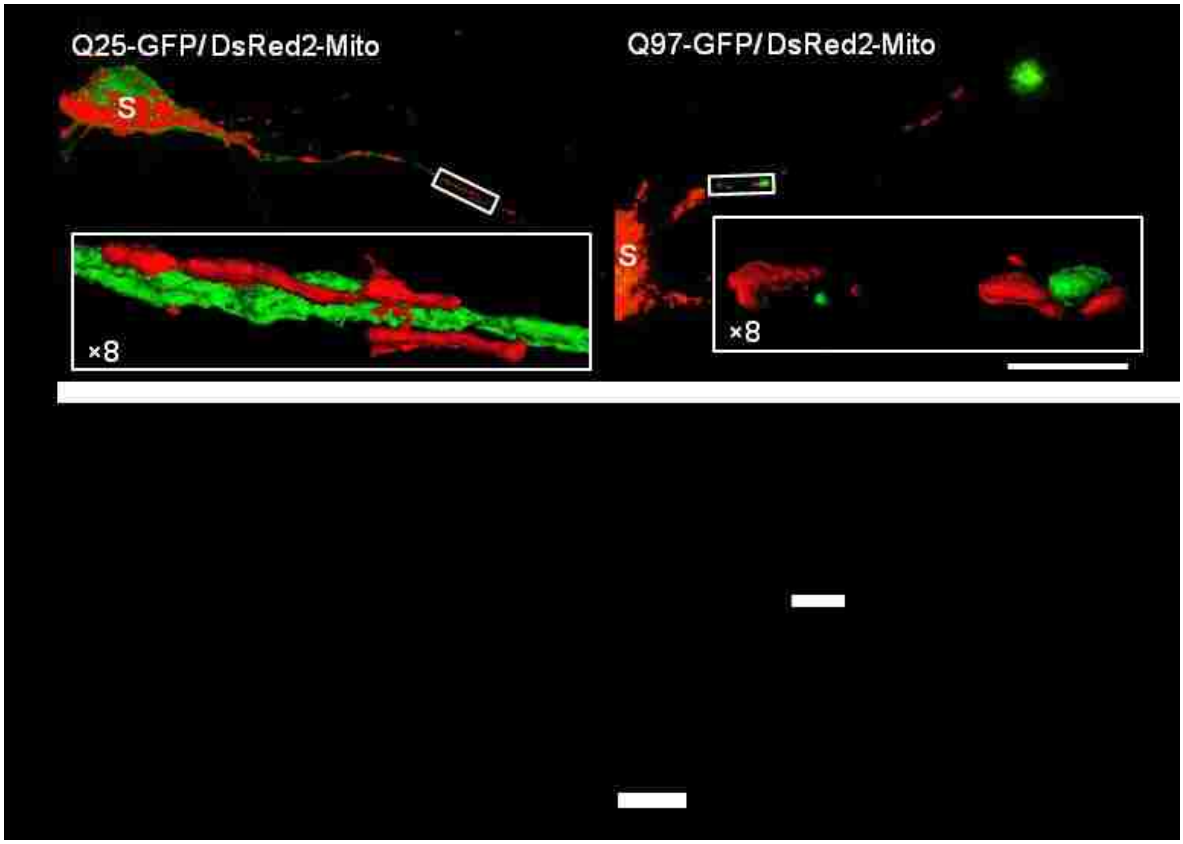

Figure 19 Mutant HTT aggregates in cortical neurons.

A) Three-dimensional fluorescent confocal micrographs and 8x zoom of boxed regions of neurons expressing HTT exon1-Q25 or -Q97 and DsRed2-Mito. Scale bar, 50 μm. B) Co-localization of mitochondria and HTT in neurons co-expressing HTT exon1-Q25 or -Q97 and DsRed2-Mito.

3.3.5 Mutant HTT interacts with DRP1 in cortical neurons

DRP1 plays an important role in both mitochondrial morphology and transport. In addition, the pattern of the localization of mutant HTT on the mitochondria is similar to DRP1. Thus, it is interesting to determine whether mutant HTT interacts with DRP1 and regulates mitochondrial fission.

To investigate whether mutant HTT interacts with DRP1 on mitochondria, three-channel co-localization was performed here. DsRed2-Mito, DRP1-YFP, and HTT exon1-Q25 or -Q97-GFP were co-transfected into primary cortical neurons. As the image shown, HTT exon1-Q25 was evenly distributed in the entire neuron, while mitochondria formed tubular network (Figure 20, top left). DRP1 was located either in the cytoplasm or forms spots on the mitochondria (Figure 20, top left). Further analysis using linescan indicated that no specific interaction between DRP1 and HTT exon1-Q25 was observed (Figure 20, top right). However, in the neuron expressing HTT exon1-Q97-GFP, both mutant HTT and DRP1 form aggregations and were localized on the mitochondria (Figure20, bottom left). Analysis using linescan revealed that mutant HTT and DRP1 co-localized at where mitochondrion was going to divide (Figure20, bottom right). Collectively, mutant HTT may have higher affinity binding to DRP1, which in turn induces mitochondrial fragmentation.

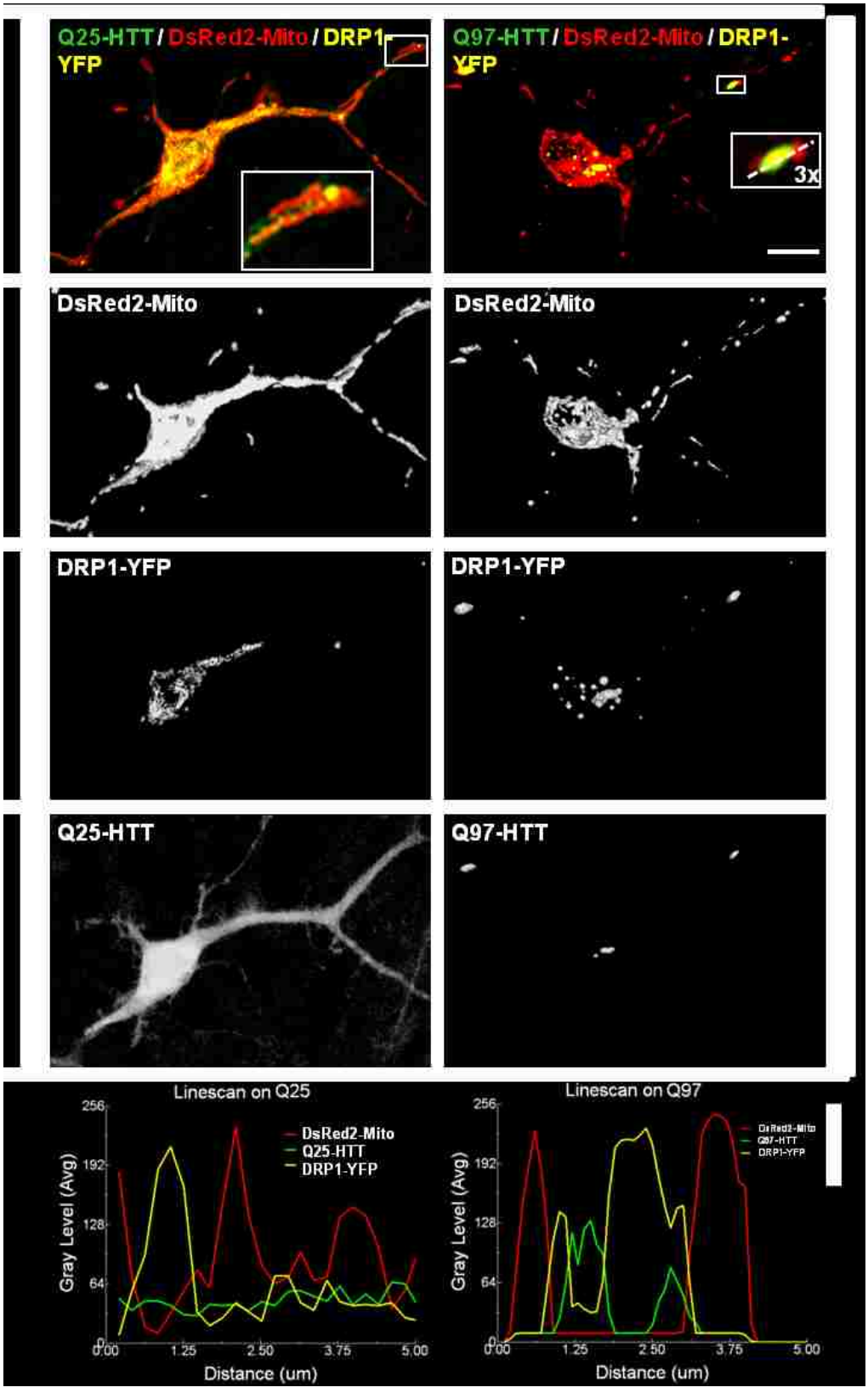
Q25-HTT / DsRed2-Mito / DRP1-YFP
Q97-HTT / DsRed2-Mito / DRP1-YFP
3x
DsRed2-Mito
DsRed2-Mito
DRP1-YFP
DRP1-YFP
Q25-HTT
Q97-HTT
Linescan on Q25
Linescan on Q97
DsRed2-Mito
Q25-HTT
DRP1-YFP
Gray Level (Avg)
Distance (um)
256
192
128
64
0
0.00
1.25
2.50
3.75
5.00

Figure 20 Mutant HTT interacts with DRP1 in cortical neurons.

Three-dimensional fluorescent confocal micrographs with line scan and 3x zoom of boxed regions of co-localization of HTT, DRP1, and mitochondria in neurons expressing DsRed2-Mito, DRP1-YFP, and HTT exon1-Q25 or -Q97. Scale bar, 10 μm.

3.3.6 Mutant HTT interacts with DRP1 in mice

To confirm this abnormal interaction between mutant HTT and DRP1, mice brains from non-transgenic mice and transgenic mice expressing HTT with 128 polyQ repeats (YAC 128) were used for analysis. Co-immunoprecipitation (CoIP) of protein lysates from 2-month-old mice brains was performed with anti-DRP1 antibodies followed by western blot with anti-HTT antibodies. The intensity of the signal for YAC 128 mice was about 50% stronger than that of control mice (Figure 21), suggesting that mutant HTT has higher affinity for DRP1.

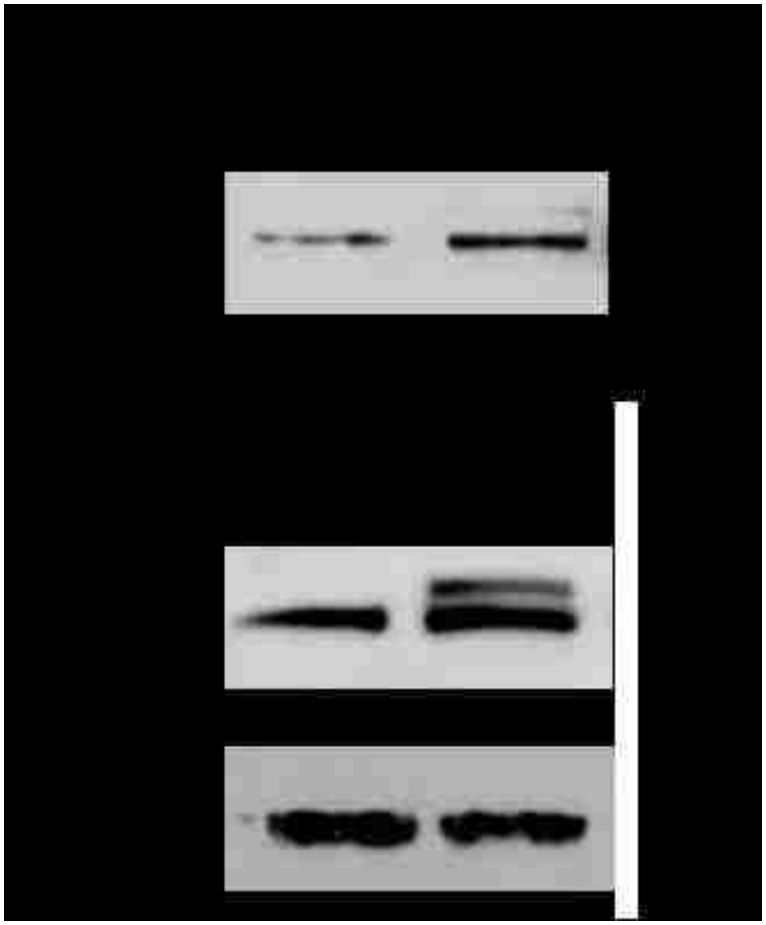

Figure 21 HTT interacts with DRP1 in mice.

Immune precipitation of lysates from 2-month-old mice brains with anti-DRP1 antibodies and western blot using anti-HTT antibodies.

3.3.7 DRP1^{K38A} and MFN2^{p82} rescue mitochondrial fragmentation and neuronal cell death

As the above results suggest, DRP1 over-activation is proposed to be the primary cause of HD. To confirm this hypothesis, we restored mitochondrial fission and fusion balance using primary neuronal cultures. Dominant-negative DRP1^{K38A} and constitutively active MFN2^{p82} were co-transfected with HTT-Q17, -Q46, and -Q97 into cortical neurons to reduce mitochondrial fission and promote mitochondrial fusion, respectively.

The percentages of mitochondrial fragmentation in neurons expressing both DRP1^{K38A} and mutant HTT (-Q46 and -Q97) were significantly decreased compared with neurons expressing mutant HTT alone, suggesting that decreased mitochondrial fission restores mitochondrial morphology (Figure 22A, left). The restoration of mitochondrial morphology was even more profound when DRP1^{K38A} and MFN2^{p82} were co-expressed (Figure 22A, right). Neurons expressing HTT-Q97 do not respond as well as neurons expressing HTT-Q46 to DRP1^{K38A} and MFN2^{p82} co-expression (Figure 22A, right). The phenotype resulting from HTT-Q97 expression is more severe and more difficult to rescue than that of HTT-Q46. Neuronal cell death was also rescued by expressing either DRP1^{K38A} alone or in combination with MFN2^{p82} in a similar pattern as mitochondrial morphology (Figure 22B). Therefore, rebalancing of mitochondrial fission and fusion by expression of DRP1^{K38A} and MFN2^{p82} restores mitochondrial morphology and is correlated with neuronal survival.

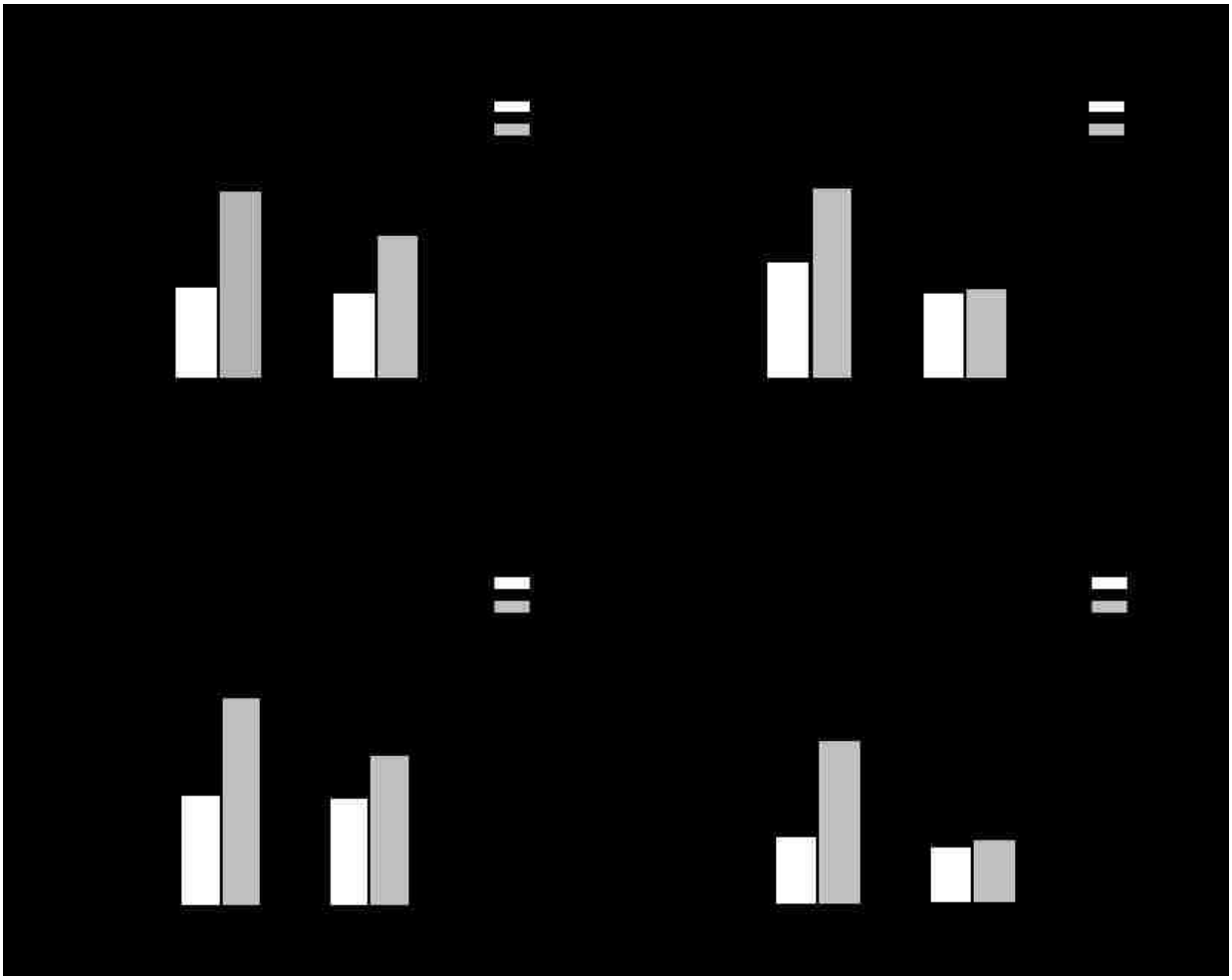

Figure 22 Restoring mitochondrial fusion by expressing DRP1^{K38A} alone or in combination with MFN2^{p82} rescues neurons from cell death.

A) Mitochondrial fragmentation of neurons expressing either HTT exon1-Q17, -Q46, or -Q97 alone or in combination with either DRP1^{K38A} alone or DRP1^{K38A} and MFN2^{p82}. B) Cell death of neurons expressing either mutant HTT exon1-Q17, -Q46, or -Q97 and DsRed2-Mito alone or in combination with either DRP1^{K38A} alone or DRP1^{K38A} and MFN2^{p82}.

3.3.8 DRP1 knockout does not prevent mutant HTT-mediated mitochondrial fragmentation

Reducing mitochondrial fission restores mutant HTT-induced fragmentation in cortical neurons. Thus, the next logical question to ask is whether deleting DRP1 can also protect against mutant HTT-induced toxicity. DRP1shRNA was co-transfected with HTT-Q17, -Q46, or -Q97. Unexpectedly, neurons expressing DRP1shRNA exhibited abnormal morphology (Figure 23). Even neurons expressing HTT-Q17 alone exhibited uneven and unsmooth neurites, correlating with fragmented mitochondria (Figure 23A). In addition, neurites far from the soma demonstrated an abnormal disc shape with mitochondrial accumulation (Figure 23B). In some cases, neurons expressing DRP1shRNA did not grow very big in size and exhibited flattened processes containing few mitochondria (Figure 23C). In sum, DRP1shRNA expression causes abnormal neuronal morphology and disturbs neuronal development, which correlates with abnormal mitochondrial morphology and distribution in neurons.

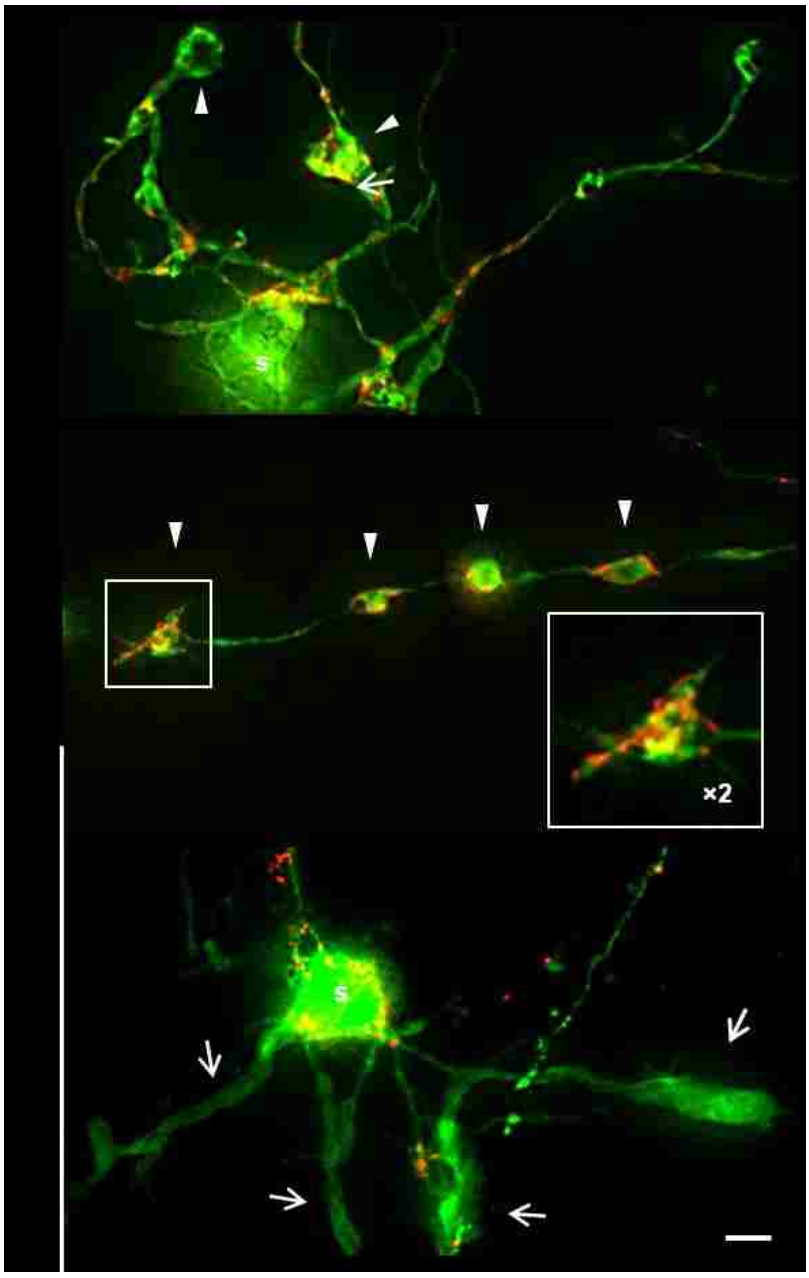

Figure 23 Neuronal morphology of primary cortical cultures expressing DRP1shRNA.

A) Abnormal morphology (arrow, arrow head) with fragmented mitochondria in primary cortical neurons expressing DsRed2-mito, HTT exon1-Q17, and DRP1shRNA during neuronal development. B) Blobby morphology of neuronal processes (arrow head) in primary cortical neurons expressing DsRed2-mito, HTT exon1-Q17, and DRP1shRNA. C) Flattened processes without mitochondria (arrow) in primary cortical neurons expressing DsRed2-mito, HTT exon1-Q17, and DRP1shRNA. Scale Bar: 10 μm.

3.3.9 DRP1^{K38A} and MFN2^{p82} rescue mitochondrial transport

Mitochondrial transport is tightly linked with mitochondrial morphology. To investigate whether restoration of the mitochondrial fission and fusion balance also rescues mitochondrial transport, live-cell imaging was performed to monitor mitochondrial movement.

Representative kymographs exhibited more horizontal lines in neurons co-expressing HTT-Q46 and DRP1^{K38A} (Figure 24B) than in HTT-Q46 neurons (Figure 24A). Neurons either expressing DRP1^{K38A} alone or in combination with MFN^{p82} exhibited improved mitochondrial movement in the anterograde and retrograde directions (Figure 25A). Further analysis revealed that DRP1^{K38A} and MFN^{p82} expression improved both mitochondrial mobility and mean velocity (Figure 25B, C). In sum, mitochondrial transport can be rescued by reducing DRP1 activity using dominant-negative DRP1^{K38A}.

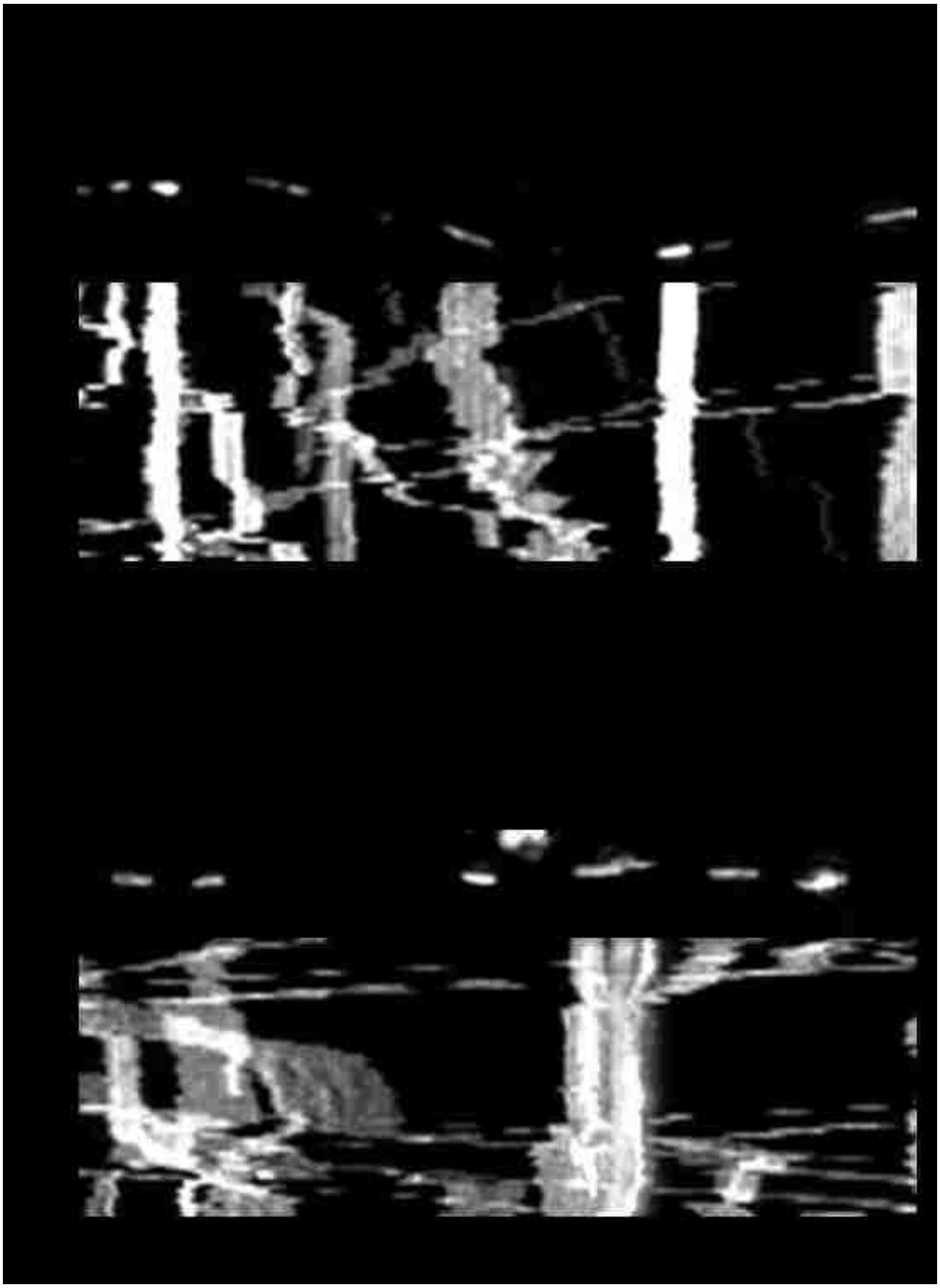

Figure 24 DRP1^{K38A} rescues mitochondrial transport defects in cortical neurons.

A) Representative kymograph of neurons transfected with HTT exon1-Q46 and DsRed2-Mito. B) Representative kymograph of neurons transfected with HTT exon1-Q46, DsRed2-Mito, and DRP1^{K38A}.

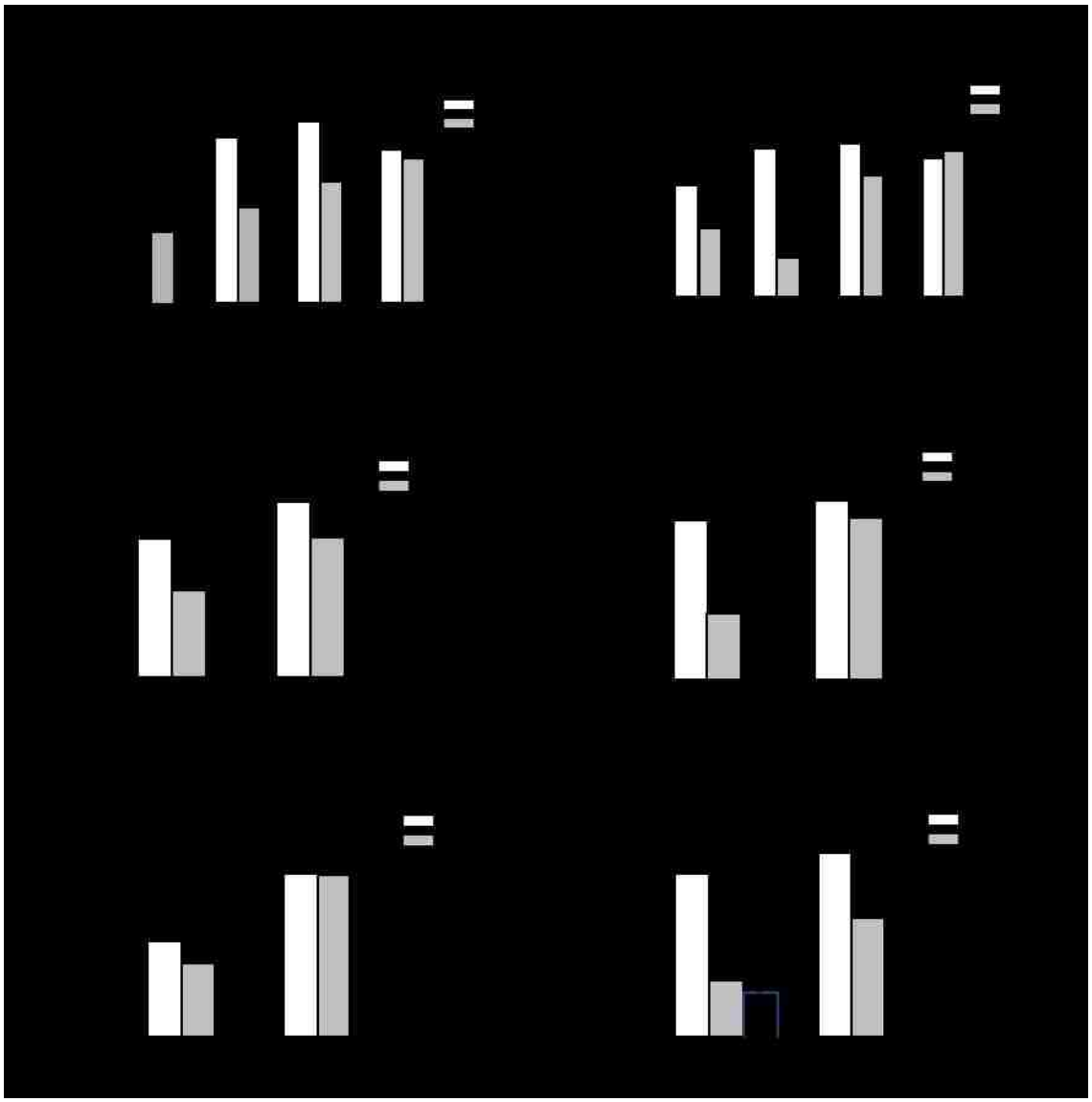

Figure 25 Restoration of mitochondrial fusion with DRP1^{K38A} or DRP1^{K38A} and MFN2^{p82} rescues neurons from neuritic trafficking defects.

A) Anterograde and retrograde movement of mitochondria in neurons expressing either HTT exon1-Q17, -Q46, or -Q97 alone or in combination with DRP1^{K38A} alone or DRP1^{K38A} and MFN2^{p82}. B) Motility of mitochondria in neurons expressing either HTT exon1-Q17, -Q46, or -Q97 alone or in combination with either DRP1^{K38A} alone or both DRP1^{K38A} and MFN2^{p82}. C) Mean velocity of mitochondria in neurons expressing either HTT exon1-Q17, -Q46, or -Q97 alone or in combination with DRP1^{K38A} alone or DRP1^{K38A} and MFN2^{p82}. Results are representative of three or more independent experiments. Statistics: Two-way ANOVA with post-hoc test.

3.4 Discussion

Mitochondrial dysfunction has been implicated in HD pathogenesis (as introduced in Section 3.1.3.4). Mitochondrial dynamics is fundamental for support and maintenance of mitochondrial function (Detmer and Chan, 2007). Imbalanced mitochondrial dynamics (fission, fusion, and transport) results in reduced ATP synthesis, elevated ROS production, and impaired Ca^{2+} buffering capacity, which in turn leads to failure in the maintenance of neuronal function and eventual neuronal death. Thus, defective mitochondrial dynamics might be the mechanism underlying mitochondrial dysfunction in HD pathogenesis.

Here, we showed that mitochondrial fragmentation occurs in mutant HTT-expressing primary neurons in a polyQ-dependent manner (Figure 16). An increased ratio of the frequency of mitochondrial fission to fusion implies that mitochondrial fragmentation may result from either excessive fission or insufficient fusion (Figure 16C). HTT is highly expressed in neurons and plays an essential role in neuronal development and survival. Mutant HTT-induced cell death seems to be specific to neurons, because HeLa cells expressing mutant HTT exon1 did not exhibit round and fragmented mitochondria. Rather, mitochondria became fragmented only when cells were treated with hydrogen peroxide (Wang et al., 2009), indicating a specific role of mutant HTT in neurons.

Due to its large molecular weight, full-length HTT is difficult to transfect into the cells. Therefore, HTT exon1, which contains the polyQ region, is always used in HD studies *in vitro*. However, whether full-length mutant HTT causes the same toxic effect as HTT exon1 in neurons

remained to be illustrated. Our data of human fibroblasts from HD patients demonstrated that full-length mutant HTT induces mitochondrial fragmentation (Figure 17), which confirms that mutant HTT-induced mitochondrial fragmentation in neuronal cultures is not an artifact of HTT exon1 overexpression. In addition to the neuronal culture data, we also investigated mitochondrial morphology in striatal neurons using YAC mice (data not shown) and our findings further confirmed that mutant HTT triggers mitochondrial fragmentation *in vivo*.

In addition to mitochondrial morphology, mitochondrial transport is also impaired in mutant HTT exon1-expressing neurons (Figure 18). Defects in mitochondrial directional movement, mean velocity, and overall mobility are all polyQ-dependent, which is in agreement with disease onset in HD patients, suggesting that defects in mitochondrial dynamics are implicated in HD progression. PolyQ length determines the consequences of defects in mitochondrial dynamics; however, whether defective mitochondrial dynamics is the primary cause of HD remains unclear. More importantly, how mutant HTT impairs mitochondrial dynamics also remains to be determined.

HTT is known to associate with mitochondria; however, the exact role of this interaction remains unclear. A previous study revealed that mutant HTT localized on mitochondria (Panov et al., 2002), and our findings that mutant HTT formed aggregates and co-localized with mitochondria are consistent with this report (Figure 19). As suggested by combined analysis of the data presented here and the findings of Panov *et al.*, it is possible that mutant HTT induces mitochondrial fragmentation by its abnormal interaction with certain mitochondrial proteins involved in mitochondrial dynamics.

As previously reported, mutant HTT forms a ring-like structure around the mitochondrion (Panov et al., 2002), which is similar to the patterns of DRP1 localization onto mitochondria. Moreover, HTT interacts with Dynamin, which is the structural homolog of DRP1, through HAP1 and regulates membrane fission during endocytosis (McGuire et al., 2006). Thus, it is no surprise that HTT interacts with DRP1 and mediates mitochondrial fission. As hypothesized, mutant HTT binds to DRP1 more strongly than WT (Figures 20, 21). Because DRP1 plays in a role in both mitochondrial morphogenesis and distribution, the abnormal interaction between HTT and DRP1 may alter DRP1 function, which in turn could lead to defects in mitochondrial dynamics and eventual cell death.

Although there are more interactions between mutant HTT and DRP1 in YAC 128 mice (Figure 21), these interactions may result from artifacts of mutant HTT overexpression. To exclude such a possibility, both lymphoblasts and postmortem tissues from HD patients were used for analysis in our lab (Song et al., 2011). We found that mutant HTT binds much more strongly to DRP1 in physiological conditions, and this increased binding strength is not caused by protein overexpression.

The structural homolog of DRP1, Dynamin, interacts with HTT through HAP1. Experiments utilizing tissues from both YAC mice and HD patients are not sufficient to determine whether HTT directly or indirectly binds to DRP1. Thus, DRP1 and HTT recombinant proteins were used to perform CoIP assays in order to examine the direct interaction between HTT and DRP1 (Song et al., 2011). My colleague Jin Chen demonstrated a high binding affinity between DRP1 and Q53 using purified recombinant protein at different concentrations. In

addition, she observed a higher DRP1 GTPase activity in the presence of HTT-Q53 than in the presence of HTT-Q20. Taken together, our data confirmed that mutant HTT binds to DRP1 and increases its GTPase activity.

Previous studies have revealed that DRP1 is not only required for mitochondrial fission and distribution (Pitts et al., 1999; Smirnova et al., 2001), but also interferes with neuronal function and even embryonic viability (Ishihara et al., 2009; Li et al., 2004; Wakabayashi et al., 2009). DRP1 activity must be balanced, as either loss of DRP1 or DRP1 overexpression jeopardizes neuronal survival (Barsoum et al., 2006; Uo et al., 2009). In HD, the elevated DRP1 GTPase activity induced by mutant HTT disrupts this balance and mediates neuronal cell death, which might be the mechanism of the disease.

Decreasing DRP1 activity by expressing dominant-negative $DRP1^{K38A}$ re-balances mitochondrial fission and fusion and transport in neurons expressing mutant HTT (Figures 22, 24). However, it is interesting that DRP1 knockdown does not rescue mutant HTT-induced mitochondrial fragmentation and neuronal cell death (Figure 23), which is consistent with a previous report that DRP1 knockdown leads to neuronal cell death (Uo et al., 2009). A possible explanation for this apparent discrepancy is that $DRP1^{K38A}$ expression does not interfere with endogenous $DRP1^{WT}$ expression, while DRP1shRNA knocks down most endogenous DRP1 expression. Therefore, the balance shifts toward mitochondrial fusion completely when DRP1shRNA is expressed, which in turn results in an opposite, but equally lethal, imbalance in mitochondrial dynamics. However, this explanation cannot account for the abnormal neuronal structure observed in DRP1shRNA expressing neurons. It is known that DRP1 knockout leads to

embryonic lethality (Ishihara et al., 2009; Wakabayashi et al., 2009), which implies that DRP1 plays a role in embryonic development. Because DRP1^{K38A} does not disturb neuronal development, it would seem that DRP1 has other functions independent of DRP1 GTPase activity.

Although abnormal binding of mutant HTT and DRP1 has been revealed, how and where this interaction occurs need to be further investigated. As previously discussed, DRP1 may play multiple roles in neuronal cells including development and survival functions. Inhibition of DRP1 using pharmacological chemicals might prevent excessive mitochondrial fission by disturbing the interaction between DRP1 and mutant HTT *in vivo*; however, inhibition might not necessarily protect against cell death, because the DRP1 inhibitor might also interfere with normal DRP1 functions. Thus, simply applying DRP1 inhibitors may not work well as a therapeutic treatment and further characterization of DRP1 and mutant HTT is required.

In sum, mutant HTT triggers excessive mitochondrial fission in a polyQ-dependent manner. The aberrant interaction between mutant HTT and DRP1 on mitochondria increases DRP1 GTPase activity and therefore induces mitochondrial fragmentation, which in turn results in elevated neuronal cell death. Decreasing DRP1 GTPase activity by expression of dominant-negative DRP1^{K38A} or active MFN2^{p82} restores the mitochondrial fission and fusion balance and rescues cell death. Thus, we conclude that defective mitochondrial dynamics is a mechanism underlying HD pathogenesis and DRP1 might be a molecular target for therapeutic treatment of HD.

CHAPTER FOUR: MITOCHONDRIAL DYNAMICS AND SIRT3

4.1 Introduction

4.1.1 Caloric restriction and aging

Caloric restriction (CR) has long been known to increase life span in rodents (Weindruch and Walford, 1988). Dietary restriction is characterized by a 30–40% reduction in food in-take. More recently, CR-mediated retardation of aging has been well recognized in a number of animal models, including yeast, mice, rats, and monkeys (Colman et al., 2009; Lee et al., 2000; Migliaccio et al., 1999; Weindruch and Walford, 1988). In addition to extending life span, CR has also been shown to delay brain function decline and prevent age-related diseases (Mattson, 2003; Patel et al., 2005; Wang et al., 2005; Weindruch and Walford, 1988).

Originally, the mechanism of CR-mediated protection was a mystery. Several hypotheses were raised, including ROS suppression. CR mice appear to be more resistant to oxidative stress (Sohal and Weindruch, 1996). This is in agreement with the "Free Radical Theory of Aging" put forth by Dr. Harman in 1956 (Harman, 1956). Recently, a microarray analysis confirmed this idea at the molecular level by demonstrating that CR up-regulates genes involved in oxidant defense in the brains of aging mice (Lee et al., 2000). Another study in p66(shc)-/- mice further indicated that resistance to oxidative stress contributes to life span extension (Migliaccio et al., 1999). Oxidants mediate phosphorylation of p66, which in turn inhibits expression of antioxidant genes (Purdom and Chen, 2003). Ablation of p66 in mice and cells resulted in more

resistance to stress and less apoptosis in response to H_2O_2 and UV exposure (Migliaccio et al., 1999). These p66-/- mice exhibit a 30–40% extension in life span, which is similar to CR mice. Thus, CR may increase life span through ROS suppression.

In the past decade, silent information regulator 2 (Sir2) was identified as a key player in CR-mediated life span expansion and protection against age-related diseases (Cohen et al., 2004). Since then, the number of studies focusing on sirtuins has dramatically increased and has helped to elucidate their roles in CR-mediated longevity.

4.1.2 Sirtuins

Sir2 was the first sirtuin gene found in *Saccharomyces cerevisiae* (Rine and Herskowitz, 1987; Shore et al., 1984), and is a class III histone deacetylases. Seven human homologs (SIRT1-7) have been identified with different subcellular localizations, suggestive of diverse cellular functions (Figure 26A).

Sirtuins are nicotinamide adenine dinucleotide (NAD^+)-dependent deacetylases which directly remove the acetyl group from lysine residues and transfer it to ADP-ribosomes, resulting in deacetylated substrates and formation of nicotinamide (NAM) (Figure 26B) (Imai et al., 2000). NAM is an inhibitor of the deacetylase reaction, while it can also be recycled to form NAD^+. As an activator, NAD^+ levels directly regulate sirtuin deacetylase activity and directly link sirtuins to the metabolic state of the cell. To date, SIRT4 is the only sirtuin for which deacetylase activity has not been identified.

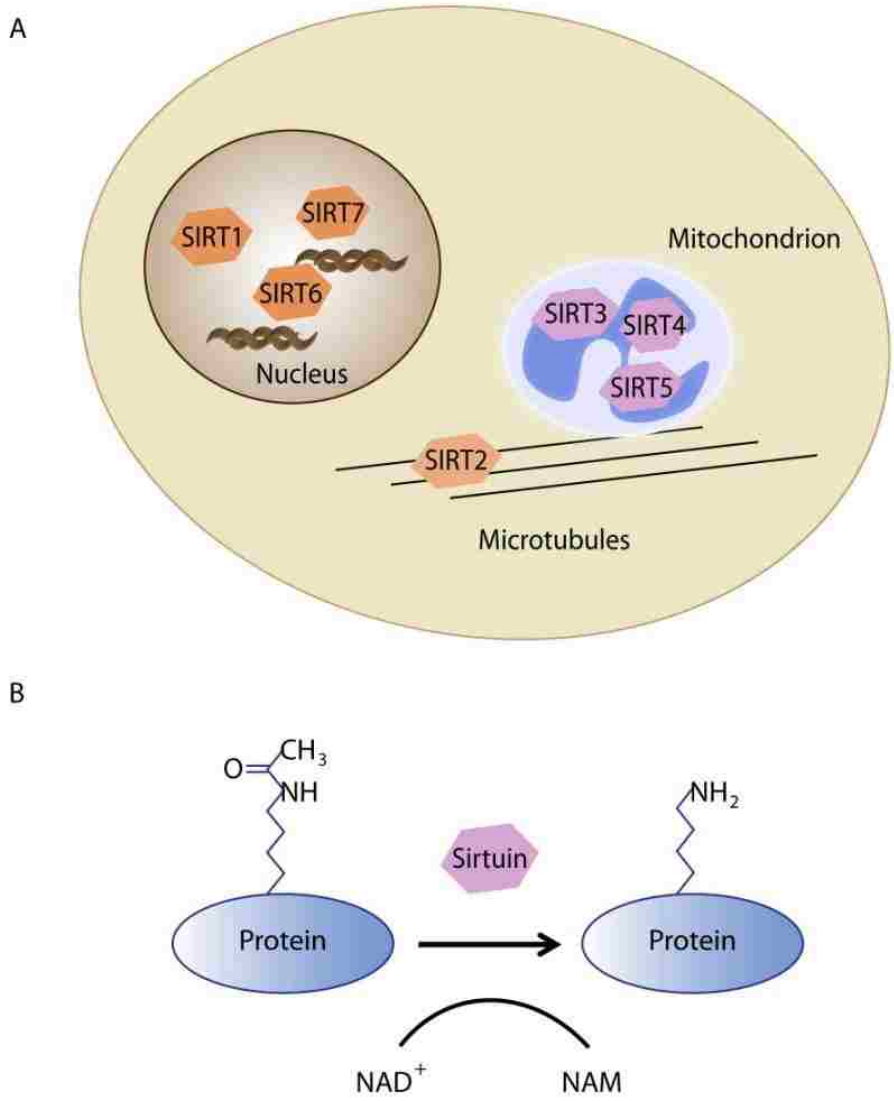

Figure 26 Sirtuins in a eukaryotic cell.

A) Illustration of localization of mammalian sirtuins. B) Schematic of the sirtuin-mediated deacetylase reaction.

4.1.3 Sirtuins, aging, and neuroprotection

As a post-translational modification, acetylation/deacetylation has been shown to modulate protein activity, stability, and subcellular localization, and thus allow adaptations to metabolic alterations and stress.

Sir2 was first identified as a longevity gene in yeast (Imai et al., 2000). Subsequent studies revealed that Sir2 was necessary for CR-mediated life span extension (Lee et al., 2000). An increase in Sir2 expression extends life span in C. *elegans* (Tissenbaum and Guarente, 2001). SIRT1 is the closest mammalian homolog to Sir2 and has been shown to be required for CR-mediated longevity in mice (Chen et al., 2005a). In addition to life span, sirtuins also play an essential role in many age-related diseases, including cancer, diabetes, and neurodegenerative diseases (Araki et al., 2004; Kim et al., 2007a; Mostoslavsky et al., 2006; Someya et al., 2010). To date, SIRT1 and SIRT3, which are involved in up-regulating a number of different cell signaling pathways, are the most extensively studied sirtuins in mammals. Because sirtuins are involved in so many pathways, it is difficult to isolate which pathway is responsible for sirtuin-mediated longevity.

Mitochondrial dysfunction has been implicated in neurodegeneration. In particular, its role in HD and ALS was extensively discussed in the previous two chapters. There is little doubt that mitochondria could play an important role in CR-mediated neuronal protection. In addition, more than 20% of mitochondrial proteins are acetylated, further supporting the idea that mitochondrial function may be regulated by sirtuin-mediated deacetylation (Kim et al.,

2006). Indeed, most mitochondrial functions, including apoptosis, ATP production, and ROS regulation, have been found to be regulated by sirtuins (Figure 27).

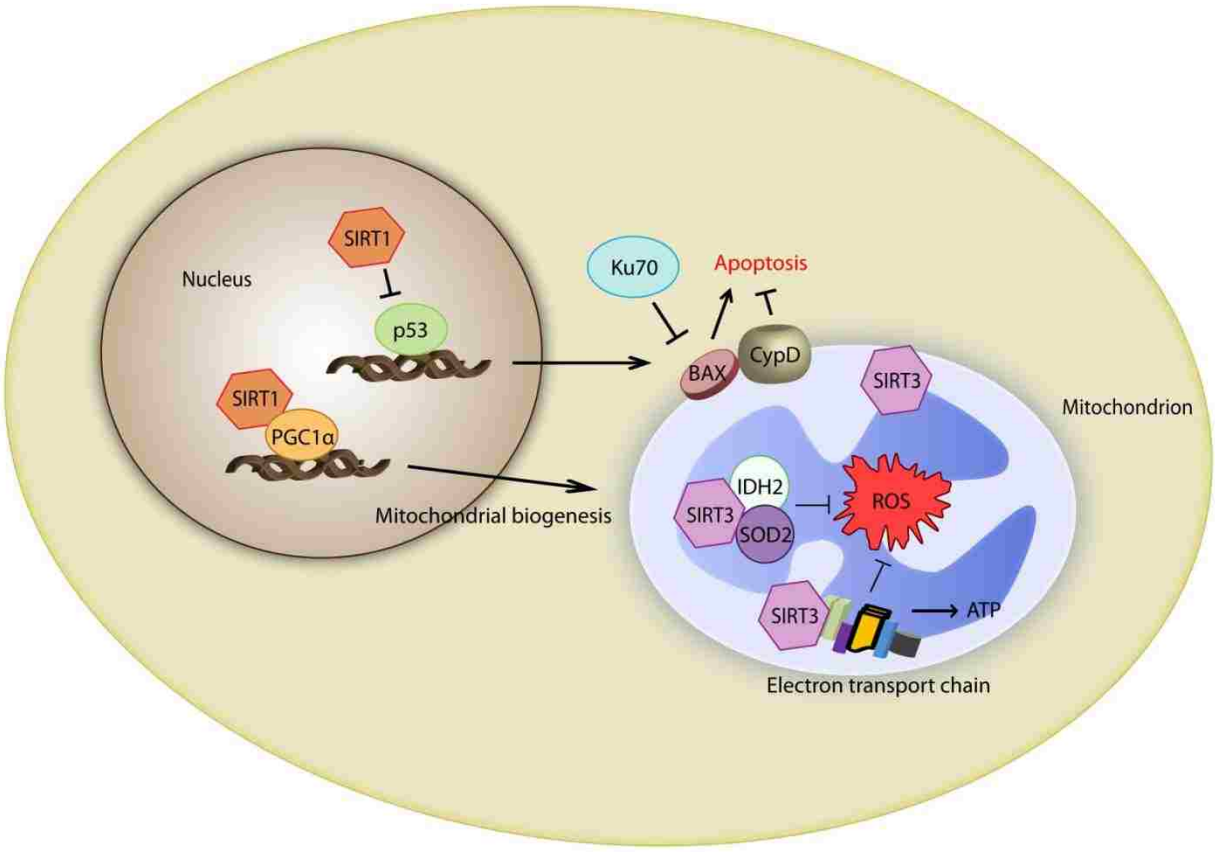

Figure 27 Pathways linking sirtuins and mitochondria.

4.1.3.1 Apoptosis in response to stress

Tumor suppressor p53, a key transcription factor in the response to DNA damage and oxidative stress, up-regulates DNA repair, cell cycle exit, and apoptosis. SIRT1 has been shown to negatively regulate p53 through deacetylation, protect against p53-mediated apoptosis, and promote cell survival (Luo et al., 2001; Vaziri et al., 2001).

Forkhead (FOXO) proteins, another family of transcription factors, trigger apoptosis in response to stress. FOXO1, 3, and 4 are SIRT1 substrates. Similar to p53, SIRT1 deacetylates FOXO proteins and represses FOXO-mediated apoptosis (Motta et al., 2004; Purdom and Chen, 2003).

Moreover, SIRT1 protects cells from apoptosis by deacetylating ku70, allowing it to sequester the pro-apoptotic protein BAX from mitochondria (Cohen et al., 2004).

Furthermore, SIRT3 promotes cell survival by deacetylating cyclophilin D (CypD), which opens the MPTP during apoptosis (Hafner et al., 2010). Deacetylation of CypD is beneficial for cardiac hypertrophy.

In sum, SIRT1 promotes cell survival against apoptosis by negatively regulating apoptosis through Bcl-2 family proteins, while SIRT3 inhibits MPTP opening through CypD, which might be the mechanism involved in CR-mediated cell survival.

4.1.3.2 Mitochondrial ROS regulation

The "Free Radical Theory of Aging" espoused by Dr. Harmon in 1956 emphasized the role of ROS in aging (Harman, 1956). Indeed, there is strong evidence suggesting a correlation between oxidative stress and life span. Mitochondria are the main source of ROS, which is a by-product of OXPHOS. To balance this highly oxidized environment, a number of anti-oxidant enzymes reside in the mitochondrial matrix. It has been proposed that either inhibition of mitochondrial OXPHOS or a reduction in the oxidative defense results in ROS induction and oxidative damage to DNA, proteins, and lipids (Wallace, 2005).

Overexpression of catalase targeted to mitochondria reduces oxidative stress and extends lifespan in mice, further suggesting that ROS plays a role in longevity and maintenance of mitochondrial function is important (Schriner et al., 2005). Put simply, increased mitochondrial ROS contributes to aging, while decreased mitochondrial ROS may participate in CR-mediated lifespan extension.

PGC-1α, a transcriptional co-activator of genes that encode mitochondrial proteins, plays a role in up-regulating mitochondrial biogenesis and ROS suppression in neurodegeneration (St-Pierre et al., 2006). Deacetylation of PGC-1α by SIRT1 has been shown to activate the transcription of its target genes (Rodgers et al., 2005). Thus, ROS suppression is implicated in CR-mediated protection because it up-regulates mitochondrial biogenesis through the SIRT1-PGC-1α pathway. Indeed, increased SIRT1 levels associated with increased mitochondrial proteins and reduced ROS have been observed in humans undergoing a 6-month

CR trial (Civitarese et al., 2007). Furthermore, resveratrol, a SIRT1 activator, up-regulates mitochondrial biogenesis through the SIRT1-PGC1α pathway in mice (Lagouge et al., 2006).

PGC-1α also up-regulates SIRT3 at the transcription level and has been shown to directly participate in mitochondrial ROS suppression during CR (Bell and Guarente, 2011). The most convincing evidence for this phenomenon comes from a recent paper on hearing loss (Someya et al., 2010). Oxidative accumulation caused death of spiral ganglia neurons in the inner ear cochlea, resulting in hearing loss, which is commonly associated with aging. SIRT3 was shown to be required for CR protection against oxidative stress and hearing loss. Isocitrate dehydrogenase 2 (IDH2), which is involved in ROS regulation, was identified as the substrate of SIRT3. Deacetylation of IDH2 leads to an increase in reduced glutathione and protection against oxidative stress. Taken together, the results of the Someya *et al.* study not only confirmed the "Free Radical Theory of Aging," but also suggested that mitochondria are important in the aging process.

Along this line of reasoning, SOD2, a critical antioxidant enzyme in the mitochondrial matrix, is also a substrate of SIRT3 (Qiu et al., 2010; Tao et al., 2010). SIRT3-mediated deacetylation of SOD2 results in increased anti-oxidant activity. Furthermore, SIRT3 directly regulates ROS by enhancing mitochondrial respiration through deacetylation of complexes I and II in addition to ROS suppression (discussion later) (Ahn et al., 2008; Cimen et al., 2010).

In sum, SIRT3 negatively regulates mitochondrial ROS production and participates in ROS suppression, which is required for CR-mediated neuroprotection.

4.1.3.3 Mitochondrial respiration and ATP production

A decline in intracellular ATP levels is commonly associated with aging and apoptosis (Tsujimoto, 1997). Decreased ATP levels were observed in SIRT3-/- mice (Ahn et al., 2008), suggesting that SIRT3 plays a role in OXPHOS and ATP production. Inhibition of mitochondrial respiration by a mutation in a subunit of complex II induces oxidative stress and decreases lifespan in nematodes (Ishii et al., 1998), suggesting an important role of mitochondrial OXPHOS in longevity. Recently, some subunits of the mitochondrial ETC have been found to be deacetylated by SIRT3 (Ahn et al., 2008; Cimen et al., 2010). Deacetylation by SIRT3 increases the activities of the respiratory complexes, which may further increase ATP production. Moreover, ATP synthase is modified by lysine acetylation and the interaction between SIRT3 and ATP synthase was identified by a proteomic study (Law et al., 2009). Although no deacetylation has been found, it is possible that SIRT3 directly regulates ATP synthesis through ATP synthase deacetylation.

In sum, SIRT3 regulates mitochondrial respiration and ATP production, which contributes to protective effects against aging.

4.1.4 Sirtuins and mitochondrial dynamics

As previously discussed, sirtuins are involved in virtually all mitochondrial-related processes including mitochondrial biogenesis, anti-oxidant defense, OXPHOS, and ATP production. Mitochondrial fission and fusion balance is crucial for maintaining these

fundamental functions in neurons. Because mutations in OPA1 and MFN2 cause ADOA and CMT-2A, respectively, there is no doubt that defects in mitochondrial fission and fusion machinery can cause neurodegeneration. Moreover, a previous study revealed that a decrease in DRP1 activity extended lifespan in yeast, further indicating that mitochondrial dynamics participates in longevity (Yang et al., 2011). Thus, it is interesting to investigate whether sirtuins can directly regulate components of the mitochondrial fission and fusion machinery, such as DRP1 and OPA1, and may represent a more bioenergetically efficient way to up-regulate mitochondrial function and promote cell survival.

Recently, a proteomic study revealed that both DRP1 and OPA1 are acetylated (Choudhary et al., 2009), which is worth further investigation to verify if these two proteins can be regulated by sirtuins (Figure 28). The acetylation site of DRP1 (K283) is located in the GTPase domain, suggesting an important role in GTPase activity regulation. More strikingly, a yeast hybrid assay revealed a direct interaction between DRP1 and SIRT3 (Stelzl et al., 2005). Therefore, we hypothesize that mitochondrial machinery may be regulated by sirtuins, indicating potential involvement in sirtuin-mediated longevity.

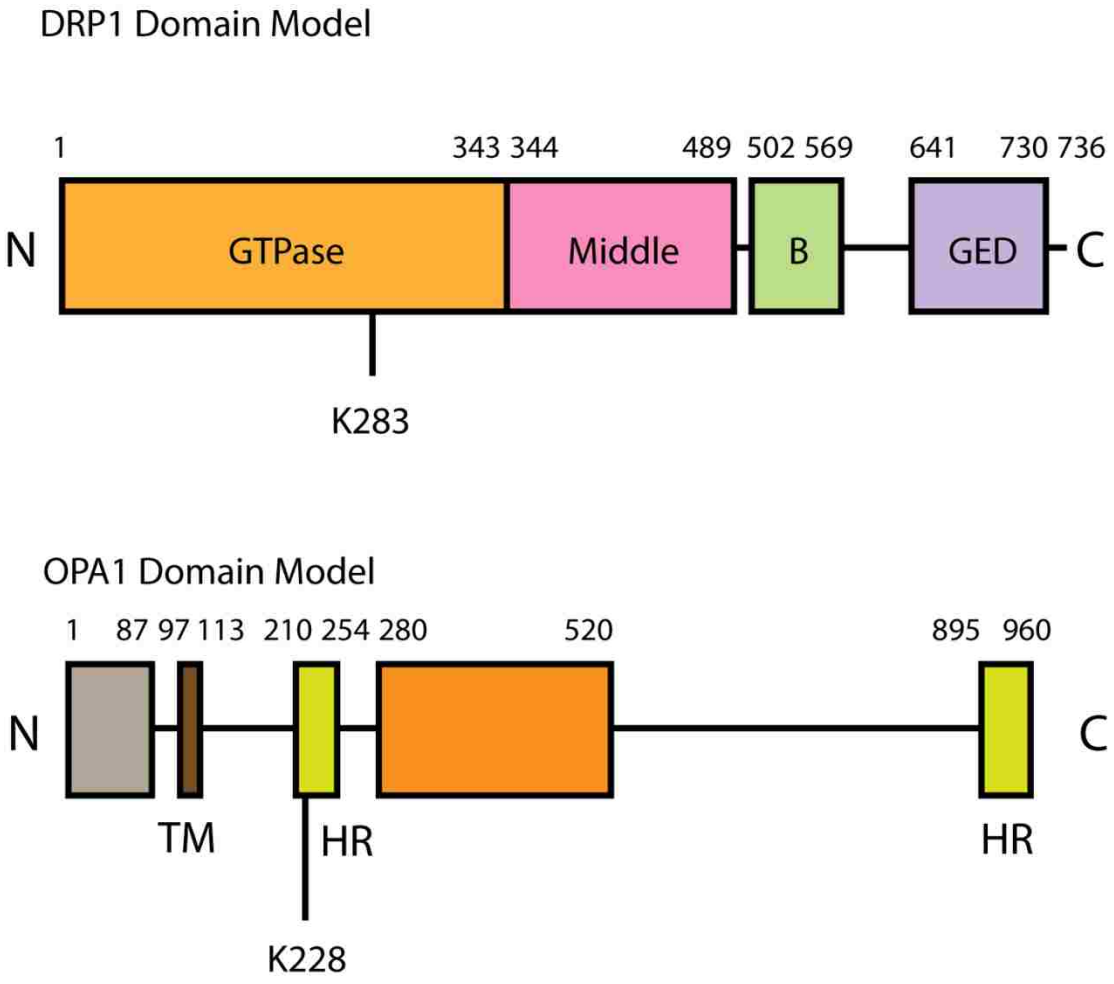

Figure 28 Domain models of the acetylation sites in DRP1 and OPA1.

4.2 Materials and Methods

4.2.1 Reagents

The pDsRed2-Mito vector was obtained from Clontech. The pcDNA3.1-SOD1^{WT} and -SOD1^{G93A} were obtained from Dr. Alvaro G. Estevez (University of Central Florida, Orlando, FL, USA). The pEGFP-C2-SOD1^{WT} and -SOD1^{G93A} were provided by Dr. Kurt J. De Vos (King's College London, London, UK). The pcDNA3.1-SIRT3-HA vector was provided by Dr. Eric M. Verdin (Gladstone Institute of Virology and Immunology at UCSF, San Francisco, CA, USA). The pcDNA-EGFP-DRP1S616A, pcDNA-EGFP-DRP1S616D, pcDNA-EGFP-DRP1S637A, and pcDNA-EGFP-DRP1S637D were made by my colleague Dr. Bossy. All plasmids were purified using the Endotoxin-free Marligen Maxiprep Kit (Diagnostic technology, Belrose, Australia). HEPES was purchased from Omega Scientific (Tarzana, CA, USA). Poly-L-lysine, Penicillin-streptomycin (Pen/Strep), NAM, N-ethylmaleimide (NEM), trichostatin A (TSA), formaldehyde, pyruvate, resveratrol, and F-12 HAM were all obtained from Sigma-Aldrich (St. Louis, MO, USA). Custom-made phenol-free DMEM/high glucose and BCS were obtained from Thermo Scientific (Rockford, IL, USA). DMEM/high glucose for MEFs was obtained from ATCC (Manassas, VA, USA). Glutamax and HBSS were purchased from Gibco (Carlsbad, CA, USA). Lipofectamine 2000, Hoechst 33342, and neurobasal medium were purchased from Invitrogen (Carlsbad, CA, USA). Protease inhibitor cocktails were purchased from Roche (Indianapolis, IN, USA). EDTA and mouse antibodies to Actin were purchased from Calbiochem (Darmstadt, Germany). 3-[(3-cholamidopropyl)dimethylammonio]-1-propanesulfonate (CHAPS) was purchased from G-

biosciences (Maryland Heights, MO, USA). Dithiothreitol (DTT) was purchased from GE Healthcare (Piscataway, NJ, USA). FBS was obtained from Atlanta Biologicals (Lawrenceville, GA, USA). SIRT2/3 Fluorimetric Drug Discovery Kit was purchased from Enzo Life Sciences (Farmingdale, NY, USA). TurboFect was obtained from Fermentas (Glen Burnie, MD, USA). Mouse antibodies to DRP1 (clone8/DLP1) and OPA1 were obtained from BD Biosciences (San Jose, CA, USA) and VDAC and SUMO1 were obtained from Cell Signaling (Danvers, MA, USA). Rabbit antibodies to pDRP1 (S616), pDRP1 (S637), acetylated-lysine, and SIRT3 were obtained from Cell Signaling (Danvers, MA, USA). Rabbit antibodies to GFP were obtained from Abcam (Cambridge, MA, USA). Costumed rabbit antibodies to acetylated DRP1 (K283) were generated from YenZym (South San Francisco, CA, USA).

4.2.2 Mice and rats

SIRT3-/- mice (129-SIRT3$^{tm1.1Fwa}$/J) were purchased from Jackson Lab and fasted for 16 h before performing the experiments.

Pregnant rats of a Sprague-Dawley background (Charles River) were used for primary cortical cultures.

All experiments were approved by the Institutional Animal Care and Use Committee of University of Central Florida College of Medicine.

4.2.3 Primary cortical neurons and transfection

Cortical neurons (400,000 cells/ml) were prepared from E18 rat embryos (Barsoum et al., 2006)and transfected at 5 DIV with Lipofectamine 2000 (Invitrogen). Cells were cultured in neurobasal medium (Gibco) supplemented with 2% Neuronal Supplement 21, 1× Pen/Strep, 2 mM GlutaMAX. Neuronal Supplement 21 was prepared according to Chen *et al.* (Chen et al., 2008). Experiments were carried out two days after transfection.

4.2.4 MEFs and HEK cells

HEK293T cells were grown in DMEM supplemented with 10% FBS, Pen/Strep, and 1 mM Pyruvate. Two days after seeding, cells were transfected with different plasmids using Turbofect according to manufacturer's instructions. 36 or 48 hours later, cells were harvested using lysis buffer containing 50 mM HEPES (pH 7.4), 2 mM $MgCl_2$, 1 mM EDTA, 2% CHAPS, 2 mM DTT, 10 mM NAM, 1 μM TSA, 10 mM NEM, and protease inhibitor cocktails (Roche), and centrifuged at 22,000 g, 4°C, for 15 min, followed by BCA test (Pierce) to determine protein concentrations.

4.2.5 Fluorescence microscopy

Both fixed and live-cell imaging of neurons were performed using an Axiovert Zeiss 100M inverted fluorescence microscope equipped with a Plan Apochromat 63×1.4 NA oil objective, a DG-4/Lambda 10-2 combo Xe-arc illumination unit (Sutter), and a Sensicam QE

cooled CCD camera (PCO AG, Germany) controlled by MetaMorph 7.1 software (Molecular Devices) as previously described (Song et al., 2008). The excitation filter for DsRed2-Mito was S555/28× (Chroma) and the emission filter was S617/73m (Chroma). The excitation filter for EGFP was S490/20× (Chroma) and the emission filter was S528/38m (Chroma). Images were acquired using the Multi Dimensional Acquisition module in MetaMorph 7.1 (2×2 binning, 0.2 μm step size, and 15-20 z-planes). The z-series were processed by de-hazing followed by Fast Fourier Transform. Images were saved and exported as TIFF files after surface rendering using MetaMorph 4D-viewer.

For live-cell imaging, cortical neurons were plated on Lab-Tek II (#1.5 German Coverglass) 8-chamber slides (Thermo Fisher) at a density of 150,000 to 200,000 cells per chamber in neurobasal medium without phenol red (see detail in 3.2.5). A region containing 100 μm neurites in 10 neurons were selected and recorded for 5 min with 5 sec intervals at 37 °C under a humidified 5% CO_2 atmosphere. To limit photobleaching and phototoxicity, a 5 μm z-stack was acquired with 1 μm step size (2×2 binning) for each time point. Each z-stack was de-hazed and maximum projected in MetaMorph 7.1. To quantify mitochondrial movement, kymographs were generated with all planes, 25 μm line width, and average projected without background subtraction. The parameters of mitochondrial velocity and moving distance were exported from MetaMorph 7.1 into Excel for further analysis. Mitochondrial velocity ≥ 20 μm/min was classified as motile, while velocity < 20 μm/min was classified as stationary.

4.2.6 Scoring of mitochondrial fragmentation and neuronal cell death

Two days after transfection, the primary cortical neurons were fixed with 3.7% formaldehyde and 5% sucrose in PBS for 15 min at 37 °C. Nuclei were stained by Hoechst 33342 (1:10,000 in PBS) at room temperature for 10 min.

Scoring was performed in three different experiments independently. Statistics: Student's *t*-test.

4.2.7 Immune precipitation and western blotting

Brain tissues from SVB and SIRT3-/- mice were lysed in lysis buffer containing 50 mM HEPES (pH 7.4), 2 mM $MgCl_2$, 1 mM EDTA, 2% CHAPS, 2 mM DTT, 10 mM NAM, 1 μM TSA, 10 mM NEM, and protease inhibitor cocktails (Roche). Protein concentrations were determined by BCA test (Pierce). Lysates (500 μg) were used to perform immune precipitation by incubating with 7 μl polyclonal rabbit-anti-AcK antibodies (Cell signaling) at 4 °C, overnight, and then incubating with 50 μl protein G sepharose (GE Healthcare) at 4 °C for 2 h. Unbound proteins were removed by washing 3 times with ice-cold lysis buffer and the remaining proteins were then loaded onto NuPAGE 4–12% Bis-Tris gels (Invitrogen) under reducing conditions and transferred to nitrocellulose membranes (Hybond-ECL Nitrocellulose, 0.22 μm, GE Healthcare). The membranes were blotted with monoclonal mouse-anti-OPA1 (BD Bioscience), mouse-anti-DRP1 (BD Bioscience), mouse-anti-Actin (Calbiochem), SUMO1 (Cell Signaling), rabbit-anti-GFP (Abcam), rabbit-anti-SIRT3 (Cell Signaling), rabbit-anti-pDRP1S616 (Cell Signaling), and rabbit-

anti-pDRP1S637 (Cell Signaling) antibodies followed by sheep-anti-mouse IgG-HRP at 1:10,000 (GE Healthcare) or donkey-anti-rabbit at 1: 5000 (GE Healthcare).

Some membranes were overnight blocked using Odyssey blocking buffer (Li-Cor Biosciences), followed by incubation with Actin (Calbiochem), OPA1 (BD Biosciences), and SIRT3 (Cell Signaling) antibodies. Protein signals were detected by Li-Cor infrared imaging system. Data were further quantified by Image J.

4.2.8 Sirtuin activity assay

Spinal cord tissues from control littermates or $SOD1^{G93A}$ transgenic mice (5–7 months old) were lysed with buffer containing 50 mM HEPES (pH 7.4), 2 mM $MgCl_2$, 1 mM EDTA, 2% CHAPS, 2 mM DTT, 10 mM NAM, 1 μM TSA, 10 mM NEM, and protease inhibitor cocktails (Roche). Eight micrograms of protein was used to perform the deacetylase activity assay using the SIRT2/3 Fluorimetric Drug Discovery Kit (Enzo Life Sciences). The data were collected using 2104 EnVision Multi-label Plate Reader (PerkinElmer) with the excitation set at 355 nm and the emission set at 435 nm.

4.3 Results

4.3.1 Fasting and resveratrol induce SIRT3 expression

CR is known to promote longevity in mammals by up-regulating sirtuins. Fasting is a procedure used to mimic CR effects in animal models. To investigate whether SIRT3 is up-regulated, mice were fasted for 24 h and analyzed. As expected, SIRT3 expression levels were significantly induced in liver tissues after 24 h fasting (Figure 29A).

In addition, resveratrol is a sirtuin activator which has been shown to extend life span in several organisms (Howitz et al., 2003; Kim et al., 2007a; Lagouge et al., 2006). We used MEFs as a cell culture model *in vitro* to examine if SIRT3 is regulated by resveratrol. As expected, elevated SIRT3 levels were observed in MEFs after resveratrol treatment (Figure 29B).

Thus, SIRT3 responds to fasting in mice and resveratrol treatment in cell culture models.

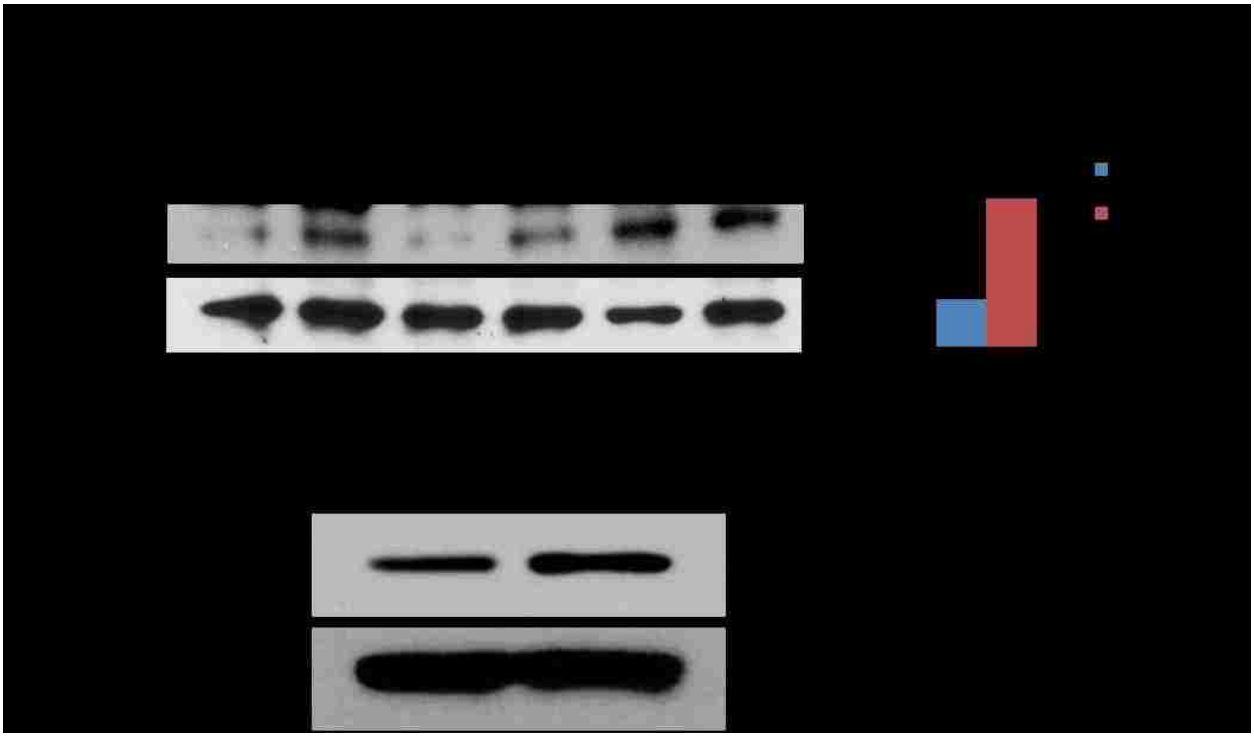

Figure 29 SIRT3 is up-regulated in response to fasting and resveratrol.

A) Western blot of cell lysates from mice with and without 24 h fasting. B) Western blot of cell lysates from MEFs with and without 5 mM resveratrol treatment for 24 h.

4.3.2 Resveratrol and nutrient depletion promote mitochondrial fusion

Having confirmed that CR/fasting and resveratrol extend life span and SIRT3 is up-regulated during this process, we next examined mitochondrial dynamics. Mitochondrial dynamics play an essential role in aging and neurodegeneration. Because SIRT3 is located inside

mitochondria, whether increased SIRT3 expression has any effect on mitochondrial dynamics in response to CR/fasting and resveratrol is an interesting question for investigation.

Primary cortical neurons treated with 100 nM resveratrol exhibited extremely long mitochondrial morphology (Figure 30A, bottom) compared with untreated neurons (Figure 30A, top). In addition, MEFs after 2 h nutrient depletion exhibited a more tubular network (Figure 30B). Thus, mitochondrial dynamics was affected by resveratrol and nutrient depletion, which might be through SIRT3 regulation.

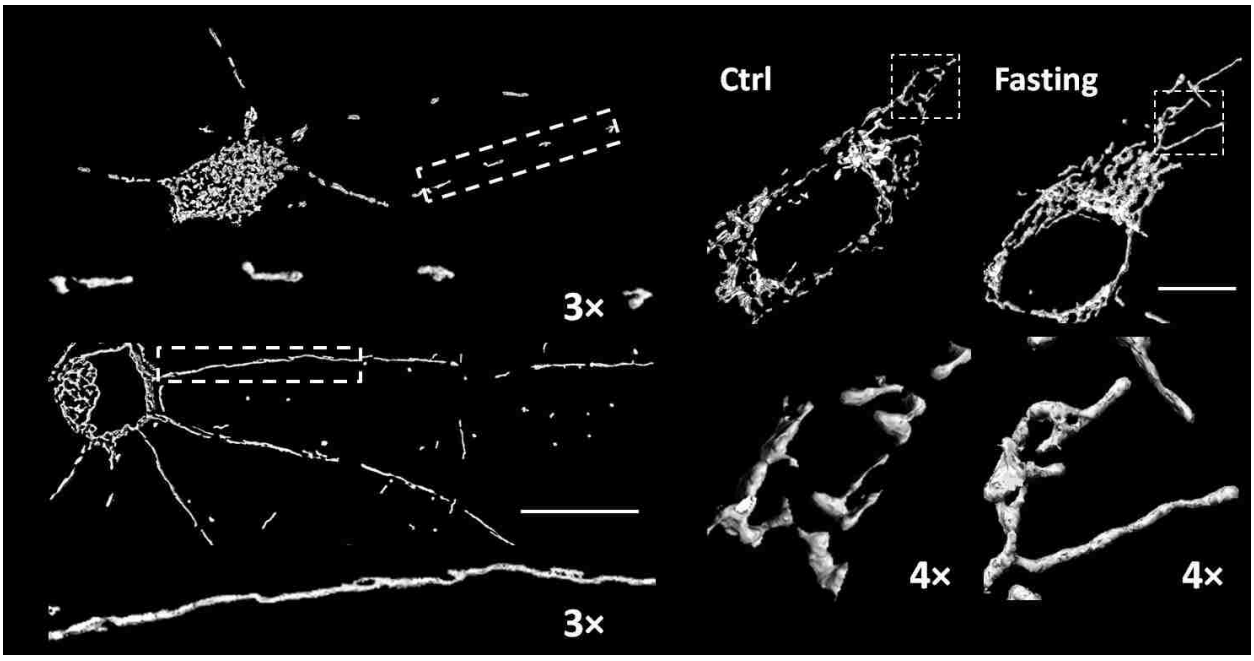

Figure 30 Resveratrol and nutrient depletion promotes mitochondrial fusion.

A) Fluorescence micrographs and close up views of cortical neurons transfected with DsRed2-Mito treated with and without 100 nM resveratrol for 24 h. Scale bar, 50 μm. B) Fluorescence micrographs and close up view of MEFs transfected with DsRed2-Mito with and without 2 h nutrient depletion. Scale bar, 25 μm.

4.3.3 Resveratrol alters post-translational modification of DRP1

Having determined that resveratrol affects mitochondrial dynamics, the next question we addressed was which protein is the target. We first examined if there was any alteration in the mitochondrial fission machinery.

Western blot was performed using MEFs treated with 5 μM resveratrol for 24 h. No change in DRP1 protein levels was observed (Figure 31); however, several post-translational modifications of DRP1 changed in response to resveratrol treatment (Figure 31). Phosphorylation of DRP1 at S616 decreased, while phosphorylation at S637 site tended to increase, suggestive of a reduction in mitochondrial fission. In addition, both acetylation and SUMOylation of DRP1 decreased, indicating that DRP1 is less stable and has faster turnover.

In sum, resveratrol induced phosphorylation of DRP1 at S637 and decreased phosphorylation at S616, acetylation, and SUMOylation. All of these changes result in decreased DRP1 activity, implying that mitochondrial fission is inhibited in response to resveratrol treatment.

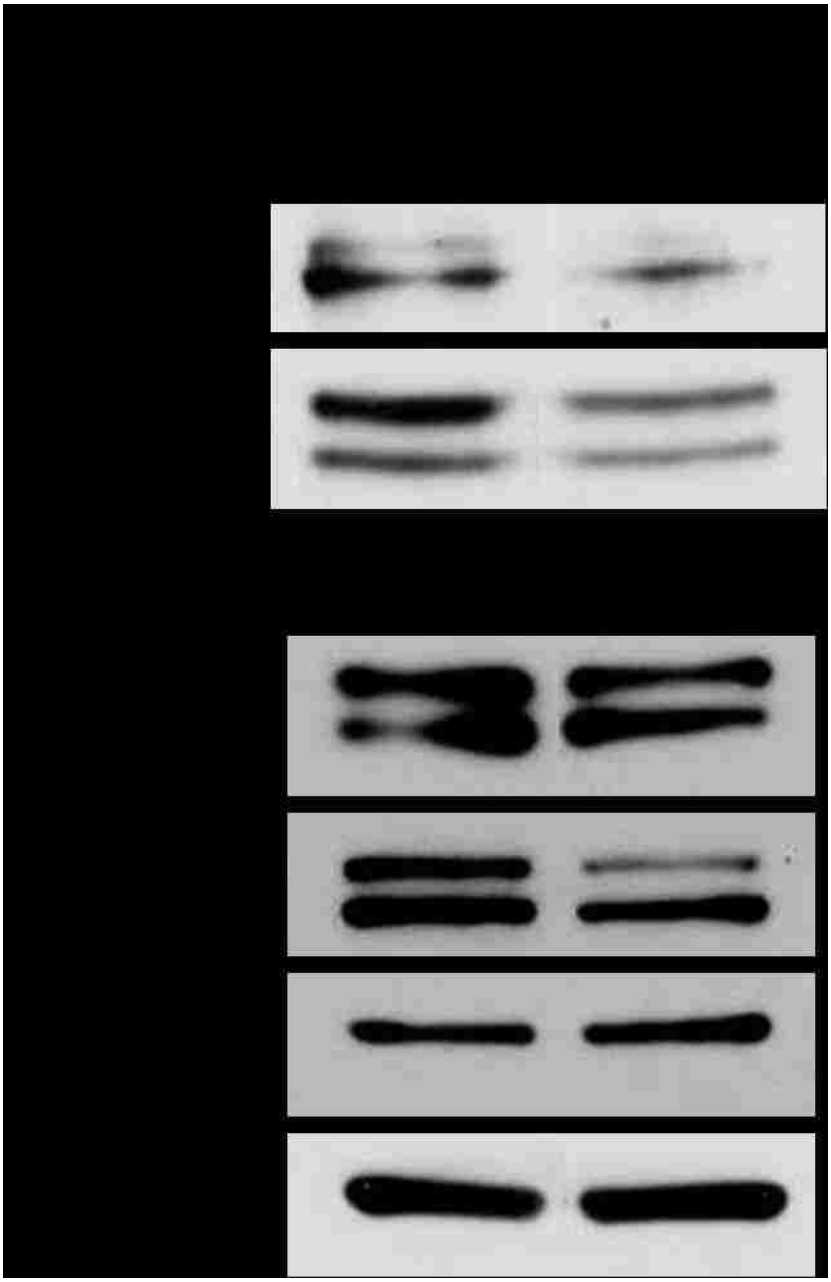

Figure 31 Western blot of lysates from MEFs treated with 5 μM resveratrol.

4.3.4 DRP1 post-translational modification directly interferes with mitochondrial dynamics

To confirm that phosphorylation of DRP1 directly regulates the mitochondrial fission and fusion balance, phospho-mimetic and phospho-resistant mutants were created and transfected into MEFs. DsRed2-Mito was also transfected and mitochondrial morphology was evaluated.

As expected, DRP1S616A MEFs exhibited elongated mitochondrial morphology, while DRP1S616D MEFs exhibited fragmented mitochondria (Figure 32 top), confirming that S616 phosphorylation induces mitochondrial fission. On the other hand, DRP1S637A MEFs exhibited short mitochondria, while DRP1S637D MEFs exhibited tubular mitochondrial shape (Figure 32, bottom). In sum, phosphorylation of DRP1 directly regulates DRP1 fission activity and interferes with mitochondrial morphology.

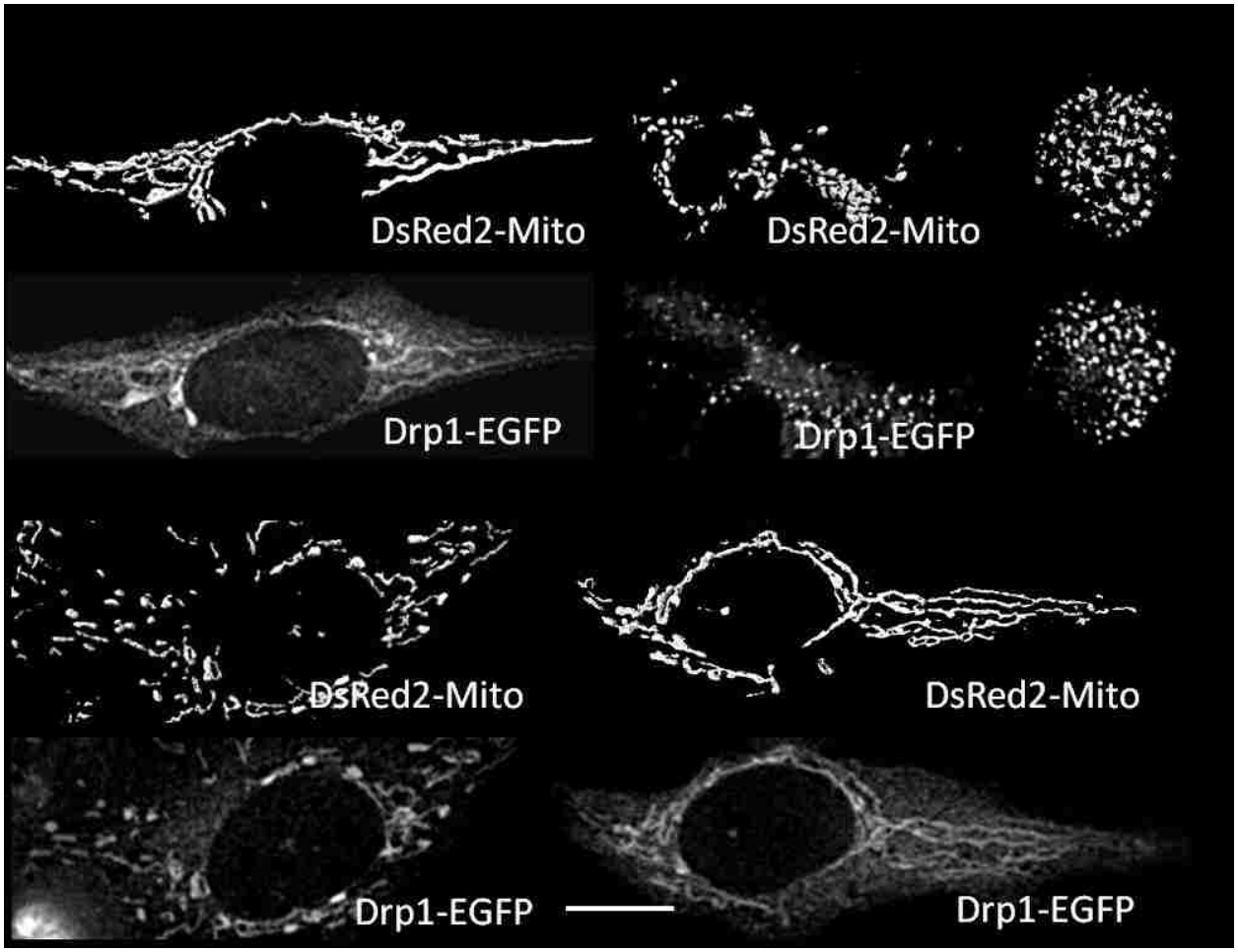

Figure 32 Fluorescence micrographs of MEFs transfected with DsRed2-Mito and different DRP1 mutants.

4.3.5 SIRT3 regulates OPA1 acetylation levels

Having established that resveratrol inhibits mitochondrial fission by altering DRP1 post-translational modifications, it is worthwhile to test if proteins mediating mitochondrial fusion are also regulated. SIRT3-/- mice were used here under 16 h fasting conditions.

Interestingly, OPA1 acetylation levels increased more than three fold in SIRT3-/- mice compared with WT mice (Figure 33). In particular, acetylation levels of the OPA1 long-isoform increased about 5 fold compared to a 2-fold increase in the short-isoform. Because the OPA1 long-isoform is more active in mediating mitochondrial fusion, we hypothesized that acetylation of OPA1 might be involved in mitochondrial fusion. In sum, OPA1 is a target of SIRT3 and may be implicated in mitochondrial fusion in response to CR/fasting.

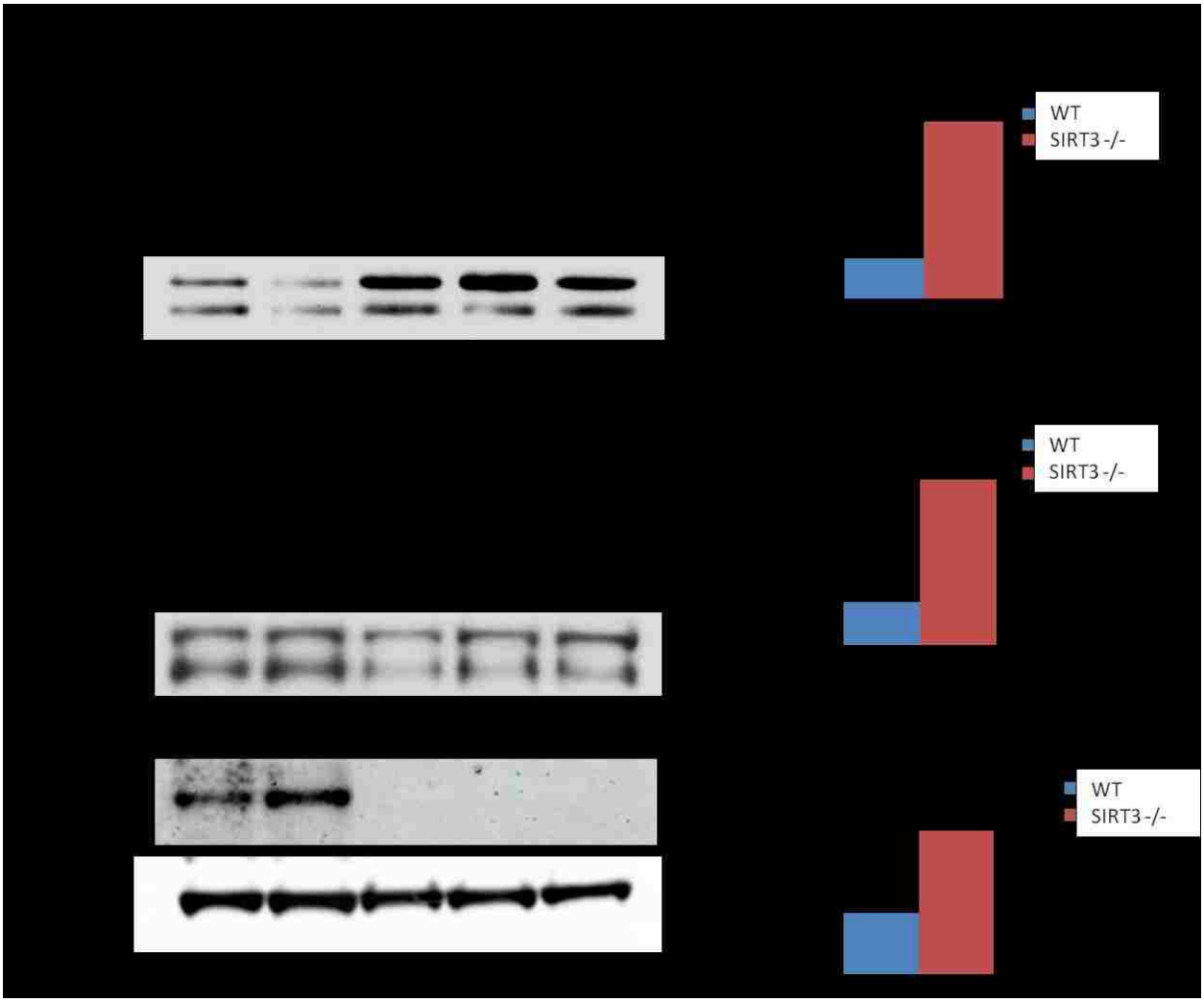

Figure 33 Immune precipitation and quantification of lysates from WT and SIRT3-/- mice using acetylation antibodies.

4.3.6 OPA1 acetylation directly interferes with mitochondrial dynamics

To evaluate if OPA1 acetylation level directly interferes with mitochondrial morphology, OPA1 plasmids with single nucleotide mutations in the acetylation site (Lys 228) were generated. To visualize mitochondria, DsRed2-Mito in combination with $OPA1^{WT}$ or $OPA1^{K228R}$ was transfected into MEFs.

WT MEF exhibited a tubular mitochondrial network, while SIRT3-/- MEFs exhibited more short and intermediate-sized mitochondrial morphology (Figure 34A, top), suggesting that SIRT3 is required for mitochondrial morphogenesis. SIRT3-/- MEFs expressing $OPA1^{WT}$ exhibited more tubular mitochondria than did SIRT3-/- MEFs (Figure 34A, bottom left), indicating that $OPA1^{WT}$ restored the mitochondrial fission and fusion balance. More strikingly, $OPA1^{K228R}$ SIRT3-/- MEFs exhibited the most tubular mitochondrial network, similar to WT MEFs (Figure 34A, bottom right). Further quantification confirmed the observations of mitochondrial morphology in these conditions (Figure 34B).

Therefore, SIRT3 plays an essential role in mitochondrial fusion, and acetylation-resistant mutant $OPA1^{K228R}$ is able to restore mitochondrial dynamics in SIRT3-/- MEFs.

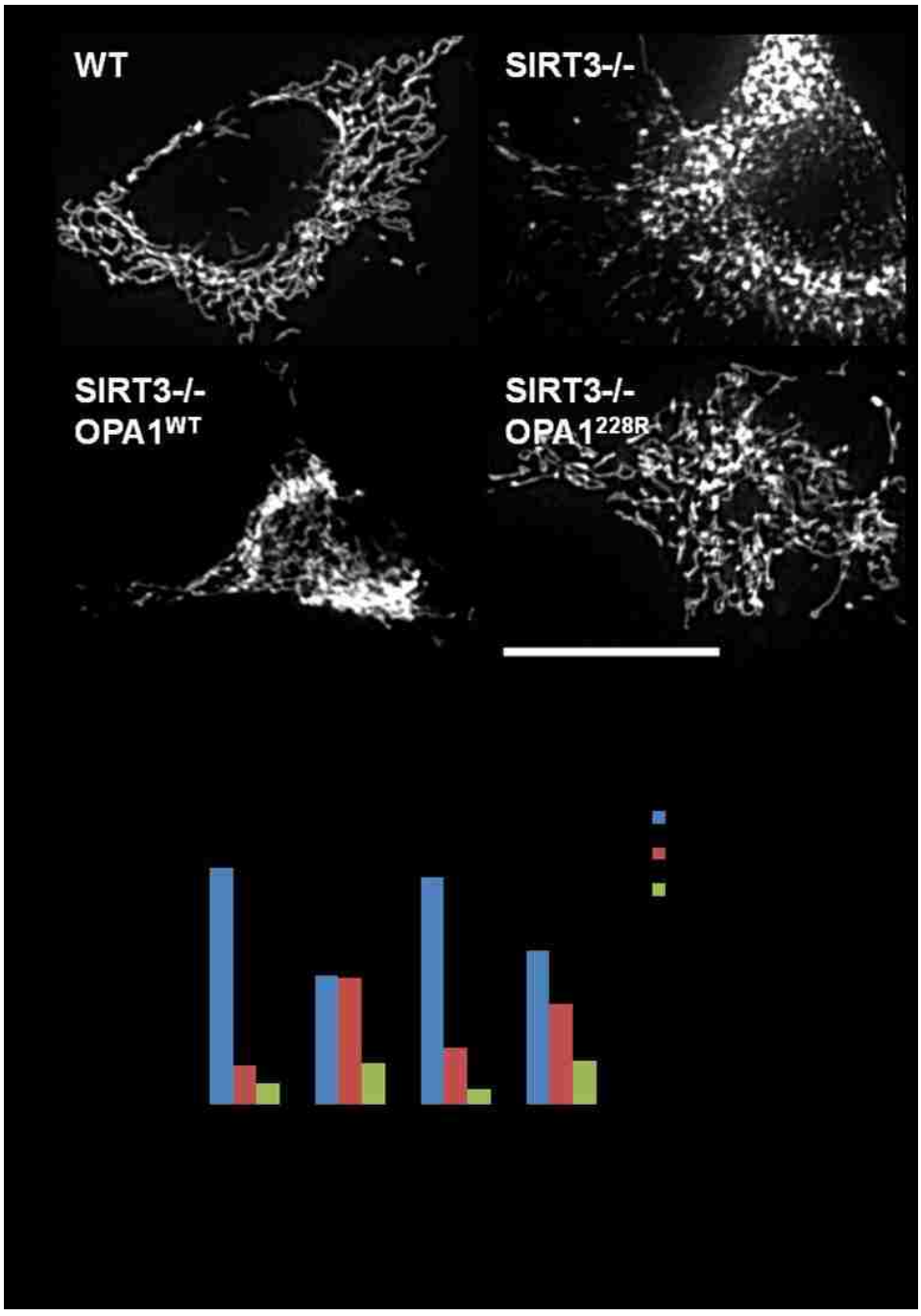

Figure 34 SIRT3 promotes mitochondrial fusion by deacetylating OPA1.

A) Fluorescence micrographs of WT and SIRT3-/- MEFs transfected with DsRed2-Mito and $OPA1^{WT}$ or $OPA1^{K228R}$. Scale bar, 50 μm. B) Percentage of mitochondrial fragmentation in WT MEFs and SIRT3-/- MEFs transfected with $OPA1^{WT}$ or $OPA1^{K228R}$.

4.3.7 SIRT3 is down-regulated by $SOD1^{G93A}$ expression

As shown above, SIRT3 is the key protein that regulates mitochondrial fission and fusion. To investigate whether defective mitochondrial dynamics characteristic of neurodegeneration results from SIRT3 down-regulation, HEK cells were transfected with DsRed2-Mito and either $SOD1^{WT}$ or $SOD1^{G93A}$.

Western blot analysis using anti-SIRT3 antibodies revealed a weak band in $SOD1^{G93A}$ HEK cells, indicating that SIRT3 expression level decreased in HEK cells expressing $SOD1^{G93A}$ (Figure 35A). In addition to protein expression level, SIRT3 activity was also measured using control mice and $SOD1^{G93A}$ mice. Tissue lysates from mice spinal cords demonstrated a reduction in sirtuin activity.

Thus, $SOD1^{G93A}$ causes a decrease in both protein expression and activity of SIRT3, which could be the cause of defective mitochondrial dynamics.

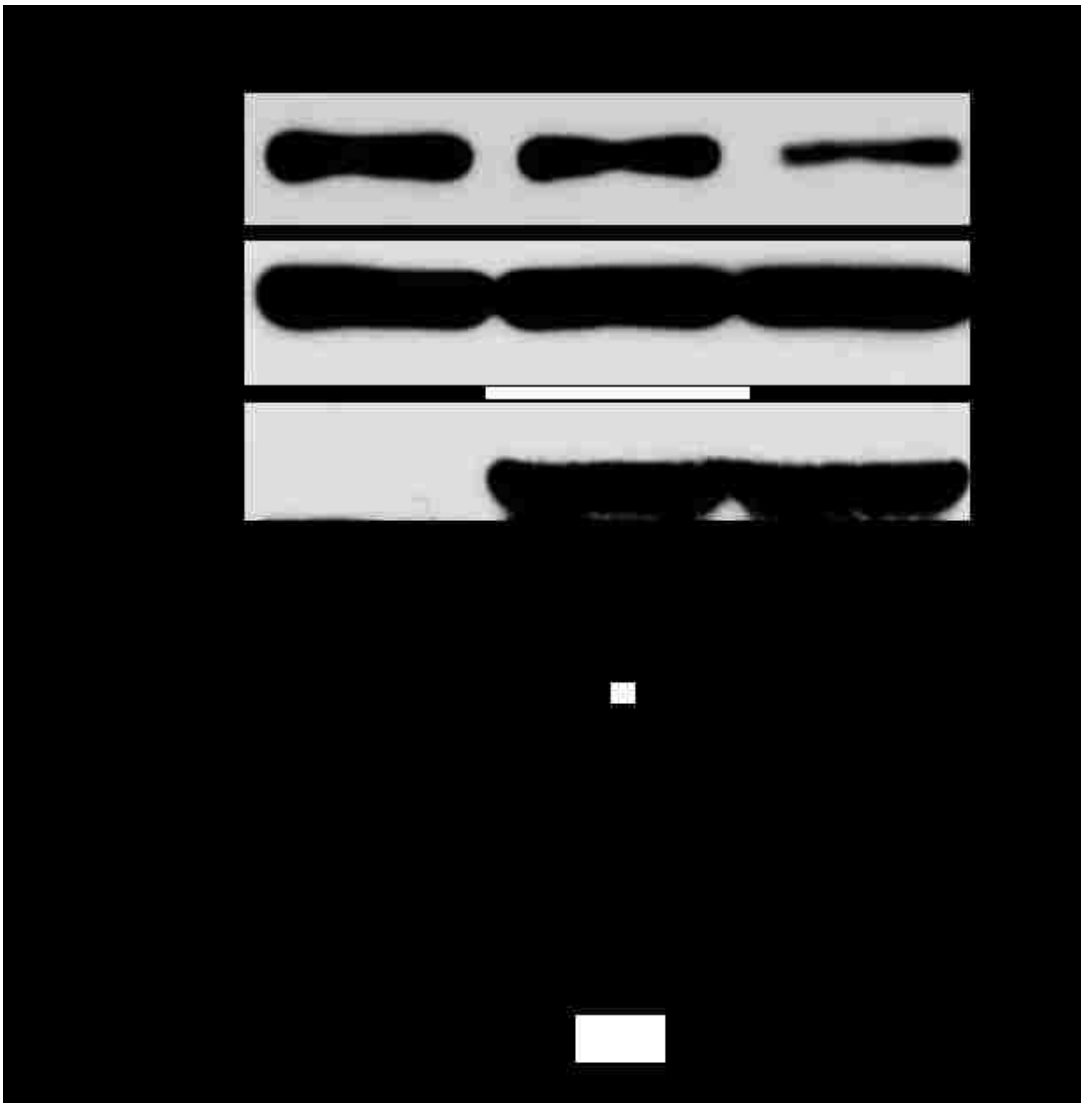

Figure 35 SOD1^{G93A} triggers a decrease in SIRT3 expression and activity.

A) Western blot of lysates from HEK cells expressing pcDNA, SOD1^{WT}, or SOD1^{G93A}. B) Sirtuin deacetylase activity of spinal cord tissue lysates isolated from non-transgenic and transgenic mutant SOD1^{G93A} mice.

4.3.8 SIRT3 restores mitochondrial dynamics in SOD1^{G93A} neurons

Defects in mitochondrial dynamics may be due to SIRT3 inhibition in SOD1^{G93A} neurons. To test whether SIRT3 is able to rescue this imbalance, DsRed2-Mito and SIRT3 were co-transfected into SOD1^{WT} and SOD1^{G93A} neurons.

As expected, both SOD1^{WT} neurons and SOD1^{WT} neurons expressing SIRT3 exhibited normal mitochondrial morphology, while SOD1^{G93A} neurons exhibited fragmented mitochondria (Figure 36A). Strikingly, SOD1^{G93A} neurons expressing SIRT3 appeared to have restored mitochondrial morphology (Figure 36B), suggesting that SIRT3 re-balanced SOD1^{G93A}-induced mitochondrial dynamics defects.

In addition to mitochondrial morphology, time-lapse imaging was also used to track mitochondrial transport. Only vertical lines were observed on kymographs of SOD1^{G93A} neurons, indicating that mitochondria were all stalled (Figure 36C, left). However, more horizontal lines on kymographs of SOD1^{G93A} neurons with SIRT3 co-expression were observed, suggesting that more anterograde and retrograde mitochondrial movement occurred (Figure 36C, right). Quantitative analysis confirmed that mitochondrial mean velocity increased in SOD1^{G93A} neurons expressing SIRT3 (Figure 36D). Further analysis revealed a decrease in the percentage of SOD1^{G93A} neurons with fragmented mitochondria when SIRT3 was co-expressed (Figure 36), correlating with neuronal cell death (Figure 36E).

Thus, SIRT3 not only restored mitochondrial dynamics including fission and fusion balance and velocity, but also rescued SOD1^{G93A}-induced neuronal cell death.

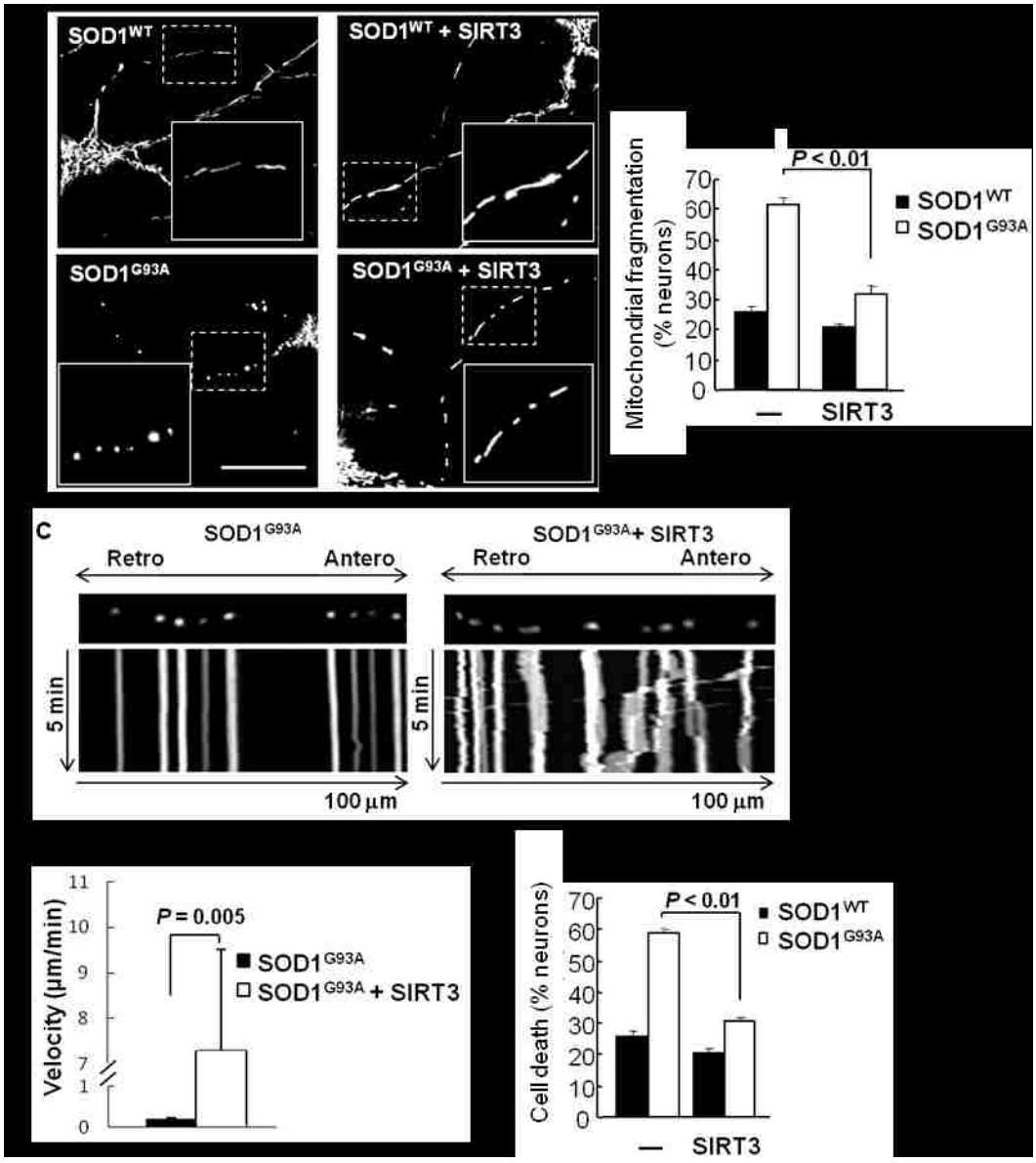

Figure 36 SIRT3 restores mitochondrial dynamics by SOD1^{G93A}.

A) Fluorescence micrographs and close up views of neurons expressing DsRed2-Mito and SOD1^{WT} or SOD1^{G93A} either alone or in combination with SIRT3. B) Percentage of mitochondrial fragmentation in neurons expressing DsRed2-Mito and SOD1^{WT} or SOD1^{G93A} either alone or in combination with SIRT3. C) Kymographs of neurons expressing DsRed2-Mito and SOD1^{G93A} either alone or in combination with SIRT3. D) Mitochondrial mean velocity of neurons expressing DsRed2-Mito and SOD1^{G93A} either alone or in combination with SIRT3 (n=10). E) Percentage of cell death in neurons expressing DsRed2-Mito and SOD1^{WT} or SOD1^{G93A} either alone or in combination with SIRT3.

4.4 Discussion

Longevity has been pursued throughout human history and since the last century, CR has been believed to be an anecdote against aging and a tool for life span extension (Weindruch and Walford, 1988). In the past ten years, Sir2 was identified as a master protein regulating multiple cell signaling pathways that promote longevity (Imai et al., 2000; Tissenbaum and Guarente, 2001). Sirtuins have been revealed to be up-regulated during CR or fasting. A number of scientists then focused on studying sirtuin-mediated life extension in different organisms (Haigis and Guarente, 2006; Tissenbaum and Guarente, 2001).

Mitochondria are key organelles in cells that are involved in cell survival and proliferation (described in 1.2.3). It has been extensively discussed in the previous chapters that mitochondrial dynamics are essential for maintenance of mitochondrial function. Mutations in genes that mediate mitochondrial dynamics, such as MFN2 and OPA1, result in neurodegenerative diseases including CMT-2A and ADOA (described in 1.3). Moreover, mitochondrial dynamics have been shown to play a role in life extension as DRP1-/- increases life span in yeast (Yang et al., 2011). Therefore, it is no doubt that mitochondrial dynamics and life span are related and both sirtuins and balanced mitochondrial dynamics contribute to longevity. However, whether mitochondrial dynamics are involved in sirtuin-mediated longevity remains unknown. In addition, SIRT3 is one of the sirtuins located in the mitochondrial matrix and whether SIRT3 regulates mitochondrial dynamics is an interesting question that is worthy of investigation.

Resveratrol, a sirtuin activator, has been commonly used to promote longevity (Howitz et al., 2003). Here, we observed elevated SIRT3 levels in cell cultures after resveratrol treatment (Figure 29), which correlated with mitochondrial elongation in primary cortical neurons (Figure 30). Thus, it seems that mitochondrial dynamics is regulated by resveratrol. Further investigation focused on specifically how mitochondrial dynamics responded to resveratrol. Interestingly, several post-translational modifications of DRP1 were altered in MEFs treated with resveratrol, including phosphorylation at S616 and S637, acetylation, and SUMOylation (Figure 31). DRP1 phosphorylation was thought to affect its GTPase activity and subcellular translocation. Phosphorylation at the DRP1 S637 site was reported to inhibit DRP1 and reduce mitochondrial fission (Cribbs and Strack, 2007), while DRP1 phosphorylation at S616 site directly induces DRP1 GTPase activity (data not shown). Post-translational modification is a fast way to regulate down-stream cellular events. How resveratrol or sirtuins alter DRP1 phosphorylation remains unclear. One possibility is sirtuins may regulate kinases, which further phosphorylate/dephosphorylate DRP1. Alterations of DRP1 acetylation may directly result from sirtuin regulation. Although what acetylation does to DRP1 is unclear, my colleague proved that SIRT3 directly deacetylates DRP1 (data not shown), suggesting that mitochondrial dynamics could be the direct target of SIRT3 in resveratrol-mediated longevity. Interestingly, OPA1 was hyper-acetylated in SIRT3-/- mice, indicating that OPA1 is also the target of SIRT3 (Figure 33). That both DRP1 and OPA1 are acetylated by SIRT3 further supports the idea that SIRT3 regulates mitochondrial dynamics by deacetylating DRP1 and OPA1. Thus, mitochondrial dynamics could be the downstream target of SIRT3-mediated protective effects.

Defective mitochondrial dynamics was observed in ALS and it may be the mechanism of the disease. A reduction in sirtuin deacetylase activity was observed in spinal cord extracts of mutant $SOD1^{G93A}$ transgenic mice (Figure 35). We cannot exclude the possibility that SIRT1 activity or the activity of other sirtuins is decreased, because the substrate may not be entirely specific. In addition, previous studies have revealed that SIRT1 up-regulates SIRT3 transcription through PGC-1α (Giralt et al., 2011; Kong et al., 2010; Rodgers et al., 2005). Thus, a decrease in SIRT1 may also lower SIRT3. SIRT3 overexpression protects against mutant $SOD1^{G93A}$-induced mitochondrial fragmentation and neuronal cell death (Figure 36). SIRT3 also protects against apoptosis linked to aging in mice and excitotoxic insults in cultured neurons (Hafner et al., 2010; Kim et al., 2011; Someya et al., 2010). The exact mechanism underlying SIRT3-mediated protection against mutant $SOD1^{G93A}$-induced toxicity remains elusive.

Nitrosative stress triggers mitochondrial fragmentation (Barsoum et al., 2006; Liot et al., 2009). SIRT3 lowers ROS by directly deacetylating SOD2 and IDH2 and increases their enzymatic activities (Qiu et al., 2010; Someya et al., 2010; Tao et al., 2010). Thus, it is possible that SIRT3 maintains mitochondrial dynamics by keeping oxidative stress in check. A decrease in SIRT3 activity might increase ROS, which in turn could lead to mitochondrial fragmentation and neuronal cell death. Another potential mechanism might involve CypD, a component of the MPTP. Reduction in CypD delays motor neuron cell death and extends the lifespan of $SOD1^{G93A}$ mice (Martin et al., 2009). Interestingly, CypD is a SIRT3 substrate. Deacetylation by SIRT3 inhibits CypD function and prevents mitochondrial permeability transition and age-related

cardiac hypertrophy (Hafner et al., 2010). Irrespective of the underlying mechanism, SIRT3 may represent a novel therapeutic target to combat ALS.

In sum, mitochondrial are elongated in response to resveratrol and nutrient depletion/fasting. SIRT3 may directly interact with DRP1 and OPA1 to promote mitochondrial fusion. In ALS, defective mitochondrial dynamics may result from decreased SIRT3 activity. SIRT3 expression restored balanced mitochondrial fission and fusion and also rescued $SOD1^{G93A}$-induced neuronal cell death. Therefore, SIRT3 represents a potential target for treatment of ALS.

CHAPTER FIVE: GENERAL DISCUSSION

Balanced mitochondrial dynamics are fundamental for maintenance of mitochondrial function. Because mitochondria are intricately involved in multiple cellular signaling pathways, mitochondrial dynamics contributes to cell functioning and even survival. Mitochondrial dysfunction is a common phenomenon in most neurodegenerative diseases, including ALS and HD (Knott et al., 2008). Due to the unique feature of neurons, e.g., long neurites, mitochondrial dynamics play a much more important role in these cells. Thus, it is not surprising that impaired mitochondrial dynamics lead to neurodegeneration. However, whether defects in mitochondrial dynamics are the primary or secondary cause of neurodegenerative diseases has yet to be determined.

Here, mitochondrial fragmentation and defective mitochondrial transport were observed in $SOD1^{G93A}$ motor neurons (Figures 7 and 8). Decreasing DRP1 activity using dominant-negative $DRP1^{K38A}$ blocks $SOD1^{G93A}$-induced mitochondrial fragmentation, defective axonal transport, and neuronal cell death (Figures 10 and 11), suggesting that defective mitochondrial dynamics could be the primary cause of ALS. Similarly, $DRP1^{K38A}$ and $MFN2^{P82}$ restored HTT-Q97-induced mitochondrial defects and rescued cell death in primary cortical neurons of HD models *in vitro* (Figures 22 and 24). Therefore, blocking mitochondrial fragmentation protects against disease-specific protein-induced toxicity in ALS and HD, suggesting that mitochondrial dynamics are not simply a symptom of, but rather a mechanism behind, neurodegenerative diseases. Currently, the only FDA approved drug for ALS is riluzole,

which blocks glutamate receptors by reducing Ca^{2+} influx and protects motor neurons against Ca^{2+}-induced excitotoxicity. Ca^{2+} buffering is one of the most important mitochondrial functions. Mitochondrial dysfunction directly results in elevated intracellular Ca^{2+} levels, while enhanced mitochondrial Ca^{2+} buffering capacity protects cells against excitotoxicity. Thus, reducing Ca^{2+} influx using riluzole may compensate for impaired Ca^{2+} buffering capacity resulting from defective mitochondrial dynamics. To date, no drugs targeting mitochondrial dynamics have been studied, despite their integral role in neuroprotection.

Mitochondrial fission is mediated by a large GTPase, DRP1, and fusion is mediated by GTPases MFN2 and OPA1. Altered activity of these GTPases directly interferes with the mitochondrial fission and fusion balance. Changes in either protein expression levels or post-translational modifications produce imbalanced mitochondrial fission and fusion, which further induces neuronal cell death. However, what interferes with mitochondrial dynamics remains elusive and it is possible that the underlying molecular mechanisms differ among various neurodegenerative diseases.

In the current work, abnormal interactions between mutant HTT and DRP1 were observed (Figures 20 and 21). Mutant HTT has a higher affinity for DRP1 and induces elevated DRP1 GTPase activity. These observations help clarify the pathway of mutant HTT-mediated mitochondrial fragmentation. Of course, this is just a starting point and many questions remain about this pathway. For example, in which domain does DRP1 interact with mutant HTT, why does mutant HTT have a higher affinity for DRP1, and how does mutant HTT stimulate DRP1 GTPase activity? In addition to the DRP1-HTT interaction, other mechanisms have also been

proposed, including defects in the BDNF and PGC-1α pathways (described in 3.1.3). Whether these pathways are dependent or independent of mitochondrial dynamics remains to be determined. In addition, mutant HTT-induced defects in cellular functions may not solely result from these molecular mechanisms. Only by answering these questions can therapeutic targets be made more specific and HD patients benefit more from HD research.

Distinct from mutant HTT in HD, $SOD1^{G93A}$ may not directly bind DRP1 or other mitochondrial fission and fusion proteins in ALS. Although more studies are required to solidify this conclusion, preliminary data demonstrated a reduction in SIRT3 expression levels and enzymatic activity in ALS (Figure 35). SIRT3 is known to be a critical enzyme that regulates ROS by deacetylating IDH2 and SOD2 inside mitochondria (Qiu et al., 2010; Someya et al., 2010; Tao et al., 2010). Nitrosative/oxidative stress has been previously shown to induce mitochondrial fragmentation. Thus, ROS dysregulation may be implicated in ALS, although how $SOD1^{G93A}$ contributes to impaired SIRT3 signaling requires further investigation. Data presented here from SIRT3-/- mice and resveratrol treated cells are the first to reveal that post-translational modifications of DRP1 including phosphorylation, acetylation, and SUMOylation interfere with mitochondrial dynamics (Figures 30–32).

In sum, our findings represent a milestone and first step toward proving that mitochondrial dynamics play a causal role in the pathogenesis of neurodegenerative diseases. However, it will be important to determine the molecular mechanisms that underlie defects in mitochondrial dynamics caused by disease-specific proteins. Studies of familial forms of

neurodegenerative diseases will continue to provide a better understanding of the sporadic cases, which will ultimately be beneficial for development of therapeutic treatments.

APPENDIX I: PERMISSION FOR REPRINT

Author Requests

If you are the author of this content (or his/her designated agent) please read the following. Since 2003, ownership of copyright in in original research articles remains with the Authors*, and provided that, when reproducing the Contribution or extracts from it, the Authors acknowledge first and reference publication in the Journal, the Authors retain the following non-exclusive rights:

a. To reproduce the Contribution in whole or in part in any printed volume (book or thesis) of which they are the author(s).

b. They and any academic institution where they work at the time may reproduce the Contribution for the purpose of course teaching.

c. To reuse figures or tables created by them and contained in the Contribution in other works created by them.

d. To post a copy of the Contribution as accepted for publication after peer review (in Word or Tex format) on the Author's own web site, or the Author's institutional repository, or the Author's funding body's archive, six months after publication of the printed or online edition of the Journal, provided that they also link to the Journal article on NPG's web site (eg through the DOI).

NPG encourages the self-archiving of the accepted version of your manuscript in your funding agency's or institution's repository, six months after publication. This policy complements the recently announced policies of the US National Institutes of Health, Wellcome Trust and other research funding bodies around the world. NPG recognizes the efforts of funding bodies to increase access to the research they fund, and we strongly encourage authors to participate in such efforts.

Authors wishing to use the published version of their article for promotional use or on a web site must request in the normal way.

If you require further assistance please read NPG's online author reuse guidelines.

Note: *British Journal of Cancer* and *Clinical Pharmacology & Therapeutics* maintain copyright polices of their own that are different from the general NPG policies. Please consult these journals to learn more.

* Commissioned material is still subject to copyright transfer conditions

Ownership of copyright in the article "Mutant huntingtin binds the mitochondrial fission GTPase dynamin-related protein-1 and increases its enzymatic activity" published in *Nature Medicine* remains with the authors. Thus, the figures which have been published are allowed to reproduce in this dissertation.

APPENDIX II: LIST OF PUBLICATIONS

Peer-reviewed journal publications:

Song W, Chen J, Petrilli A, Liot G, Klinglmayr E, Zhou Y, Poquiz P, Tjong J, Pouladi MA, Hayden MR, Masliah E, Ellisman M, Rouiller I, Schwarzenbacher R, Bossy B, Perkins G, Bossy-Wetzel E. Mutant huntingtin binds the mitochondrial fission GTPase dynamin-related protein-1 and increases its enzymatic activity. ***Nature Medicine***. 2011 Mar; 17(3):377-82.

Song W, Bossy B, Martin OJ, Hicks A, Lubitz S, Knott AB, Bossy-Wetzel E. Assessing mitochondrial morphology and dynamics using fluorescence wide-field microscopy and 3D image processing. ***Methods***. 2008 Dec; 46(4):295-303.

Liang J, **Song W**, Tromp G, Kolattukudy PE, Fu M. Genome-wide survey and expression profiling of CCCH-zinc finger family reveals a functional module in macrophage activation. ***PLoS One***. 2008 Aug 6; 3(8):e2880.

Liang J, Wang J, Azfer A**, Song W**, Tromp G, Kolattukudy PE, Fu M. A novel CCCH-zinc finger protein family regulates proinflammatory activation of macrophages. ***Journal of Biological Chemistry***. 2008 Mar 7; 283(10):6337-46.

Song W, Song Y, Kincaid B, Bossy B, Bossy-Wetzel E. Mutant $SOD1^{G93A}$ triggers mitochondrial fragmentation in spinal cord motor neurons: neuronal protection by Sirt3. ***Neurobiology of Disease*** (Accepted).

Dowding J, **Song W**, Karakoti A, Kumar A, Kim A, Lubitz S, Bossy K, Bossy B, Seal S, Ellisman M, Perkins G, Self W, Bossy-Wetzel E. Cerium oxide nanoparticles mediate neuroprotection by scavenging peroxynitrite. (To be submitted)

Abstracts:

Song W, DeAssis V, Bossy B, Lubitz S, Bossy-Wetzel E. Defects in Mitochondrial Dynamics Participate in Amyotrophic Lateral Sclerosis. Neuroscience Meeting, Chicago, IL. Oct. 19, 2009. (Oral presentation)

Song W, DeAssis V, Bossy B, Lubitz S, Bossy-Wetzel E. Motor Neuron Degeneration in Amyotrophic Lateral Sclerosis is Linked with Mitochondrial Fission. American Society for Cell Biology annual meeting, San Diego, CA. Dec.7, 2009.

Petrilli Guinart A, **Song W**, Liot G, Bossy B, Lubitz S, DeAssis V, Jonhson J, Poquiz P, Tjong J, Pouladi M, Ghassemadeh S, Hayden M, Masliah E, Ellisman M, Perkins G, Rouiller I, Bossy-Wetzel E. Mutant Huntington mediates neuronal injury by impairing the mitochondrial fission and fusion balance. Society for Neuroscience Annual Meeting, Chicago, IL. Oct. 19, 2009.

LIST OF REFERENCES

Abdelwahid, E., et al., 2007. Mitochondrial disruption in Drosophila apoptosis. Dev Cell. 12**,** 793-806.

Ackerley, S., et al., 2004. p38alpha stress-activated protein kinase phosphorylates neurofilaments and is associated with neurofilament pathology in amyotrophic lateral sclerosis. Mol Cell Neurosci. 26**,** 354-64.

Ahn, B. H., et al., 2008. A role for the mitochondrial deacetylase Sirt3 in regulating energy homeostasis. Proc Natl Acad Sci U S A. 105**,** 14447-52.

Akepati, V. R., et al., 2008. Characterization of OPA1 isoforms isolated from mouse tissues. J Neurochem. 106**,** 372-83.

Albin, R. L., et al., 1990. Abnormalities of striatal projection neurons and N-methyl-D-aspartate receptors in presymptomatic Huntington's disease. N Engl J Med. 322**,** 1293-8.

Alexander, C., et al., 2000. OPA1, encoding a dynamin-related GTPase, is mutated in autosomal dominant optic atrophy linked to chromosome 3q28. Nat Genet. 26**,** 211-5.

Andrade, M. A., Bork, P., 1995. HEAT repeats in the Huntington's disease protein. Nat Genet. 11**,** 115-6.

Araki, T., et al., 2004. Increased nuclear NAD biosynthesis and SIRT1 activation prevent axonal degeneration. Science. 305**,** 1010-3.

Arzberger, T., et al., 1997. Changes of NMDA receptor subunit (NR1, NR2B) and glutamate transporter (GLT1) mRNA expression in Huntington's disease--an in situ hybridization study. J Neuropathol Exp Neurol. 56**,** 440-54.

Bae, B. I., et al., 2005. p53 mediates cellular dysfunction and behavioral abnormalities in Huntington's disease. Neuron. 47**,** 29-41.

Baloh, R. H., et al., 2007. Altered axonal mitochondrial transport in the pathogenesis of Charcot-Marie-Tooth disease from mitofusin 2 mutations. J Neurosci. 27**,** 422-30.

Baquet, Z. C., et al., 2004. Early striatal dendrite deficits followed by neuron loss with advanced age in the absence of anterograde cortical brain-derived neurotrophic factor. J Neurosci. 24**,** 4250-8.

Barsoum, M. J., et al., 2006. Nitric oxide-induced mitochondrial fission is regulated by dynamin-related GTPases in neurons. EMBO J. 25**,** 3900-11.

Beers, D. R., et al., 2006. Wild-type microglia extend survival in PU.1 knockout mice with familial amyotrophic lateral sclerosis. Proc Natl Acad Sci U S A. 103**,** 16021-6.

Bell, E. L., Guarente, L., 2011. The SirT3 divining rod points to oxidative stress. Mol Cell. 42**,** 561-8.

Benard, G., et al., 2007. Mitochondrial bioenergetics and structural network organization. J Cell Sci. 120**,** 838-48.

Bendotti, C., et al., 2001. Transgenic SOD1 G93A mice develop reduced GLT-1 in spinal cord without alterations in cerebrospinal fluid glutamate levels. J Neurochem. 79**,** 737-46.

Bereiter-Hahn, J., Voth, M., 1994. Dynamics of mitochondria in living cells: shape changes, dislocations, fusion, and fission of mitochondria. Microsc Res Tech. 27**,** 198-219.

Betarbet, R., et al., 2000. Chronic systemic pesticide exposure reproduces features of Parkinson's disease. Nat Neurosci. 3**,** 1301-6.

Bleazard, W., et al., 1999. The dynamin-related GTPase Dnm1 regulates mitochondrial fission in yeast. Nat Cell Biol. 1, 298-304.

Borchelt, D. R., et al., 1994. Superoxide dismutase 1 with mutations linked to familial amyotrophic lateral sclerosis possesses significant activity. Proc Natl Acad Sci U S A. 91, 8292-6.

Bosco, D. A., et al., 2010. Wild-type and mutant SOD1 share an aberrant conformation and a common pathogenic pathway in ALS. Nat Neurosci. 13, 1396-403.

Bossy-Wetzel, E., et al., 2004. Crosstalk between nitric oxide and zinc pathways to neuronal cell death involving mitochondrial dysfunction and p38-activated K+ channels. Neuron. 41, 351-65.

Bossy, B., et al., 2010. S-Nitrosylation of DRP1 does not affect enzymatic activity and is not specific to Alzheimer's disease. J Alzheimers Dis. 20 Suppl 2, S513-26.

Boston-Howes, W., et al., 2006. Caspase-3 cleaves and inactivates the glutamate transporter EAAT2. J Biol Chem. 281, 14076-84.

Brennan, W. A., Jr., et al., 1985. Regional mitochondrial respiratory activity in Huntington's disease brain. J Neurochem. 44, 1948-50.

Browne, S. E., Beal, M. F., 2006. Oxidative damage in Huntington's disease pathogenesis. Antioxid Redox Signal. 8, 2061-73.

Browne, S. E., et al., 1997. Oxidative damage and metabolic dysfunction in Huntington's disease: selective vulnerability of the basal ganglia. Ann Neurol. 41, 646-53.

Bruijn, L. I., et al., 1997. ALS-linked SOD1 mutant G85R mediates damage to astrocytes and promotes rapidly progressive disease with SOD1-containing inclusions. Neuron. 18**,** 327-38.

Brustovetsky, N., et al., 2005. Age-dependent changes in the calcium sensitivity of striatal mitochondria in mouse models of Huntington's Disease. J Neurochem. 93**,** 1361-70.

Burns, A., et al., 1990. Clinical assessment of irritability, aggression, and apathy in Huntington and Alzheimer disease. J Nerv Ment Dis. 178**,** 20-6.

Butterworth, J., et al., 1985. Distribution of phosphate-activated glutaminase, succinic dehydrogenase, pyruvate dehydrogenase and gamma-glutamyl transpeptidase in post-mortem brain from Huntington's disease and agonal cases. J Neurol Sci. 67**,** 161-71.

Byers, R. K., et al., 1973. Huntington's disease in children. Neuropathologic study of four cases. Neurology. 23**,** 561-9.

Candiani, S., et al., 2007. Characterization, developmental expression and evolutionary features of the huntingtin gene in the amphioxus Branchiostoma floridae. BMC Dev Biol. 7**,** 127.

Cassina, P., et al., 2008. Mitochondrial dysfunction in SOD1G93A-bearing astrocytes promotes motor neuron degeneration: prevention by mitochondrial-targeted antioxidants. J Neurosci. 28**,** 4115-22.

Cassina, P., et al., 2005. Astrocyte activation by fibroblast growth factor-1 and motor neuron apoptosis: implications for amyotrophic lateral sclerosis. J Neurochem. 93**,** 38-46.

Cassina, P., et al., 2002. Peroxynitrite triggers a phenotypic transformation in spinal cord astrocytes that induces motor neuron apoptosis. J Neurosci Res. 67**,** 21-9.

Cerveny, K. L., Jensen, R. E., 2003. The WD-repeats of Net2p interact with Dnm1p and Fis1p to regulate division of mitochondria. Mol Biol Cell. 14**,** 4126-39.

Chan, D. C., 2006. Mitochondrial fusion and fission in mammals. Annu Rev Cell Dev Biol. 22**,** 79-99.

Chang, C. R., Blackstone, C., 2007. Cyclic AMP-dependent protein kinase phosphorylation of Drp1 regulates its GTPase activity and mitochondrial morphology. J Biol Chem. 282**,** 21583-7.

Chang, D. T., et al., 2006. Mutant huntingtin aggregates impair mitochondrial movement and trafficking in cortical neurons. Neurobiol Dis. 22**,** 388-400.

Chen, D., et al., 2005a. Increase in activity during calorie restriction requires Sirt1. Science. 310**,** 1641.

Chen, H., et al., 2005b. Disruption of fusion results in mitochondrial heterogeneity and dysfunction. J Biol Chem. 280**,** 26185-92.

Chen, H., et al., 2003. Mitofusins Mfn1 and Mfn2 coordinately regulate mitochondrial fusion and are essential for embryonic development. J Cell Biol. 160**,** 189-200.

Chen, H., et al., 2007a. Mitochondrial fusion protects against neurodegeneration in the cerebellum. Cell. 130**,** 548-62.

Chen, X. J., et al., 2007b. Proprioceptive sensory neuropathy in mice with a mutation in the cytoplasmic Dynein heavy chain 1 gene. J Neurosci. 27**,** 14515-24.

Chen, Y., et al., 2008. NS21: re-defined and modified supplement B27 for neuronal cultures. J Neurosci Methods. 171**,** 239-47.

Cho, D. H., et al., 2009. S-nitrosylation of Drp1 mediates beta-amyloid-related mitochondrial fission and neuronal injury. Science. 324, 102-5.

Choo, Y. S., et al., 2004. Mutant huntingtin directly increases susceptibility of mitochondria to the calcium-induced permeability transition and cytochrome c release. Hum Mol Genet. 13, 1407-20.

Chung, K. W., et al., 2006. Early onset severe and late-onset mild Charcot-Marie-Tooth disease with mitofusin 2 (MFN2) mutations. Brain. 129, 2103-18.

Cimen, H., et al., 2010. Regulation of succinate dehydrogenase activity by SIRT3 in mammalian mitochondria. Biochemistry. 49, 304-11.

Cipolat, S., et al., 2004. OPA1 requires mitofusin 1 to promote mitochondrial fusion. Proc Natl Acad Sci U S A. 101, 15927-32.

Civitarese, A. E., et al., 2007. Calorie restriction increases muscle mitochondrial biogenesis in healthy humans. PLoS Med. 4, e76.

Clark, I. E., et al., 2006. Drosophila pink1 is required for mitochondrial function and interacts genetically with parkin. Nature. 441, 1162-6.

Cohen, H. Y., et al., 2004. Calorie restriction promotes mammalian cell survival by inducing the SIRT1 deacetylase. Science. 305, 390-2.

Colin, E., et al., 2008. Huntingtin phosphorylation acts as a molecular switch for anterograde/retrograde transport in neurons. EMBO J. 27, 2124-34.

Colman, R. J., et al., 2009. Caloric restriction delays disease onset and mortality in rhesus monkeys. Science. 325, 201-4.

Cornett, J., et al., 2005. Polyglutamine expansion of huntingtin impairs its nuclear export. Nat Genet. 37, 198-204.

Cribbs, J. T., Strack, S., 2007. Reversible phosphorylation of Drp1 by cyclic AMP-dependent protein kinase and calcineurin regulates mitochondrial fission and cell death. EMBO Rep. 8, 939-44.

Cui, L., et al., 2006. Transcriptional repression of PGC-1alpha by mutant huntingtin leads to mitochondrial dysfunction and neurodegeneration. Cell. 127, 59-69.

Damiano, M., et al., 2006. Neural mitochondrial Ca2+ capacity impairment precedes the onset of motor symptoms in G93A Cu/Zn-superoxide dismutase mutant mice. J Neurochem. 96, 1349-61.

Davies, V. J., et al., 2007. Opa1 deficiency in a mouse model of autosomal dominant optic atrophy impairs mitochondrial morphology, optic nerve structure and visual function. Hum Mol Genet. 16, 1307-18.

De Vos, K., et al., 2000. Tumor necrosis factor induces hyperphosphorylation of kinesin light chain and inhibits kinesin-mediated transport of mitochondria. J Cell Biol. 149, 1207-14.

De Vos, K. J., et al., 2007. Familial amyotrophic lateral sclerosis-linked SOD1 mutants perturb fast axonal transport to reduce axonal mitochondria content. Hum Mol Genet. 16, 2720-8.

del Toro, D., et al., 2006. Mutant huntingtin impairs the post-Golgi trafficking of brain-derived neurotrophic factor but not its Val66Met polymorphism. J Neurosci. 26, 12748-57.

Delettre, C., et al., 2001. Mutation spectrum and splicing variants in the OPA1 gene. Hum Genet. 109, 584-91.

Delettre, C., et al., 2000. Nuclear gene OPA1, encoding a mitochondrial dynamin-related protein, is mutated in dominant optic atrophy. Nat Genet. 26, 207-10.

Deng, H., et al., 2008. The Parkinson's disease genes pink1 and parkin promote mitochondrial fission and/or inhibit fusion in Drosophila. Proc Natl Acad Sci U S A. 105, 14503-8.

Deng, H. X., et al., 1993. Amyotrophic lateral sclerosis and structural defects in Cu,Zn superoxide dismutase. Science. 261, 1047-51.

Detmer, S. A., Chan, D. C., 2007. Functions and dysfunctions of mitochondrial dynamics. Nat Rev Mol Cell Biol. 8, 870-9.

Dodson, M. W., Guo, M., 2007. Pink1, Parkin, DJ-1 and mitochondrial dysfunction in Parkinson's disease. Curr Opin Neurobiol. 17, 331-7.

Dunah, A. W., et al., 2002. Sp1 and TAFII130 transcriptional activity disrupted in early Huntington's disease. Science. 296, 2238-43.

Exner, N., et al., 2007. Loss-of-function of human PINK1 results in mitochondrial pathology and can be rescued by parkin. J Neurosci. 27, 12413-8.

Fan, M. M., Raymond, L. A., 2007. N-methyl-D-aspartate (NMDA) receptor function and excitotoxicity in Huntington's disease. Prog Neurobiol. 81, 272-93.

Ferre, M., et al., 2005. eOPA1: an online database for OPA1 mutations. Hum Mutat. 25, 423-8.

Ferri, A., et al., 2006. Familial ALS-superoxide dismutases associate with mitochondria and shift their redox potentials. Proc Natl Acad Sci U S A. 103, 13860-5.

Fischer, L. R., et al., 2004. Amyotrophic lateral sclerosis is a distal axonopathy: evidence in mice and man. Exp Neurol. 185**,** 232-40.

Frank, S., et al., 2001. The role of dynamin-related protein 1, a mediator of mitochondrial fission, in apoptosis. Dev Cell. 1**,** 515-25.

Fransson, S., et al., 2006. The atypical Rho GTPases Miro-1 and Miro-2 have essential roles in mitochondrial trafficking. Biochem Biophys Res Commun. 344**,** 500-10.

Fusco, F. R., et al., 1999. Cellular localization of huntingtin in striatal and cortical neurons in rats: lack of correlation with neuronal vulnerability in Huntington's disease. J Neurosci. 19**,** 1189-202.

Gandre-Babbe, S., van der Bliek, A. M., 2008. The novel tail-anchored membrane protein Mff controls mitochondrial and peroxisomal fission in mammalian cells. Mol Biol Cell. 19**,** 2402-12.

Gauthier, L. R., et al., 2004. Huntingtin controls neurotrophic support and survival of neurons by enhancing BDNF vesicular transport along microtubules. Cell. 118**,** 127-38.

Gautier, C. A., et al., 2008. Loss of PINK1 causes mitochondrial functional defects and increased sensitivity to oxidative stress. Proc Natl Acad Sci U S A. 105**,** 11364-9.

Giralt, A., et al., 2011. Peroxisome proliferator-activated receptor-gamma coactivator-1alpha controls transcription of the Sirt3 gene, an essential component of the thermogenic brown adipocyte phenotype. J Biol Chem. 286**,** 16958-66.

Gissi, C., et al., 2006. Huntingtin gene evolution in Chordata and its peculiar features in the ascidian Ciona genus. BMC Genomics. 7**,** 288.

Glater, E. E., et al., 2006. Axonal transport of mitochondria requires milton to recruit kinesin heavy chain and is light chain independent. J Cell Biol. 173**,** 545-57.

Goyal, G., et al., 2007. Role of mitochondrial remodeling in programmed cell death in Drosophila melanogaster. Dev Cell. 12**,** 807-16.

Griffin, E. E., Chan, D. C., 2006. Domain interactions within Fzo1 oligomers are essential for mitochondrial fusion. J Biol Chem. 281**,** 16599-606.

Griffin, E. E., et al., 2005. The WD40 protein Caf4p is a component of the mitochondrial fission machinery and recruits Dnm1p to mitochondria. J Cell Biol. 170**,** 237-48.

Griparic, L., et al., 2004. Loss of the intermembrane space protein Mgm1/OPA1 induces swelling and localized constrictions along the lengths of mitochondria. J Biol Chem. 279**,** 18792-8.

Group, T. H. s. D. C. R., 1993. A novel gene containing a trinucleotide repeat that is expanded and unstable on Huntington's disease chromosomes. Cell. 72**,** 971-83.

Gu, M., et al., 1996. Mitochondrial defect in Huntington's disease caudate nucleus. Ann Neurol. 39**,** 385-9.

Gunawardena, S., et al., 2003. Disruption of axonal transport by loss of huntingtin or expression of pathogenic polyQ proteins in Drosophila. Neuron. 40**,** 25-40.

Guo, X., et al., 2005. The GTPase dMiro is required for axonal transport of mitochondria to Drosophila synapses. Neuron. 47**,** 379-93.

Gurney, M. E., et al., 1994. Motor neuron degeneration in mice that express a human Cu,Zn superoxide dismutase mutation. Science. 264**,** 1772-5.

Hafner, A. V., et al., 2010. Regulation of the mPTP by SIRT3-mediated deacetylation of CypD at lysine 166 suppresses age-related cardiac hypertrophy. Aging (Albany NY). 2, 914-23.

Haigis, M. C., Guarente, L. P., 2006. Mammalian sirtuins--emerging roles in physiology, aging, and calorie restriction. Genes Dev. 20, 2913-21.

Harder, Z., et al., 2004. Sumo1 conjugates mitochondrial substrates and participates in mitochondrial fission. Curr Biol. 14, 340-5.

Harjes, P., Wanker, E. E., 2003. The hunt for huntingtin function: interaction partners tell many different stories. Trends Biochem Sci. 28, 425-33.

Harman, D., 1956. Aging: a theory based on free radical and radiation chemistry. J Gerontol. 11, 298-300.

Harraz, M. M., et al., 2008. SOD1 mutations disrupt redox-sensitive Rac regulation of NADPH oxidase in a familial ALS model. J Clin Invest. 118, 659-70.

Hassel, B., et al., 2008. Glutamate uptake is reduced in prefrontal cortex in Huntington's disease. Neurochem Res. 33, 232-7.

Hayden, M. R., et al., 1986. Positron emission tomography in the early diagnosis of Huntington's disease. Neurology. 36, 888-94.

Ho, L. W., et al., 2001. Wild type Huntingtin reduces the cellular toxicity of mutant Huntingtin in mammalian cell models of Huntington's disease. J Med Genet. 38, 450-2.

Hollenbeck, P. J., Saxton, W. M., 2005. The axonal transport of mitochondria. J Cell Sci. 118, 5411-9.

Hoppins, S., et al., 2007. The machines that divide and fuse mitochondria. Annu Rev Biochem. 76**,** 751-80.

Horton, T. M., et al., 1995. Marked increase in mitochondrial DNA deletion levels in the cerebral cortex of Huntington's disease patients. Neurology. 45**,** 1879-83.

Howitz, K. T., et al., 2003. Small molecule activators of sirtuins extend Saccharomyces cerevisiae lifespan. Nature. 425**,** 191-6.

Howland, D. S., et al., 2002. Focal loss of the glutamate transporter EAAT2 in a transgenic rat model of SOD1 mutant-mediated amyotrophic lateral sclerosis (ALS). Proc Natl Acad Sci U S A. 99**,** 1604-9.

Huang, C. C., et al., 1998. Amyloid formation by mutant huntingtin: threshold, progressivity and recruitment of normal polyglutamine proteins. Somat Cell Mol Genet. 24**,** 217-33.

Ilieva, H., et al., 2009. Non-cell autonomous toxicity in neurodegenerative disorders: ALS and beyond. J Cell Biol. 187**,** 761-72.

Imai, S., et al., 2000. Transcriptional silencing and longevity protein Sir2 is an NAD-dependent histone deacetylase. Nature. 403**,** 795-800.

Ingerman, E., et al., 2005. Dnm1 forms spirals that are structurally tailored to fit mitochondria. J Cell Biol. 170**,** 1021-7.

Ishihara, N., et al., 2006. Regulation of mitochondrial morphology through proteolytic cleavage of OPA1. EMBO J. 25**,** 2966-77.

Ishihara, N., et al., 2009. Mitochondrial fission factor Drp1 is essential for embryonic development and synapse formation in mice. Nat Cell Biol. 11**,** 958-66.

Ishii, N., et al., 1998. A mutation in succinate dehydrogenase cytochrome b causes oxidative stress and ageing in nematodes. Nature. 394**,** 694-7.

Israelson, A., et al., 2010. Misfolded mutant SOD1 directly inhibits VDAC1 conductance in a mouse model of inherited ALS. Neuron. 67**,** 575-87.

Jaarsma, D., et al., 2000. Human Cu/Zn superoxide dismutase (SOD1) overexpression in mice causes mitochondrial vacuolization, axonal degeneration, and premature motoneuron death and accelerates motoneuron disease in mice expressing a familial amyotrophic lateral sclerosis mutant SOD1. Neurobiol Dis. 7**,** 623-43.

Jaarsma, D., et al., 2001. CuZn superoxide dismutase (SOD1) accumulates in vacuolated mitochondria in transgenic mice expressing amyotrophic lateral sclerosis-linked SOD1 mutations. Acta Neuropathol. 102**,** 293-305.

Jenkins, B. G., et al., 2005. Effects of CAG repeat length, HTT protein length and protein context on cerebral metabolism measured using magnetic resonance spectroscopy in transgenic mouse models of Huntington's disease. J Neurochem. 95**,** 553-62.

Jope, R. S., Johnson, G. V., 2004. The glamour and gloom of glycogen synthase kinase-3. Trends Biochem Sci. 29**,** 95-102.

Kabashi, E., et al., 2004. Focal dysfunction of the proteasome: a pathogenic factor in a mouse model of amyotrophic lateral sclerosis. J Neurochem. 89**,** 1325-35.

Kaltenbach, L. S., et al., 2007. Huntingtin interacting proteins are genetic modifiers of neurodegeneration. PLoS Genet. 3**,** e82.

Kang, J. S., et al., 2008. Docking of axonal mitochondria by syntaphilin controls their mobility and affects short-term facilitation. Cell. 132**,** 137-48.

Karbowski, M., et al., 2002. Spatial and temporal association of Bax with mitochondrial fission sites, Drp1, and Mfn2 during apoptosis. J Cell Biol. 159**,** 931-8.

Karbowski, M., et al., 2007. The mitochondrial E3 ubiquitin ligase MARCH5 is required for Drp1 dependent mitochondrial division. J Cell Biol. 178**,** 71-84.

Kashatus, D. F., et al., 2011. RALA and RALBP1 regulate mitochondrial fission at mitosis. Nat Cell Biol. 13**,** 1108-15.

Kegel, K. B., et al., 2002. Huntingtin is present in the nucleus, interacts with the transcriptional corepressor C-terminal binding protein, and represses transcription. J Biol Chem. 277**,** 7466-76.

Kijima, K., et al., 2005. Mitochondrial GTPase mitofusin 2 mutation in Charcot-Marie-Tooth neuropathy type 2A. Hum Genet. 116**,** 23-7.

Kim, D., et al., 2007a. SIRT1 deacetylase protects against neurodegeneration in models for Alzheimer's disease and amyotrophic lateral sclerosis. EMBO J. 26**,** 3169-79.

Kim, I., et al., 2007b. Selective degradation of mitochondria by mitophagy. Arch Biochem Biophys. 462**,** 245-53.

Kim, J. Y., et al., 2005. Mitochondrial DNA content is decreased in autosomal dominant optic atrophy. Neurology. 64**,** 966-72.

Kim, M. W., et al., 2009. Secondary structure of Huntingtin amino-terminal region. Structure. 17**,** 1205-12.

Kim, S. C., et al., 2006. Substrate and functional diversity of lysine acetylation revealed by a proteomics survey. Mol Cell. 23**,** 607-18.

Kim, S. H., et al., 2011. Neuronal Sirt3 protects against excitotoxic injury in mouse cortical neuron culture. PLoS One. 6**,** e14731.

Kirkinezos, I. G., et al., 2005. Cytochrome c association with the inner mitochondrial membrane is impaired in the CNS of G93A-SOD1 mice. J Neurosci. 25**,** 164-72.

Knott, A. B., et al., 2008. Mitochondrial fragmentation in neurodegeneration. Nat Rev Neurosci. 9**,** 505-18.

Kong, J., Xu, Z., 1998. Massive mitochondrial degeneration in motor neurons triggers the onset of amyotrophic lateral sclerosis in mice expressing a mutant SOD1. J Neurosci. 18**,** 3241-50.

Kong, X., et al., 2010. Sirtuin 3, a new target of PGC-1alpha, plays an important role in the suppression of ROS and mitochondrial biogenesis. PLoS One. 5**,** e11707.

Koshiba, T., et al., 2004. Structural basis of mitochondrial tethering by mitofusin complexes. Science. 305**,** 858-62.

Kuhl, D. E., et al., 1982. Cerebral metabolism and atrophy in Huntington's disease determined by 18FDG and computed tomographic scan. Ann Neurol. 12**,** 425-34.

Kunst, C. B., et al., 1997. Mutations in SOD1 associated with amyotrophic lateral sclerosis cause novel protein interactions. Nat Genet. 15**,** 91-4.

Kuwert, T., et al., 1990. Cortical and subcortical glucose consumption measured by PET in patients with Huntington's disease. Brain. 113 (Pt 5)**,** 1405-23.

Kwiatkowski, T. J., Jr., et al., 2009. Mutations in the FUS/TLS gene on chromosome 16 cause familial amyotrophic lateral sclerosis. Science. 323, 1205-8.

Lagouge, M., et al., 2006. Resveratrol improves mitochondrial function and protects against metabolic disease by activating SIRT1 and PGC-1alpha. Cell. 127, 1109-22.

Law, I. K., et al., 2009. Identification and characterization of proteins interacting with SIRT1 and SIRT3: implications in the anti-aging and metabolic effects of sirtuins. Proteomics. 9, 2444-56.

Lee, C. K., et al., 2000. Gene-expression profile of the ageing brain in mice. Nat Genet. 25, 294-7.

Lee, K. D., Hollenbeck, P. J., 1995. Phosphorylation of kinesin in vivo correlates with organelle association and neurite outgrowth. J Biol Chem. 270, 5600-5.

Lee, Y. J., et al., 2004. Roles of the mammalian mitochondrial fission and fusion mediators Fis1, Drp1, and Opa1 in apoptosis. Mol Biol Cell. 15, 5001-11.

Li, S. H., et al., 2002. Interaction of Huntington disease protein with transcriptional activator Sp1. Mol Cell Biol. 22, 1277-87.

Li, S. H., Li, X. J., 2004. Huntingtin-protein interactions and the pathogenesis of Huntington's disease. Trends Genet. 20, 146-54.

Li, Z., et al., 1999. A putative Drosophila homolog of the Huntington's disease gene. Hum Mol Genet. 8, 1807-15.

Li, Z., et al., 2004. The importance of dendritic mitochondria in the morphogenesis and plasticity of spines and synapses. Cell. 119, 873-87.

Ligon, L. A., Steward, O., 2000. Role of microtubules and actin filaments in the movement of mitochondria in the axons and dendrites of cultured hippocampal neurons. J Comp Neurol. 427**,** 351-61.

Lin, M. T., Beal, M. F., 2006. Mitochondrial dysfunction and oxidative stress in neurodegenerative diseases. Nature. 443**,** 787-95.

Liot, G., et al., 2009. Complex II inhibition by 3-NP causes mitochondrial fragmentation and neuronal cell death via an NMDA- and ROS-dependent pathway. Cell Death Differ. 16**,** 899-909.

Liu, J., et al., 2004. Toxicity of familial ALS-linked SOD1 mutants from selective recruitment to spinal mitochondria. Neuron. 43**,** 5-17.

Lobsiger, C. S., Cleveland, D. W., 2007. Glial cells as intrinsic components of non-cell-autonomous neurodegenerative disease. Nat Neurosci. 10**,** 1355-60.

Lodi, R., et al., 2000. Abnormal in vivo skeletal muscle energy metabolism in Huntington's disease and dentatorubropallidoluysian atrophy. Ann Neurol. 48**,** 72-6.

Lodi, R., et al., 2004. Deficit of in vivo mitochondrial ATP production in OPA1-related dominant optic atrophy. Ann Neurol. 56**,** 719-23.

Low, H. H., Lowe, J., 2006. A bacterial dynamin-like protein. Nature. 444**,** 766-9.

Luo, J., et al., 2001. Negative control of p53 by Sir2alpha promotes cell survival under stress. Cell. 107**,** 137-48.

Lustbader, J. W., et al., 2004. ABAD directly links Abeta to mitochondrial toxicity in Alzheimer's disease. Science. 304**,** 448-52.

Magrane, J., et al., 2009. Mutant SOD1 in neuronal mitochondria causes toxicity and mitochondrial dynamics abnormalities. Hum Mol Genet. 18**,** 4552-64.

Magrane, J., Manfredi, G., 2009. Mitochondrial function, morphology, and axonal transport in amyotrophic lateral sclerosis. Antioxid Redox Signal. 11**,** 1615-26.

Magrane, J., et al., 2012. Mitochondrial Dynamics and Bioenergetic Dysfunction Is Associated with Synaptic Alterations in Mutant SOD1 Motor Neurons. J Neurosci. 32**,** 229-42.

Manczak, M., et al., 2011. Impaired mitochondrial dynamics and abnormal interaction of amyloid beta with mitochondrial protein Drp1 in neurons from patients with Alzheimer's disease: implications for neuronal damage. Hum Mol Genet. 20**,** 2495-509.

Martin, L. J., et al., 2009. The mitochondrial permeability transition pore in motor neurons: involvement in the pathobiology of ALS mice. Exp Neurol. 218**,** 333-46.

Mattiazzi, M., et al., 2002. Mutated human SOD1 causes dysfunction of oxidative phosphorylation in mitochondria of transgenic mice. J Biol Chem. 277**,** 29626-33.

Mattson, M. P., 2003. Gene-diet interactions in brain aging and neurodegenerative disorders. Ann Intern Med. 139**,** 441-4.

McGuire, J. R., et al., 2006. Interaction of Huntingtin-associated protein-1 with kinesin light chain: implications in intracellular trafficking in neurons. J Biol Chem. 281**,** 3552-9.

Meeusen, S., et al., 2006. Mitochondrial inner-membrane fusion and crista maintenance requires the dynamin-related GTPase Mgm1. Cell. 127**,** 383-95.

Meeusen, S., et al., 2004. Mitochondrial fusion intermediates revealed in vitro. Science. 305**,** 1747-52.

Migliaccio, E., et al., 1999. The p66shc adaptor protein controls oxidative stress response and life span in mammals. Nature. 402**,** 309-13.

Miller, B. R., et al., 2008. Up-regulation of GLT1 expression increases glutamate uptake and attenuates the Huntington's disease phenotype in the R6/2 mouse. Neuroscience. 153**,** 329-37.

Morfini, G., et al., 2006. JNK mediates pathogenic effects of polyglutamine-expanded androgen receptor on fast axonal transport. Nat Neurosci. 9**,** 907-16.

Mostoslavsky, R., et al., 2006. Genomic instability and aging-like phenotype in the absence of mammalian SIRT6. Cell. 124**,** 315-29.

Motta, M. C., et al., 2004. Mammalian SIRT1 represses forkhead transcription factors. Cell. 116**,** 551-63.

Murata, T., et al., 2008. Increased mitochondrial oxidative damage in patients with sporadic amyotrophic lateral sclerosis. J Neurol Sci. 267**,** 66-9.

Nagai, M., et al., 2007. Astrocytes expressing ALS-linked mutated SOD1 release factors selectively toxic to motor neurons. Nat Neurosci. 10**,** 615-22.

Nangaku, M., et al., 1994. KIF1B, a novel microtubule plus end-directed monomeric motor protein for transport of mitochondria. Cell. 79**,** 1209-20.

Narendra, D., et al., 2008. Parkin is recruited selectively to impaired mitochondria and promotes their autophagy. J Cell Biol. 183**,** 795-803.

Nasir, J., et al., 1995. Targeted disruption of the Huntington's disease gene results in embryonic lethality and behavioral and morphological changes in heterozygotes. Cell. 81**,** 811-23.

Naylor, K., et al., 2006. Mdv1 interacts with assembled dnm1 to promote mitochondrial division. J Biol Chem. 281**,** 2177-83.

Neumann, M., et al., 2006. Ubiquitinated TDP-43 in frontotemporal lobar degeneration and amyotrophic lateral sclerosis. Science. 314**,** 130-3.

Niwa, J., et al., 2002. Dorfin ubiquitylates mutant SOD1 and prevents mutant SOD1-mediated neurotoxicity. J Biol Chem. 277**,** 36793-8.

Nunnari, J., et al., 1997. Mitochondrial transmission during mating in Saccharomyces cerevisiae is determined by mitochondrial fusion and fission and the intramitochondrial segregation of mitochondrial DNA. Mol Biol Cell. 8**,** 1233-42.

Okado-Matsumoto, A., Fridovich, I., 2001. Subcellular distribution of superoxide dismutases (SOD) in rat liver: Cu,Zn-SOD in mitochondria. J Biol Chem. 276**,** 38388-93.

Olichon, A., et al., 2003. Loss of OPA1 perturbates the mitochondrial inner membrane structure and integrity, leading to cytochrome c release and apoptosis. J Biol Chem. 278**,** 7743-6.

Ooi, L., Wood, I. C., 2007. Chromatin crosstalk in development and disease: lessons from REST. Nat Rev Genet. 8**,** 544-54.

Palacino, J. J., et al., 2004. Mitochondrial dysfunction and oxidative damage in parkin-deficient mice. J Biol Chem. 279**,** 18614-22.

Pandey, M., et al., 2008. Mitochondrial NAD+-linked State 3 respiration and complex-I activity are compromised in the cerebral cortex of 3-nitropropionic acid-induced rat model of Huntington's disease. J Neurochem. 104**,** 420-34.

Panov, A. V., et al., 2002. Early mitochondrial calcium defects in Huntington's disease are a direct effect of polyglutamines. Nat Neurosci. 5**,** 731-6.

Paradies, G., et al., 2009. Role of cardiolipin peroxidation and Ca2+ in mitochondrial dysfunction and disease. Cell Calcium. 45**,** 643-50.

Pasinelli, P., et al., 2004. Amyotrophic lateral sclerosis-associated SOD1 mutant proteins bind and aggregate with Bcl-2 in spinal cord mitochondria. Neuron. 43**,** 19-30.

Patel, N. V., et al., 2005. Caloric restriction attenuates Abeta-deposition in Alzheimer transgenic models. Neurobiol Aging. 26**,** 995-1000.

Pehar, M., et al., 2004. Astrocytic production of nerve growth factor in motor neuron apoptosis: implications for amyotrophic lateral sclerosis. J Neurochem. 89**,** 464-73.

Perutz, M. F., et al., 1994. Glutamine repeats as polar zippers: their possible role in inherited neurodegenerative diseases. Proc Natl Acad Sci U S A. 91**,** 5355-8.

Pilling, A. D., et al., 2006. Kinesin-1 and Dynein are the primary motors for fast transport of mitochondria in Drosophila motor axons. Mol Biol Cell. 17**,** 2057-68.

Pitts, K. R., et al., 1999. The dynamin-like protein DLP1 is essential for normal distribution and morphology of the endoplasmic reticulum and mitochondria in mammalian cells. Mol Biol Cell. 10**,** 4403-17.

Puigserver, P., Spiegelman, B. M., 2003. Peroxisome proliferator-activated receptor-gamma coactivator 1 alpha (PGC-1 alpha): transcriptional coactivator and metabolic regulator. Endocr Rev. 24**,** 78-90.

Puls, I., et al., 2003. Mutant dynactin in motor neuron disease. Nat Genet. 33**,** 455-6.

Purdom, S., Chen, Q. M., 2003. p66(Shc): at the crossroad of oxidative stress and the genetics of aging. Trends Mol Med. 9**,** 206-10.

Qin, Z. H., et al., 2004. Huntingtin bodies sequester vesicle-associated proteins by a polyproline-dependent interaction. J Neurosci. 24**,** 269-81.

Qiu, X., et al., 2010. Calorie restriction reduces oxidative stress by SIRT3-mediated SOD2 activation. Cell Metab. 12**,** 662-7.

Ranen, N. G., et al., 1995. Anticipation and instability of IT-15 (CAG)n repeats in parent-offspring pairs with Huntington disease. Am J Hum Genet. 57**,** 593-602.

Reaume, A. G., et al., 1996. Motor neurons in Cu/Zn superoxide dismutase-deficient mice develop normally but exhibit enhanced cell death after axonal injury. Nat Genet. 13**,** 43-7.

Reddy, P. H., et al., 1999a. Transgenic mice expressing mutated full-length HD cDNA: a paradigm for locomotor changes and selective neuronal loss in Huntington's disease. Philos Trans R Soc Lond B Biol Sci. 354**,** 1035-45.

Reddy, P. H., et al., 1999b. Recent advances in understanding the pathogenesis of Huntington's disease. Trends Neurosci. 22**,** 248-55.

Reid, E., et al., 2002. A kinesin heavy chain (KIF5A) mutation in hereditary spastic paraplegia (SPG10). Am J Hum Genet. 71**,** 1189-94.

Reilmann, R., et al., 1994. Huntington's disease: the neuroexcitotoxin aspartate is increased in platelets and decreased in plasma. J Neurol Sci. 127**,** 48-53.

Reiner, A., et al., 2003. Wild-type huntingtin plays a role in brain development and neuronal survival. Mol Neurobiol. 28**,** 259-76.

Rigamonti, D., et al., 2000. Wild-type huntingtin protects from apoptosis upstream of caspase-3. J Neurosci. 20**,** 3705-13.

Rine, J., Herskowitz, I., 1987. Four genes responsible for a position effect on expression from HML and HMR in Saccharomyces cerevisiae. Genetics. 116**,** 9-22.

Rockabrand, E., et al., 2007. The first 17 amino acids of Huntingtin modulate its sub-cellular localization, aggregation and effects on calcium homeostasis. Hum Mol Genet. 16**,** 61-77.

Rodgers, J. T., et al., 2005. Nutrient control of glucose homeostasis through a complex of PGC-1alpha and SIRT1. Nature. 434**,** 113-8.

Rosen, D. R., 1993. Mutations in Cu/Zn superoxide dismutase gene are associated with familial amyotrophic lateral sclerosis. Nature. 364**,** 362.

Rothstein, J. D., et al., 1995. Selective loss of glial glutamate transporter GLT-1 in amyotrophic lateral sclerosis. Ann Neurol. 38**,** 73-84.

Sasaki, S., Iwata, M., 2007. Mitochondrial alterations in the spinal cord of patients with sporadic amyotrophic lateral sclerosis. J Neuropathol Exp Neurol. 66**,** 10-6.

Sayer, J. A., et al., 2005. Interaction of the nuclear matrix protein NAKAP with HypA and huntingtin: implications for nuclear toxicity in Huntington's disease pathogenesis. Neuromolecular Med. 7**,** 297-310.

Schriner, S. E., et al., 2005. Extension of murine life span by overexpression of catalase targeted to mitochondria. Science. 308**,** 1909-11.

Selkoe, D. J., 2003. Folding proteins in fatal ways. Nature. 426**,** 900-4.

Sesaki, H., et al., 2003. Cells lacking Pcp1p/Ugo2p, a rhomboid-like protease required for Mgm1p processing, lose mtDNA and mitochondrial structure in a Dnm1p-dependent manner, but remain competent for mitochondrial fusion. Biochem Biophys Res Commun. 308**,** 276-83.

Shaw, P. J., 2005. Molecular and cellular pathways of neurodegeneration in motor neurone disease. J Neurol Neurosurg Psychiatry. 76**,** 1046-57.

Shaw, P. J., Ince, P. G., 1997. Glutamate, excitotoxicity and amyotrophic lateral sclerosis. J Neurol. 244 Suppl 2**,** S3-14.

Shimohata, T., et al., 2000. Expanded polyglutamine stretches interact with TAFII130, interfering with CREB-dependent transcription. Nat Genet. 26**,** 29-36.

Shimojo, M., 2008. Huntingtin regulates RE1-silencing transcription factor/neuron-restrictive silencer factor (REST/NRSF) nuclear trafficking indirectly through a complex with REST/NRSF-interacting LIM domain protein (RILP) and dynactin p150 Glued. J Biol Chem. 283**,** 34880-6.

Shore, D., et al., 1984. Characterization of two genes required for the position-effect control of yeast mating-type genes. EMBO J. 3**,** 2817-23.

Sidoryk-Wegrzynowicz, M., et al., 2011. Role of astrocytes in brain function and disease. Toxicol Pathol. 39**,** 115-23.

Smirnova, E., et al., 2001. Dynamin-related protein Drp1 is required for mitochondrial division in mammalian cells. Mol Biol Cell. 12**,** 2245-56.

Smirnova, E., et al., 1998. A human dynamin-related protein controls the distribution of mitochondria. J Cell Biol. 143**,** 351-8.

Smith, R., et al., 2005. Synaptic dysfunction in Huntington's disease: a new perspective. Cell Mol Life Sci. 62**,** 1901-12.

Sohal, R. S., Weindruch, R., 1996. Oxidative stress, caloric restriction, and aging. Science. 273**,** 59-63.

Someya, S., et al., 2010. Sirt3 mediates reduction of oxidative damage and prevention of age-related hearing loss under caloric restriction. Cell. 143**,** 802-12.

Son, M., et al., 2007. Overexpression of CCS in G93A-SOD1 mice leads to accelerated neurological deficits with severe mitochondrial pathology. Proc Natl Acad Sci U S A. 104**,** 6072-7.

Song, W., et al., 2008. Assessing mitochondrial morphology and dynamics using fluorescence wide-field microscopy and 3D image processing. Methods. 46**,** 295-303.

Song, W., et al., 2011. Mutant huntingtin binds the mitochondrial fission GTPase dynamin-related protein-1 and increases its enzymatic activity. Nat Med. 17**,** 377-82.

Song, Z., et al., 2007. OPA1 processing controls mitochondrial fusion and is regulated by mRNA splicing, membrane potential, and Yme1L. J Cell Biol. 178**,** 749-55.

Spalloni, A., et al., 2004. Cu/Zn-superoxide dismutase (GLY93-->ALA) mutation alters AMPA receptor subunit expression and function and potentiates kainate-mediated toxicity in motor neurons in culture. Neurobiol Dis. 15**,** 340-50.

St-Pierre, J., et al., 2006. Suppression of reactive oxygen species and neurodegeneration by the PGC-1 transcriptional coactivators. Cell. 127**,** 397-408.

Stelzl, U., et al., 2005. A human protein-protein interaction network: a resource for annotating the proteome. Cell. 122**,** 957-68.

Stowers, R. S., et al., 2002. Axonal transport of mitochondria to synapses depends on milton, a novel Drosophila protein. Neuron. 36**,** 1063-77.

Strehlow, A. N., et al., 2007. Wild-type huntingtin participates in protein trafficking between the Golgi and the extracellular space. Hum Mol Genet. 16**,** 391-409.

Sugars, K. L., Rubinsztein, D. C., 2003. Transcriptional abnormalities in Huntington disease. Trends Genet. 19**,** 233-8.

Taguchi, N., et al., 2007. Mitotic phosphorylation of dynamin-related GTPase Drp1 participates in mitochondrial fission. J Biol Chem. 282**,** 11521-9.

Tanaka, Y., et al., 1998. Targeted disruption of mouse conventional kinesin heavy chain, kif5B, results in abnormal perinuclear clustering of mitochondria. Cell. 93**,** 1147-58.

Tao, R., et al., 2010. Sirt3-mediated deacetylation of evolutionarily conserved lysine 122 regulates MnSOD activity in response to stress. Mol Cell. 40**,** 893-904.

Tartari, M., et al., 2008. Phylogenetic comparison of huntingtin homologues reveals the appearance of a primitive polyQ in sea urchin. Mol Biol Evol. 25**,** 330-8.

Tissenbaum, H. A., Guarente, L., 2001. Increased dosage of a sir-2 gene extends lifespan in Caenorhabditis elegans. Nature. 410**,** 227-30.

Tohgi, H., et al., 1999. Remarkable increase in cerebrospinal fluid 3-nitrotyrosine in patients with sporadic amyotrophic lateral sclerosis. Ann Neurol. 46**,** 129-31.

Trushina, E., et al., 2004. Mutant huntingtin impairs axonal trafficking in mammalian neurons in vivo and in vitro. Mol Cell Biol. 24**,** 8195-209.

Tsujimoto, Y., 1997. Apoptosis and necrosis: intracellular ATP level as a determinant for cell death modes. Cell Death Differ. 4**,** 429-34.

Turner, B. J., Talbot, K., 2008. Transgenics, toxicity and therapeutics in rodent models of mutant SOD1-mediated familial ALS. Prog Neurobiol. 85**,** 94-134.

Twig, G., et al., 2008. Fission and selective fusion govern mitochondrial segregation and elimination by autophagy. EMBO J. 27**,** 433-46.

Uo, T., et al., 2009. Drp1 levels constitutively regulate mitochondrial dynamics and cell survival in cortical neurons. Exp Neurol. 218**,** 274-85.

van der Bliek, A. M., et al., 1993. Mutations in human dynamin block an intermediate stage in coated vesicle formation. J Cell Biol. 122**,** 553-63.

Vance, C., et al., 2009. Mutations in FUS, an RNA processing protein, cause familial amyotrophic lateral sclerosis type 6. Science. 323**,** 1208-11.

Vande Velde, C., et al., 2008. Selective association of misfolded ALS-linked mutant SOD1 with the cytoplasmic face of mitochondria. Proc Natl Acad Sci U S A. 105**,** 4022-7.

Varadi, A., et al., 2004. Cytoplasmic dynein regulates the subcellular distribution of mitochondria by controlling the recruitment of the fission factor dynamin-related protein-1. J Cell Sci. 117**,** 4389-400.

Vaziri, H., et al., 2001. hSIR2(SIRT1) functions as an NAD-dependent p53 deacetylase. Cell. 107**,** 149-59.

Verhoeven, K., et al., 2006. MFN2 mutation distribution and genotype/phenotype correlation in Charcot-Marie-Tooth type 2. Brain. 129**,** 2093-102.

Verstreken, P., et al., 2005. Synaptic mitochondria are critical for mobilization of reserve pool vesicles at Drosophila neuromuscular junctions. Neuron. 47**,** 365-78.

Vonsattel, J. P., et al., 1985. Neuropathological classification of Huntington's disease. J Neuropathol Exp Neurol. 44**,** 559-77.

Wakabayashi, J., et al., 2009. The dynamin-related GTPase Drp1 is required for embryonic and brain development in mice. J Cell Biol. 186**,** 805-16.

Wallace, D. C., 2005. A mitochondrial paradigm of metabolic and degenerative diseases, aging, and cancer: a dawn for evolutionary medicine. Annu Rev Genet. 39**,** 359-407.

Wallace, D. C., Fan, W., 2009. Energetics, epigenetics, mitochondrial genetics. Mitochondrion. 10**,** 12-31.

Walz, W., The neuronal environment brain homeostasis in health and disease. Contemporary neuroscience. Humana Press, Totowa, N.J., 2002.

Wang, H., et al., 2009. Effects of overexpression of huntingtin proteins on mitochondrial integrity. Hum Mol Genet. 18**,** 737-52.

Wang, J., et al., 2005. Caloric restriction attenuates beta-amyloid neuropathology in a mouse model of Alzheimer's disease. FASEB J. 19**,** 659-61.

Wang, X., Schwarz, T. L., 2009. The mechanism of Ca2+ -dependent regulation of kinesin-mediated mitochondrial motility. Cell. 136**,** 163-74.

Warby, S. C., et al., 2005. Huntingtin phosphorylation on serine 421 is significantly reduced in the striatum and by polyglutamine expansion in vivo. Hum Mol Genet. 14**,** 1569-77.

Warita, H., et al., 1999. Selective impairment of fast anterograde axonal transport in the peripheral nerves of asymptomatic transgenic mice with a G93A mutant SOD1 gene. Brain Res. 819**,** 120-31.

Wasiak, S., et al., 2007. Bax/Bak promote sumoylation of DRP1 and its stable association with mitochondria during apoptotic cell death. J Cell Biol. 177**,** 439-50.

Weindruch, R., Walford, R. L., 1988. The retardation of aging and disease by dietary restriction. C.C. Thomas, Springfield, Ill., U.S.A.

Weydt, P., et al., 2006. Thermoregulatory and metabolic defects in Huntington's disease transgenic mice implicate PGC-1alpha in Huntington's disease neurodegeneration. Cell Metab. 4**,** 349-62.

Wiedemann, F. R., et al., 2002. Mitochondrial DNA and respiratory chain function in spinal cords of ALS patients. J Neurochem. 80**,** 616-25.

Williamson, T. L., Cleveland, D. W., 1999. Slowing of axonal transport is a very early event in the toxicity of ALS-linked SOD1 mutants to motor neurons. Nat Neurosci. 2**,** 50-6.

Xia, J., et al., 2003. Huntingtin contains a highly conserved nuclear export signal. Hum Mol Genet. 12, 1393-403.

Yamanaka, K., et al., 2008. Astrocytes as determinants of disease progression in inherited amyotrophic lateral sclerosis. Nat Neurosci. 11, 251-3.

Yang, C. C., et al., 2011. The dynamin-related protein DRP-1 and the insulin signaling pathway cooperate to modulate Caenorhabditis elegans longevity. Aging Cell. 10, 724-8.

Yang, Y., et al., 2008. Pink1 regulates mitochondrial dynamics through interaction with the fission/fusion machinery. Proc Natl Acad Sci U S A. 105, 7070-5.

Youle, R. J., Karbowski, M., 2005. Mitochondrial fission in apoptosis. Nat Rev Mol Cell Biol. 6, 657-63.

Young, A. B., et al., 1988. NMDA receptor losses in putamen from patients with Huntington's disease. Science. 241, 981-3.

Young, A. B., et al., 1986. PET scan investigations of Huntington's disease: cerebral metabolic correlates of neurological features and functional decline. Ann Neurol. 20, 296-303.

Yuan, H., et al., 2007. Mitochondrial fission is an upstream and required event for bax foci formation in response to nitric oxide in cortical neurons. Cell Death Differ. 14, 462-71.

Zala, D., et al., 2008. Phosphorylation of mutant huntingtin at S421 restores anterograde and retrograde transport in neurons. Hum Mol Genet. 17, 3837-46.

Zhang, F., et al., 2007. Interaction between familial amyotrophic lateral sclerosis (ALS)-linked SOD1 mutants and the dynein complex. J Biol Chem. 282, 16691-9.

Zhang, Y., et al., 2006. Huntingtin inhibits caspase-3 activation. EMBO J. 25, 5896-906.

Zhang, Y., et al., 2004. Rat kinesin light chain 3 associates with spermatid mitochondria. Dev Biol. 275**,** 23-33.

Zhao, C., et al., 2001. Charcot-Marie-Tooth disease type 2A caused by mutation in a microtubule motor KIF1Bbeta. Cell. 105**,** 587-97.

Zuccato, C., Cattaneo, E., 2007. Role of brain-derived neurotrophic factor in Huntington's disease. Prog Neurobiol. 81**,** 294-330.

Zuccato, C., et al., 2001. Loss of huntingtin-mediated BDNF gene transcription in Huntington's disease. Science. 293**,** 493-8.

Zuccato, C., et al., 2003. Huntingtin interacts with REST/NRSF to modulate the transcription of NRSE-controlled neuronal genes. Nat Genet. 35**,** 76-83.

Zuchner, S., et al., 2004. Mutations in the mitochondrial GTPase mitofusin 2 cause Charcot-Marie-Tooth neuropathy type 2A. Nat Genet. 36**,** 449-51.